

PhD Thesis

Novel biomarkers in the era of modern stroke management



Dóra Spántler MD

Doctoral School of Clinical Medicine

Supervisors:

Tihamér Molnár MD, PhD, DSc

Péter Csécsei MD, PhD

Head of the doctoral program: Gábor Jancsó MD, PhD

Head of the doctoral school: Lajos Bogár MD, PhD, D.Sc

University of Pécs

Pécs, 2023

Table of contents

Abbreviations	4
I. Introduction	8
1.1. <i>Definition and epidemiology of stroke</i>	8
1.2. <i>Stroke education and prevention</i>	8
1.3. <i>Consequences of stroke</i>	9
1.4. <i>Biomarkers</i>	10
II. Ischemic stroke	13
2.1. <i>Definition and epidemiology of acute ischemic stroke</i>	13
2.2. <i>Etiology, classification, and pathogenesis of acute ischemic stroke</i>	13
2.3. <i>Diagnostic approach to acute ischemic stroke</i>	18
2.4. <i>Treatment of acute ischemic stroke and outcome</i>	20
2.5. <i>Collateral system</i>	25
2.6. <i>Biomarkers in acute ischemic stroke</i>	27
III. Aneurysmal subarachnoid hemorrhage (aSAH)	29
3.1. <i>Definition and epidemiology of aSAH</i>	29
3.2. <i>Etiology and pathogenesis of aSAH</i>	29
3.3. <i>Diagnostic approach and treatment of aSAH</i>	32
3.4. <i>Classification of aSAH</i>	35
3.5. <i>Complications after aSAH and outcome</i>	37
3.6. <i>Biomarkers in aSAH</i>	40
IV. Aims	44
4.1. <i>Ischemic stroke</i>	44
4.2. <i>Aneurysmal subarachnoid hemorrhage</i>	44
V. Methods	45
5.1. <i>Ischemic stroke</i>	45
5.1.1. <i>Study design</i>	45
5.1.2. <i>Clinical protocol</i>	45
5.1.3. <i>Sampling and laboratory analysis</i>	46
5.1.4. <i>Statistical analysis</i>	46
5.2. <i>Aneurysmal subarachnoid hemorrhage</i>	47

5.2.1. <i>Study design</i>	47
5.2.2. <i>Clinical protocol</i>	47
5.2.3. <i>Sampling and laboratory analysis</i>	48
5.2.4. <i>Statistical analysis</i>	49
VI. Results	50
6.1. <i>Ischemic stroke</i>	50
6.1.1. <i>Clinical characteristics</i>	50
6.1.2. <i>Admission periostin level, comorbidities and outcome</i>	53
6.1.3. <i>Variables associated with poor collaterals</i>	54
6.2. <i>Aneurysmal subarachnoid hemorrhage</i>	56
6.2.1. <i>Clinical characteristics</i>	56
6.2.2. <i>Cytokines associated with DCI and functional outcome</i>	58
6.2.3. <i>Clinical variables associated with DCI and Day 30 functional outcome</i>	60
6.2.4. <i>Correlations between biomarkers in aSAH patients</i>	63
VII. Discussion	66
7.1. <i>Ischemic stroke</i>	66
7.2. <i>Aneurysmal subarachnoid hemorrhage</i>	69
VIII. Conclusion	72
IX. Own findings	74
X. List of publications and presentations	75
XI. Acknowledgement	76
XII. References	77

Abbreviations

ACom: anterior communicating artery

AF: atrial fibrillation

AHA/ASA: Stroke Council of the American Heart Association/American Stroke Association

aSAH: aneurysmal subarachnoid hemorrhage

ASPECTS: Alberta Stroke Program Early CT Score

ATP: adenosin-5'- triphosphate

BBB: blood–brain barrier

BMP: bone morphogenic protein

CBF: cerebral blood flow

CCL11: C-C motif chemokine 11/eotaxin-1

CEI: cardioembolism infarct

CNS: central nervous system

CPP: cerebral perfusion pressure

CRP: C-reactive protein

CSF: cerebrospinal fluid

CTA: CT angiography

CTP: CT perfusion

CV: cerebral vasospasm

CX3CL1: CX3C chemokine ligand 1/fractalkine

DAMPs: damage-associated molecular patterns

DCI: delayed cerebral ischemia

DSA: Digital Subtraction Angiography

DWI: diffusion-weighted imaging

EAE: experimental autoimmune encephalitis

EBI: early brain injury

ECG: electrocardiogram

ECM: extracellular matrix

EVT: endovascular therapy

FGF: fibroblast growth factor

FLT-3L: fms-like tyrosine kinase-3 ligand

FLAIR: fluid-attenuated inversion recovery

GCS: Glasgow Coma Scale

HRQoL: Health-Related Quality of Life

IA: intraarterial

IAT: intraarterial thrombolysis

ICA: internal carotid artery

ICH: intracerebral hemorrhage

ICP: intracranial pressure

IFN: interferon

IL: interleukin

IV: intravenous

IVT: intravenous thrombolysis

IVtPA: intravenous tissue plasminogen activator

IS: ischemic stroke

LAAS: large artery atherosclerosis

MCA: middle cerebral artery

mFisher: modified Fisher score

MCP: monocyte chemotactic protein

MIP: macrophage inflammatory protein

MMPs: matrix metalloproteinases

MRA: MR angiogram

MRI: magnetic resonance imaging

mRS: modified Rankin scale

MT: mechanical thrombectomy

NCCT: non-contrast computed tomography

NIHSS: Neurological Institutes of Health Stroke Scale

NLR: neutrophil-lymphocyte ratio

NMDA: N-methyl-D-aspartate

NO: nitric oxide

ODE: other determined etiology

PCA: posterior cerebral artery

PCom: posterior communicating artery

PWI: perfusion-weighted imaging

ROS: reactive oxygen species

RBC: red blood cell count

SAH: subarachnoid hemorrhage

TBI: traumatic brain injury

TCD: transcranial Doppler

TGF- β : transforming growth factor beta

TIA: transient ischemic attack

TNF- α : tumor necrosis factor alpha

UDE: stroke of undetermined etiology

UTP: Uridine-5'-triphosphate

WBC: white blood cell count

WFNS: Federation of Neurological Surgeons

WHO: World Health Organization

I. Introduction

1.1. Definition and epidemiology of stroke

Stroke was defined by the World Health Organization (WHO) in 1970, as rapidly developing clinical signs of focal (or global) cerebral deficits, with symptoms lasting 24 hours or longer, or leading to death, with no apparent cause other than vascular origin [1]. Typically, stroke is characterized as a neurological deficit attributed to an acute focal injury of the central nervous system (CNS) by a vascular cause, including cerebral infarction, intracerebral hemorrhage (ICH), and subarachnoid hemorrhage (SAH) [2]. As our knowledge has grown over the years, the Stroke Council of the American Heart Association (AHA)/ American Stroke Association (ASA) proposed a new definition in 2013 and now the CNS infarction is interpreted as brain, spinal cord, or retinal cell death attributed to ischemia, based on neuropathological, neuroimaging, and/or clinical evidence of permanent injury [2].

Stroke is the second leading cause of disability and death worldwide [3], affecting 15 million people per year, 5 million of them die, and another 5 million are permanently physically challenged [4]. Stroke burden has become the leading cause of death and disability in Canada, the United States and China [5,6,7]. The incidence of stroke is correlated with ethnicity [8]. In the United States, the number of cases is higher in black and Hispanic people than in Caucasians, as multiple studies reported [4]. The chance of stroke is proportional to age, and almost 75% of all strokes occur in patients older than 64 years [4], but the incidence of stroke among people aged 20-54 years increased globally between 1990 and 2016 [9]. The incidence in men (62.8/100,000 people/year) is higher than in women (59/100,000 people/year) [8], although younger ages in women due to pregnancy-related cases, such as preeclampsia, contraception use and hormonal therapy, as well as migraine with aura are at higher risk [9].

1.2. Stroke education and prevention

The high incidence of stroke is probably due to poor community knowledge [3]. Evidence from studies in developed and developing countries shows that less than 50% of responders can recognize risk factors or warning signs of stroke [3]. Stroke represents a medical emergency that requires immediate recognition and treatment within a narrow time window [10]. Timely access to therapy may depend on patients or witnesses recognizing the signs and symptoms of stroke [5,6]. Several studies found that delays in seeking stroke treatment were

primarily caused by a lack of recognition of symptoms and not calling emergency services [6].

Educational efforts such as stroke awareness campaigns are one way to inform the public about prevention and risk factors, signs and symptoms of stroke, and to draw attention to immediate action [5]. WHO supports initiatives to prevent stroke and other types of cardiovascular disease [11]. The prevention strategy targets several behavioral and lifestyle risk factors, and even small changes in the distribution of risk factors could lead to significant reductions in the incidence of stroke and cardiovascular disease. Primary prevention strategies for stroke include community education programs and digital health technology [12]. Children should be considered an important potential target audience, on the one hand, due to the importance of educating them about healthy lifestyles, on the other hand, they need to understand the importance of seeking immediate medical attention if an adult in their environment exhibits stroke symptoms [5]. Another important approach in stroke prevention is to avoid secondary vascular events. After an ischaemic or hemorrhagic stroke, appropriate control of blood pressure can reduce the risk of subsequent stroke, as well as antiplatelet therapy and reduction of cholesterol in ischaemic stroke are also important for secondary prevention [13,14].

1.3. Consequences of stroke

As a result of effective new technologies and therapies, more and more patients survive stroke and live with its sequelae, especially in the western world. The rising number of survivors has raised the idea of measuring the outcomes associated with stroke treatment and rehabilitation. The concept of Health-Related Quality of Life (HRQoL) is used as an important parameter to assess the impact of disease on the patient's life, to measure outcomes, and to evaluate the utility and disability associated with different health states [15,16]. It also measures emotional, physical, social, and subjective feelings of well-being, useful in evaluating the effectiveness of prophylactic, therapeutic, and rehabilitative interventions, in addition, facilitating patient-caregiver communication and clinical decision-making [16,17]. In a study of stroke patients in Auckland, HRQoL was found to be relatively good for stroke patients who psychologically adjusted well to their illness despite the significant ongoing physical disability. In contrast, a Canadian study supported by the Kansas City study showed impairment of certain HRQoL domains [18,19,20]. However, stroke studies that have applied

HRQoL show different results, but outcome measures are important to identify and determine the prognosis in stroke patients.

Beyond doubt, stroke has serious economic and social consequences. The public health burden of stroke is likely to increase in the future decades and places stroke high on the agenda of public health issues in the 21st century. Therefore, there is an urgent need to find reliable markers that predict complications, support decision-making and be promising in treatment.

1.4. Biomarkers

In 2001 the National Institute of Health Biomarkers Definitions Working Group created the first interpretation of biomarkers and defined them as objectively measured characteristics evaluated as an indication of normal biological processes, pathogenic processes, or pharmacological responses to a therapeutic intervention [21]. A more recent definition (2016) describes a biomarker as „a functional variant or quantitative index of a biological process that predicts or reflects the evolution of or predisposition to a disease or a response to therapy” [22]. Based on this, it does not mean exclusively a molecule but includes a wide range of test areas such as imaging procedures, pathology, laboratory diagnostics, electrocardiography, body temperature, etc. [23,24].

Biomarkers play a critical role in biomedical research to better understand disease mechanisms and identify novel disease targets, in drug discovery and development, and can be used as part of personalized medicine to customize treatment to the specific disease characteristics of an individual patient [25,26]. They can be used in many aspects, as **Table 1** shows.

Table 1. Uses of biomarkers.

Biomarkers in disease	Biomarkers in drug discovery and development	Biomarkers in tumors
<ul style="list-style-type: none"> • screen for diseases • characterize diseases • rule out, diagnose, stage, and monitor diseases • inform prognosis • prediction and monitoring of clinical response to an intervention (help to individualize therapeutic interventions) • identify cell types e.g., histological markers 	<ul style="list-style-type: none"> • as targets for screening compounds during drug discovery • as endpoints for pharmacodynamic studies • in studying the relationship between the concentration or dose of a drug and its effect • to measure efficacy in clinical trials • to help define the adverse effects of drug candidates. 	<ul style="list-style-type: none"> • to assess the risk of cancer • to study tumor-host interactions • to reflect tumor burden • to reflect cellular function, such as pathways of apoptosis • identification of tumor markers that predict responses to particular medications

Source: reference [21,27]

In the chain of events leading from pathogenesis to clinical manifestation, a biomarker can be identified at any point in the chain, at the molecular, cellular, tissue, organ or whole organism level [25]. The first step is to find an appropriate biomarker. Clinical biomarkers have the advantages of being simpler and less expensive than direct measurement of final clinical endpoints, and they can be analyzed repeatedly and over a shorter period of time. Good biomarkers should have several specific features listed in **Table 2**. Most importantly, they should be measurable with little or no variability, have a significant signal-to-noise ratio, and change immediately and reliably in response to changes in the disease or its therapy [25]. The second stage of biomarker development also called the qualification phase, is when the candidate biomarker level is determined in the diagnostic sample and confirms the different concentrations measured in samples from individual patients and their controls. In the subsequent verification phase, population-level studies are performed on healthy controls, and it is aimed to verify the specificity of the test. Then, in the validation phase, we have an opportunity to develop and test the clinical assay in which samples are taken from patients

and their controls. In this phase, the sensitivity/specificity data and the potential clinical applications of the new marker are also investigated [28].

Table 2. Characteristics of useful biomarkers according to Bradford Hill’s guidelines.

Characteristics of useful biomarkers	
Strength	- Strong association between marker and outcome, or between the effects of a treatment on each.
Consistency	- The association persists in different individuals, in different places, in different circumstances, and at different times.
Specificity	- The marker is associated with a specific disease.
Temporality	- The time-courses of changes in the marker and outcome occur in parallel.
Biological gradient (dose-responsiveness)	- Increasing exposure to an intervention produces increasing effects on the marker and the disease.
Plausibility	- Credible mechanisms connect the marker, the pathogenesis of the disease, and the mode of action of the intervention.
Coherence	- The association is consistent with the natural history of the disease and the marker.
Experimental evidence	- An intervention gives results consistent with the association.
Analogy	- There is a similar result from which we can adduce a relationship.

Source: reference [25]

II. Ischemic stroke

2.1. Definition and epidemiology of acute ischemic stroke

A comprehensive definition of ischemic stroke (IS) requires clinical symptoms and evidence of infarction to provide an accurate description of the ischemia process that occurs in a patient [2]. The Stroke Council of AHA/ASA defined ischemic stroke as „an episode of neurological dysfunction caused by focal cerebral, spinal or retinal infarction” [2].

The incidence of stroke varies considerably throughout the world, the highest in developing countries, with ischemic stroke being the most common type [8,29]. Of all strokes, 85% are ischemic, 10% are intracerebral hemorrhage, and 5% are subarachnoid hemorrhage [2,10,30]. According to the first INTERSTROKE study, involving 22 countries, the proportions of ischaemic and hemorrhagic stroke in Africa were about 66% and 34%, compared to high-income countries with 91% and 9% [31]. It is partly confirmed by the SIREN (Stroke Investigative Research and Educational Network) study [32].

2.2. Etiology, classification, and pathogenesis of acute ischemic stroke

Most strokes of ischemic origin are caused by atherosclerosis affecting large arteries and by embolism of cardiac origin, with an estimated loss of 2 million neurons for every minute delay in reperfusion therapies [9]. Approximately 45% of ischemic strokes are caused by a thrombus, cardioembolic stroke accounts for 14–30% of all cerebral infarctions, while the lacunar subtype is 15–25% of all ischemic strokes [8]. The TOAST (Trial of ORG10172 in Acute Stroke Treatment) classification is used to categorize IS. It distinguishes five different stroke subtypes listed in **Table 3** [8,33].

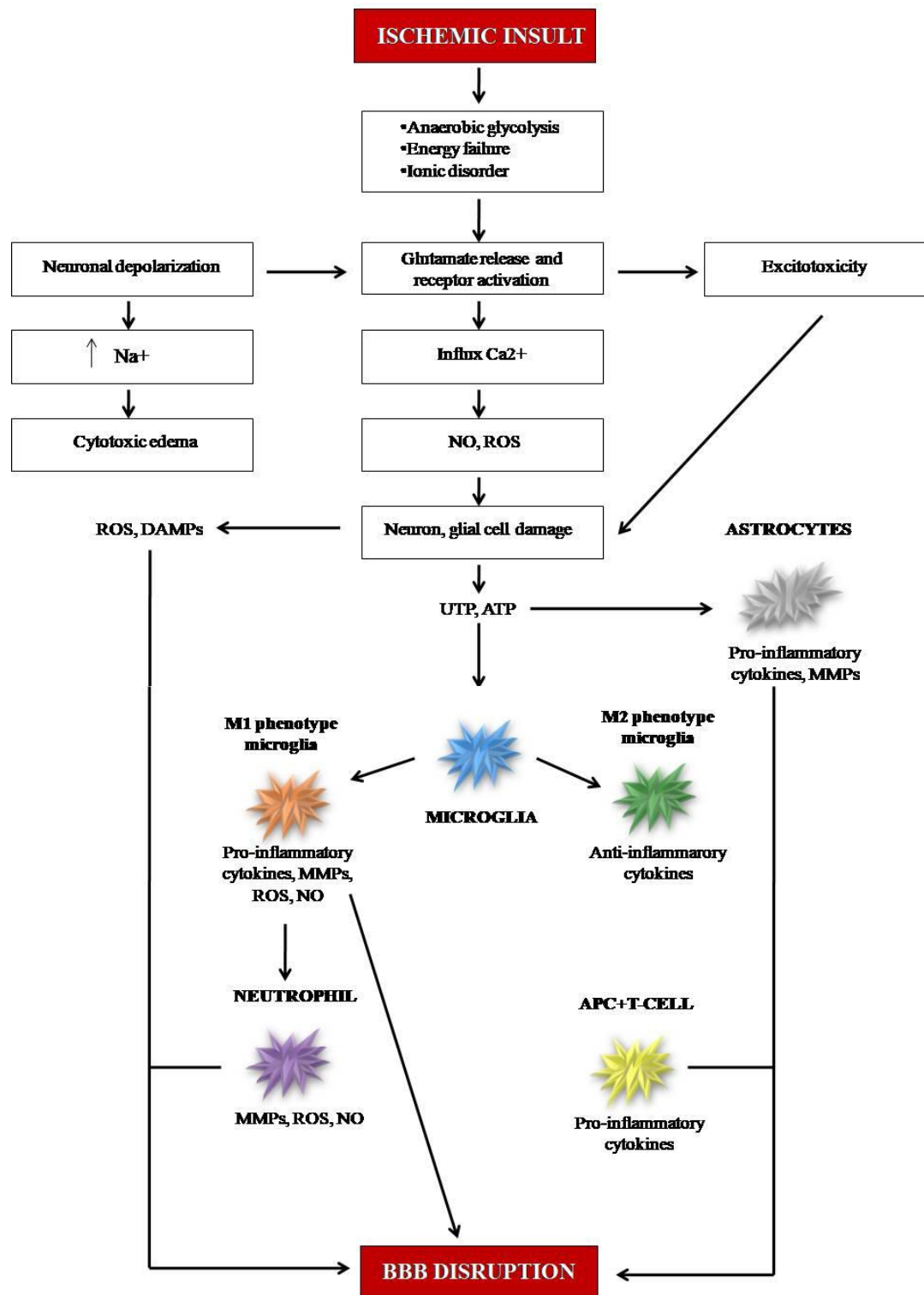
Table 3. Types of IS based on the TOAST classification.

	Types of stroke	Causes	The incidence of stroke types (%)
1	large artery atherosclerosis (LAAS)	Atherosclerotic plaques in the large blood vessels of the brain lead to ischemia and infarction.	20%
2	cardioembolism infarction (CEI)	Associated with cardiac dysrhythmias, valvular heart disease, and thrombi in the left ventricles.	15%
3	small artery occlusion (lacune)	One or more vessels in the brain are affected (microatheromatosis).	25%
4	stroke of other determined etiology (ODE)	Such as arterial dissection, cancer-related coagulopathy, intrinsic disease of the arterial wall, primary hemostatic disease/coagulopathy, hypoperfusion syndromes, infectious/ inflammatory diseases, hereditary syndromes, iatrogenic, migraine and drugs.	20-25%
5	stroke of undetermined etiology (UDE)	Cause is unknown.	5-10%

Abbreviations: TOAST, Trial of ORG10172 in Acute Stroke Treatment *Source:* reference [3,8,33,34]

The blood supply to the brain is managed by two internal carotids anteriorly and two vertebral arteries posteriorly. In thrombotic stroke, the build-up of plaque constricts the vascular chamber and forms clots that narrow the vessels and block the blood flow. In an embolic stroke, the embolism decreases blood flow in the brain, causing severe stress [9]. The occlusion of a cerebral artery results in a deficiency of oxygen, glucose and lipids, whilst the neurons are unable to sustain their normal transmembrane ionic gradient and homeostasis. On the one hand, neuronal damage causes significant release of glutamate, activation of N-methyl-D-aspartate (NMDA) receptors, and increased intracellular calcium levels, resulting in excitotoxicity and cell death. Damaged neurons and astrocytes produce reactive oxygen species (ROS) and endogenous danger molecules, called damage-associated molecular patterns (DAMPs). On the other hand, the loss of membrane ion pump function resulting in loss of potassium in exchange for sodium accompanied by an inflow of water causes cytotoxic edema. As the extracellular adenosine-5'- triphosphate (ATP) level rises due to injured plasma membranes of dying cells, microglia and astrocytes become active. The activated microglia, phenotype M2, remove debris and dead tissue, promote the production of growth factors and improve neuronal protection through anti-inflammatory mediators, while M1 phenotype microglia secretes pro-inflammatory agents and take part in neuronal damage. Damaged cells and remnants cause inflammation and oxidative stress contributing to blood–brain barrier (BBB) disruption. [8,9]. As cells die and brain tissue is injured, molecular danger signals further increase phlogosis by activating more microglia and infiltrating leukocytes in a feed-forward response releasing more cytokines with pro-inflammatory action (**Figure 1**). These mechanisms lead to increased neuronal cell necrosis, brain edema, and hemorrhagic transformation [8,9].

Figure 1. Pathomechanism of ischemic brain damage.



Abbreviations: Na⁺, sodium ion; Ca²⁺, calcium ion; NO, nitric oxide; ROS, reactive oxygen species; DAMPs, Damage-associated molecular patterns; UTP, Uridine-5'-triphosphate; ATP, adenosine-5'-triphosphate; MMPs, matrix metalloproteinases; APC, antigen presenting cell; BBB, blood-brain barrier. *Source:* reference [8,9]

Several risk factors play an important role in the development of IS. Some of these factors are modifiable, and some are non-modifiable (**Table 4**) [9]. Non-modifiable risk factors include age, sex, ethnicity, genetics, and transient ischemic attack (TIA). TIA occurs when the blood supply is temporarily blocked in a region of the brain. Nearly 60% of strokes are in patients with a history of TIA [9]. Modifiable risk factors are of paramount importance, as timely and appropriate medical intervention can reduce the risk of stroke in susceptible individuals. Hypertension is one of the most significant risk factors. Diabetes doubles the risk of IS and confers an approximately 20% higher mortality rate. The prognosis for diabetic patients after a stroke is worse than for non-diabetic patients, including higher rates of severe disability and slower recovery. Atrial fibrillation (AF) increases the risk of stroke two- to five-fold depending upon the age of the individual, concern and contributes to 15% of all strokes. Hyperlipidemia, alcohol and drug abuse, smoking, insufficient physical inactivity and poor diet are also associated with an increased risk of stroke [3,9,35].

Table 4. Risk factors associated with stroke

Modifiable risk factors	Non-modifiable risk factors
Hypertension	Age
Diabetes	Sex
Atrial fibrillation	Race/ethnicity
Hyperlipidemia	Transient ischemic attack
Alcohol and drug abuse	Genetics
Smoking	
Physical inactivity	
Poor diet	

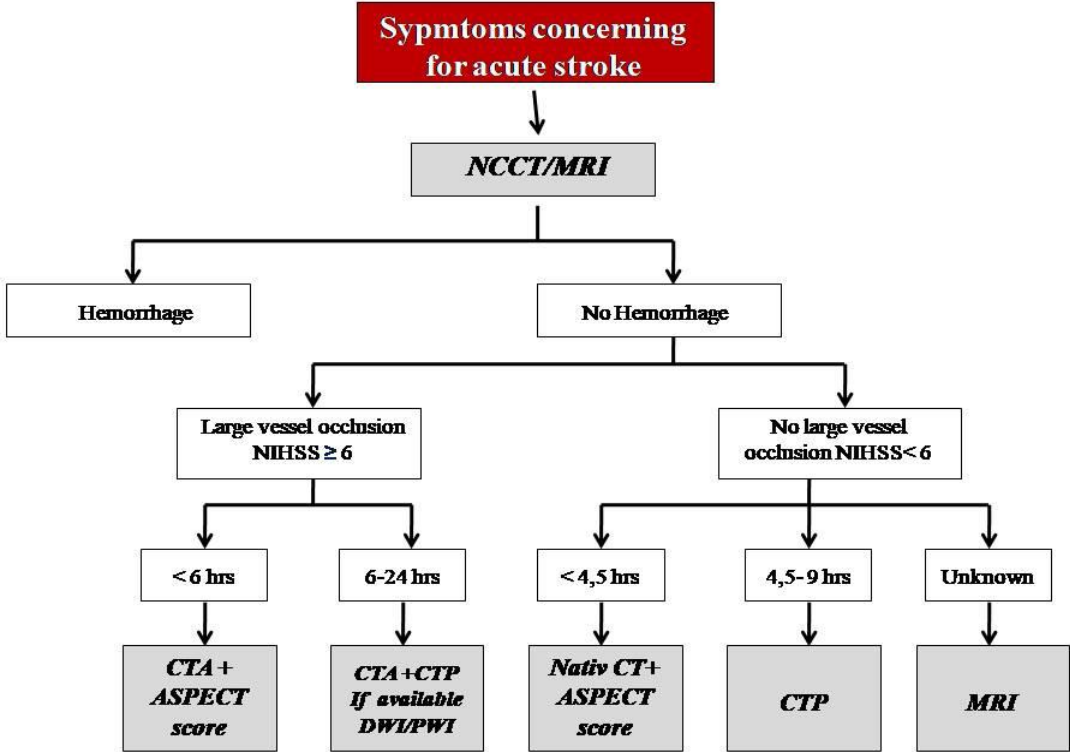
Source: reference [3,9,35]

2.3. Diagnostic approach to acute ischemic stroke

Patients with IS may present with many clinical manifestations, such as sudden onset of focal neurological deficit, confusion, speech abnormalities, impaired vision, or numbness and weakness in the upper and/or lower extremities. Public health campaigns to increase stroke awareness and several tools for prehospital stroke recognition, like the FAST acronym (face drops, arm weakness, speech abnormalities, time to call emergency medical services), can help identify stroke patients and activate a stroke-specific chain of survival [10]. In addition to clinical examination, establishing the exact time of onset is a critical component of stroke care. **Figure 2** below, summarises the imaging techniques recommended in stroke. Patients with suspected stroke should be evaluated with reproducible standardized scales such as the Neurological Institutes of Health Stroke Scale (NIHSS) in order to determine the severity of the patient's condition [10,35]. The confirmation of acute IS depends heavily on neuroimaging performed on the first arrival at a hospital. Non-contrast computed tomography (NCCT) and magnetic resonance imaging (MRI) are able to exclude stroke mimics such as brain tumor or subdural hematoma and to separate brain ischemia from hemorrhage [2,36]. The Alberta Stroke Program Early CT Score (ASPECTS) is a 10-point quantitative topographic CT score, where one point is subtracted from a maximum score of 10 for any sign of early ischemia. It helps to assess the extent of ischemic changes on non-contrast CT and, as several studies have proven, is useful in assessing the collateral system by helping to estimate the core-penumbra ratio and thus the extent of the collateral network [35,36]. The ASPECT score has been shown to have prognostic value among patients treated with thrombolysis for acute IS within 3 hours of symptoms onset [37]. Furthermore, ASPECT score of 7 or less is associated with a higher chance of thrombolysis-related parenchymal hemorrhage [37]. Vascular imaging can be performed by CT angiography (CTA), which involves the introduction of intravenous contrast during imaging. This technique allows visualization of the extracranial and intracranial arteries and veins, informs about collateral blood flow, clot burden and its characteristics [35,37]. MR angiogram (MRA) can also provide useful information about the patient's vascular status and stroke etiology using two different techniques: (i) without contrast, using time of flight and phase contrast, or (ii) with contrast, using gadolinium. Duplex Doppler imaging of the cervical, and transcranial Doppler (TCD) imaging of the intracranial arteries and veins can help identify occlusive vascular lesions and malformations. CT perfusion technology (CTP) using contrast material enables real-time visualization of cerebrovascular physiology parameters, including cerebral blood flow, cerebral blood volume, and mean transit time through brain parenchyma. Furthermore, the quantification of the ischemic core

and the estimation of the tissue at risk known as the penumbra, can provide immediate information for the treatment decision-making [35,37]. Modern imaging such as diffusion-weighted imaging (DWI) can detect tissue changes after several minutes to days after transient or permanent ischemic events by perceiving the movement of the water molecule between two closely spaced radiofrequency pulses. DWI, fluid-attenuated inversion recovery (FLAIR) and perfusion-weighted imaging (PWI) are used to identify potentially reversible lesions. The importance of early diagnosis is that if the blood supply is not restored, the penumbra will suffer permanent damage and result in negative clinical outcome [2,37].

Figure 2. Summarizing the imaging techniques in acute stroke



Abbreviations: NCCT, Non-contrast computed tomography; MRI, magnetic resonance imaging; NIHSS, Neurological Institutes of Health Stroke Scale; hrs, hours; CTA, CT angiography; ASPECT score, Alberta Stroke Program Early CT Score; CTP, CT perfusion; DWI, diffusion-weighted imaging; PWI, perfusion-weighted imaging. *Source:* refrence [10,35-37]

2.4. Treatment of acute ischemic stroke and outcome

Treatment of acute IS consists of a multidisciplinary approach, which focuses on restoring blood flow to the brain and treating stroke-induced neurological damage. Before the 1990s, treatment focused mainly on symptomatic management, secondary prevention, and rehabilitation. Since then, two major innovations have transformed acute stroke care. Besides intravenous (IV) or intraarterial (IA) thrombolysis treatment, endovascular therapy (EVT) has become available for patients with stroke [9,35].

Originally, IV treatment was developed for coronary thrombolysis but was found to be effective in stroke. The efficiency of thrombolytic drugs depends on different factors including the age of the clot, the specificity of the thrombolytic agent for fibrin, the presence and half-life of neutralizing antibodies [9]. The aim of these drugs is to promote fibrinolysin formation, which catalyzes the dissolution of the clot blocking the cerebral vessel [9]. In 1995, the intravenous tissue plasminogen activator (IVtPA), which was developed from research conducted by the US NINDS (National Institute of Neurological Disorders and Stroke), became the mainstay of treatment, within 4.5 hours of the onset of symptoms in eligible patients [9,35,36]. The main reasons for the low treatment rate nowadays, are the limited time window, the resistance of an old or large thrombus to fibrinolysis, the risks of hemorrhage, and the lower rates of recanalization in patients with proximal vessel occlusion [35,36]. Other drugs including alteplase, reteplase, and tenecteplase are fibrin activators that convert plasminogen to plasmin directly, whereas non-fibrin activators like streptokinase and staphylokinase do so indirectly. Intravenous thrombolysis (IVT) with alteplase has been proven to be effective initially within 4.5 hours and has been more recently proven in patients with IS at awakening [9,38]. Intraarterial thrombolysis (IAT) is another approach that requires experienced clinicians and angiographic techniques, and is most effective in the first 6 hours of onset of middle cerebral artery (MCA) occlusion. In two small clinical trials, thrombolytics and glycoprotein IIb/IIIa antagonists were combined, which seemed to be helpful in the treatment of atherosclerotic occlusions [39,40]. While the IMS (Interventional Management of Stroke) III trial tested IVT and IAT together to assess the benefits of combining rapid administration of therapy and a superior recanalization methodology for faster relief. This combined therapy was fruitful compared to IVT alone [41]. A correlation was found between high fibrinogen levels in stroke patients and poor diagnosis for clinical outcomes [42]. The use of fibrinogen-depleting agents such as anicrod helps to decrease blood plasma levels of fibrinogen, thus reducing blood thickness, removing the blood clot in the artery and restoring

blood flow in the affected regions of the brain. On the other hand, some studies reported hemorrhage after treatment [43]. Ancrod is a snake (Malaysian pit viper) venom that has been studied and found to be effective in IS within three hours of onset. The ESTAT (European Stroke Treatment with Ancrod Trial) concluded that controlled administration of ancrod at 70 mg/dL fibrinogen was effective and safe as it achieved a lower prevalence of hemorrhage [44].

Over the years, endovascular therapy for the management of acute IS has evolved tremendously. The success of EVT is measured by the degree or quality of revascularization, therefore, the Thrombolysis in Cerebral Infarction scale was created to standardize the different degrees of reperfusion, ranging from no perfusion to complete perfusion [45]. Multiple trials have proven the efficacy of EVT and showed an improved clinical outcome in patients with proximal MCA or internal carotid artery (ICA) occlusion when EVT was performed within either 6 hours, 8 hours or 12 hours of symptom onset [35]. Five randomized controlled trials demonstrated improved clinical outcomes and rates of recanalization of the occluded arteries with the use of new-generation mechanical thrombectomy devices. These results led to the updating of the guideline in acute IS with large vessel occlusion in the anterior circulation [46]. A meta-analysis was performed by the HERMES (Highly Effective Reperfusion Evaluated in Multiple Endovascular Stroke) Trials collaborators involving 1287 patient's data. The results showed that the proportion of patients who achieved functional independence at 90 days (defined as modified Rankin Score of 0–2) in the intervention group was 46.0% compared to the control group with 26.5% [44]. Two clinical trials showed that the time window can be further extended to 24 hours post-symptom onset if there is a mismatch between the clinical deficit and the infarct size or a perfusion mismatch on imaging [48,49]. Some suggest that patients older than 80 years may benefit from EVT and should not be excluded only on the basis of age [47]. These findings emphasized the benefit of endovascular therapy and made it a standard of care for the treatment of acute IS in select patient populations.

Guidelines and scores help to select the appropriate endovascular approach. AHA/ASA guidelines published in 2019, suggest head NCCT or MRI at admission to exclude underlying hemorrhage and determine whether patients are candidates for acute therapy [50]. CTA or MRA of the head and neck is recommended in patients who meet the criteria for EVT without any delay in the administration of IVtPA [50]. These two imaging techniques allow rapid identification of large vessel occlusion, clinically significant vascular disease, presence of

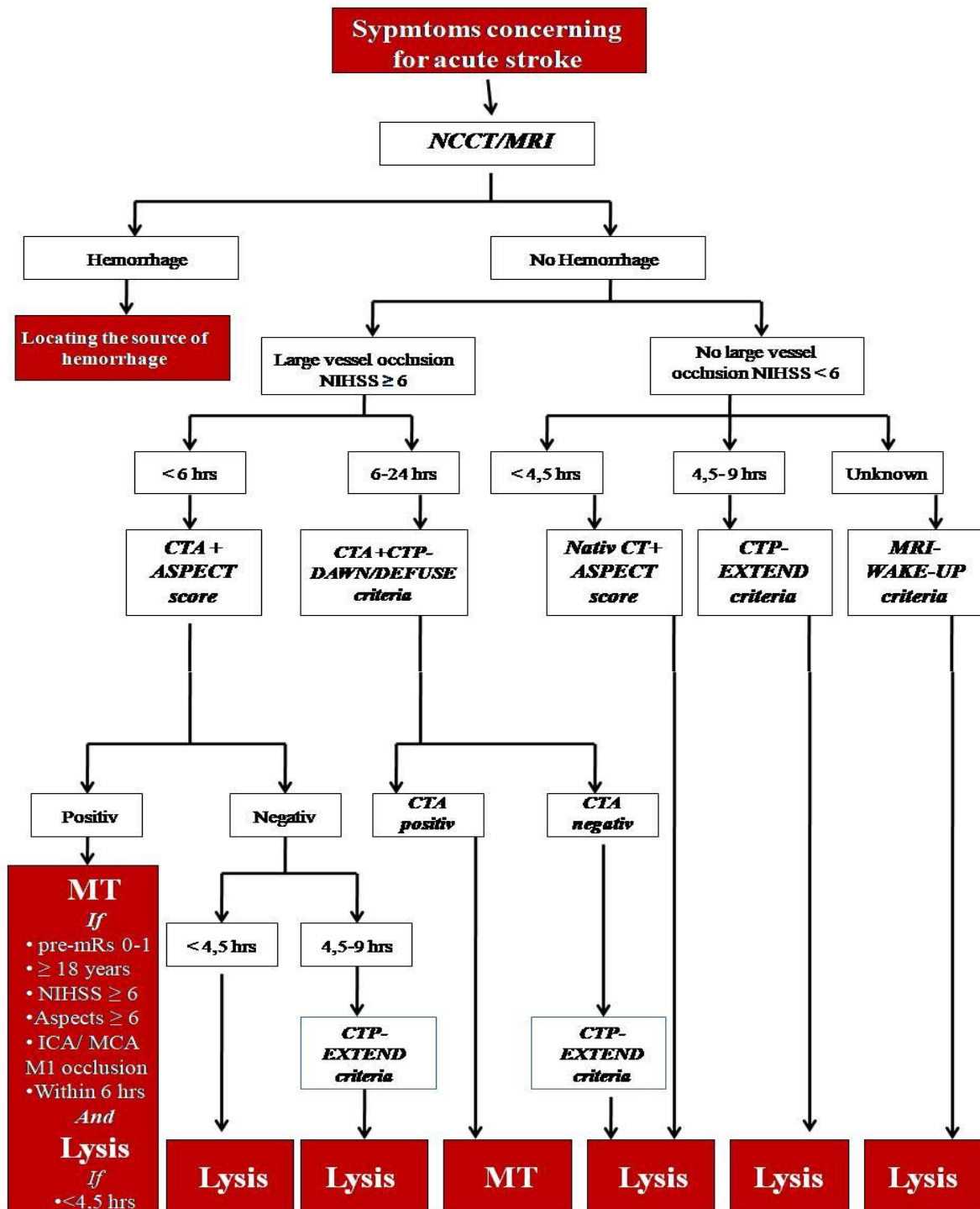
collaterals as well as the aortic arch, and great vessel anatomy. Moreover, ASPECTS aids in the rapid identification of patients who would benefit from EVT [51]. Four major randomized controlled clinical trials were published, which showed encouraging findings in relation to the extension of the time window in stroke treatment (**Table 5**). These trials are the following: DAWN (DWI or CTP Assessment with Clinical Mismatch in the Triage of Wake-Up and Late Presenting Strokes Undergoing Neurointervention with Trevo) [49], DEFUSE-3 (The Endovascular Therapy Following Imaging Evaluation for Ischemic Stroke) [48], EXTEND (Extending the Time for Thrombolysis in Emergency Neurological Deficits) [52] and WAKE-UP [53]. Patients with large vessel occlusion should undergo mechanical thrombectomy (MT) if they meet all the criteria and the onset of symptoms is between 0-6 hours (**Figure 3**) [50]. Within 4.5 hours after symptom onset, MT is recommended with IVT whenever indicated, to improve functional outcome. If the patient is eligible for both treatments, IVT with MT appears to be more beneficial than MT alone. Both treatments should be performed as soon as possible after hospital arrival, and should not delay each other. If occlusion is not proven by CTA, thrombolysis is the appropriate treatment. In patients with acute IS within 6 to 24 hours of the last known normal with large vessel occlusion in the anterior circulation, CTA, CTP, or DWI, MR-perfusion are recommended, if available. If patients meet the eligibility criteria of one of the trials (DAWN or DEFUSE), the patient is also selected for MT (**Figure 3**) [48,49]. In the case of no large vessel occlusion, after NCCT or CTP, or MRI, depending on the time window, IVT is required (**Figure 3**). During EVT, due to the lack of evidence, whether patient undergo general anesthesia or conscious sedation should be individualized based on clinical characteristics, tolerance to the procedure and patient risk factors [46-50].

Table 5. Criteria for stroke treatment.

DAWN	DEFUSE-3	EXTEND	WAKE-UP
6-24 hrs	6-16 hrs	4,5-9 hrs	unknown
NIHSS \geq 10	NIHSS \geq 6	NIHSS 4-26	NIHSS $<$ 25
Prestroke mRs $<$ 1	Baseline mRs $<$ 2		
$<$ 1/3 MCA occlusion	ASPECT $>$ 6	$<$ 1/3 MCA occlusion	$<$ 1/3 MCA, $<$ 1/2 PCA occlusion
<ul style="list-style-type: none"> • \geq 80 years • NIHSS \geq 10 • infarct volume $<$ 21ml 	<ul style="list-style-type: none"> • core $<$ 70 • ischemic tissue/infarct \geq 1,8 • penumbra \geq 15ml • DWI core $<$ 25ml 	<ul style="list-style-type: none"> • core $<$ 70 • ischemic tissue/infarct \geq 1,2 • penumbra \geq 10ml 	<ul style="list-style-type: none"> • FLAIR-DWI mismatch • pos DWI • no marked parenchymal FLAIR hyperintensity
<ul style="list-style-type: none"> • $<$ 80 years • NIHSS \geq 10 • infarct volume $<$ 31ml 			
<ul style="list-style-type: none"> • $<$ 80 years • NIHSS \geq 20 • infarct volume 31-51ml 			

Abbreviations: DAWN, diffusion-weighted imaging or CT perfusion Assessment with Clinical Mismatch in the Triage of Wake-Up and Late Presenting Strokes Undergoing Neurointervention with Trevo; DEFUSE-3, Endovascular Therapy Following Imaging Evaluation for Ischemic Stroke; EXTEND, Extending the Time for Thrombolysis in Emergency Neurological Deficits; hrs, hours; NIHSS, Neurological Institutes of Health Stroke Scale; mRs, modified Rankin scale; MCA, middle cerebral artery; PCA, posterior cerebral artery; DWI, diffusion-weighted imaging; FLAIR, fluid-attenuated inversion recovery; ASPECTS, Alberta Stroke Program Early CT Score. *Source:* reference [48,49,52,53]

Figure 3. Stroke treatment.



Abbreviations: NCCT, Non-contrast computed tomography; MRI, magnetic resonance imaging; NIHSS, Neurological Institutes of Health Stroke Scale; hrs, hours; CTA, CT angiography; ASPECT score, Alberta Stroke Program Early CT Score; CTP, CT perfusion; DAWN, diffusion-weighted imaging or CT perfusion Assessment with Clinical Mismatch in the Triage of Wake-Up and Late Presenting Strokes Undergoing Neurointervention with Trevo; DEFUSE-3, Endovascular Therapy Following Imaging Evaluation for Ischemic Stroke; EXTEND, Extending the Time for Thrombolysis in Emergency Neurological Deficits; MT, mechanical thrombectomy; NIHSS, Neurological Institutes of Health Stroke Scale; mRs, modified Rankin scale; MCA, middle cerebral artery; ICA, internal carotid artery. *Source:* reference [48-53]

Patients with acute IS who undergo EVT should be admitted to neurological critical care units. During hospitalization, monitoring vital signs and verification of hemodynamic and respiratory stability are crucial [10,35]. Patient management includes antihypertensive therapy, glucose management, oxygenation, antiplatelet therapy and antipyretics. The follow-up head CT can range from immediately post-procedure to 24 hours. Standardized protocols must be followed to avoid complications such as bleeding at the puncture site, malignant cerebral edema, stroke evolution, and vessel rethrombosis. Improvement in pre-clinical and clinical care contributes to successful stroke treatment, recovery, rehabilitation and prevention [9,36].

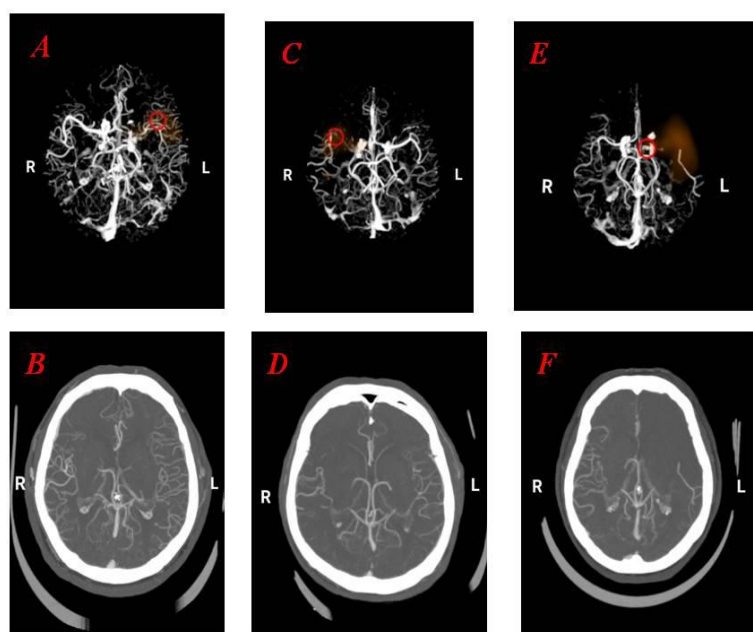
The multiple new innovations give more patients a lean on acute treatment, leading to better outcomes. Despite the changes, the constant decline in stroke mortality has slowed down, mainly because of the increasing number of patients with stroke risk factors [9,35]. In Western European countries, stroke mortality declined by 30-50% from 1975 to around 2005 mostly in Iceland, Italy, Austria, and Germany [3]. Stroke survivors sometimes require lifelong pharmaceutical treatment, rehabilitation and care. Managing sequelae such as swallowing difficulties, depression, and spasticity takes a long time [3].

2.5. Collateral system

Collateral circulation represents an alternative pre-existing vascular pathway that allows blood flow to reach the target tissue when the primary conduit is blocked [54]. The collateral circulation in the brain includes venous collaterals, the primary (short arterial segments in the Circle of Willis), and secondary (pial also called leptomeningeal) arterial collaterals. Primary arterial collaterals allow blood flow between the territories of the internal carotid arteries and the vertebrobasilar system or between the cerebral hemispheres. Secondary collaterals cross-connect a small number of distal arterioles of the cerebral arteries [54,55]. Multiple scores have been described for the evaluation of collaterals in acute IS. However, there is no gold standard for collateral assessment. The CTA collateral score also called the Tan score [56], the ASPECTS on collaterals, and the scores of Christoforidis et al. [57,58] and Miteff et al. [59] are generally used for collateral assessment (**Figure 4**). Previous stroke studies proved that a greater degree of collaterals at baseline has been associated with a smaller infarct size [60], an improved recanalization rate after endovascular treatment [61] and better clinical outcome [59]. A study involving 857 patients with acute IS highlights lower stroke severity,

lower frequency of cortical signs (except for hemineglect), higher ASPECT score, lower clot burden, statin use, and shorter delay from symptoms onset to baseline imaging were associated with better collaterals. On the other hand, smoking, aging, hypertension, and impaired renal function could reduce collateral extent by either causing endothelial dysfunction or decreasing the dilatatory capacity of the pial arteries [55]. Another study found that infarct volume and modified Rankin scale (mRS) scores at discharge are significantly lower for patients with better angiographically-assessed pial collaterals, while NIHSS score and collateral flow scores show an inverse relationship [58]. As collateral blood flow maintains tissue viability until definitive treatment like thrombectomy can be performed, thereby preventing penumbral tissue infarction and improving clinical outcomes [56]. A secondary analysis of CTA collateral status from the MR CLEAN randomized clinical trial showed a positive correlation between the collateral score and the degree of the benefit of EVT. Such studies suggest that collateral status may be a useful factor in the management of patients with acute IS [62]. Several studies have shown that the ASPECT score is an effective tool for assessing the collateral system by helping to estimate the core-penumbra ratio and thus the extent of the collateral network [55,63-65]. Based on the analysis of a large stroke register database, we can state that better collaterals are associated with lower core volumes and higher ASPECT scores, but not with higher penumbra volumes [49]. This suggests a major role of collaterals in early tissue loss.

Figure 4. CTA collateral status in ischemic stroke



Note:

A,B: Left ACM occlusion on CTA with good collaterals

- ASPECT: 10
- CTA collateral score: 3
- mCTA: 5

C,D: Right ACM occlusion on CTA with intermediate collaterals

- ASPECT: 7
- CTA collateral score: 2
- mCTA: 3

E,F: ICA and ACM occlusion on CTA with bad collaterals

- ASPECT: 6
- CTA collateral score: 1
- mCTA: 2

Abbreviations: ACM, arteria cerebri media; CTA, CT angiography; ASPECT, Alberta Stroke Program Early CT Score; mCTA, multiphase CT angiography, ICA, arteria carotis interna.

Source: Brainomx.com

2.6. Biomarkers in acute ischemic stroke

Matricellular proteins are non-structural extracellular matrix (ECM) proteins that are highly expressed at sites of injury or inflammation. They bind to growth factors and their activity is modulated by cytokines. They interact with other ECM proteins, while mediating cell-matrix interactions and tissue remodeling [66].

Periostin, also termed osteoblast-specific factor 2, is a 93.3 kDa-secreted matricellular protein, initially isolated from mouse osteoblast cell line [66,67]. The periostin molecule is composed of an N-terminal secretory signal peptide, followed by a cysteine-rich domain (EMI domain), four internal homologous repeats (FAS domains), and a C-terminal hydrophilic domain that is alternatively spliced [66,68]. Periostin is encoded by the POSTN gene in humans. Its expression can be induced by transforming growth factor beta (TGF- β) 1, 2, and 3, bone morphogenetic proteins (BMP) 2 and 4, VEGF (vascular endothelial growth factor), connective tissue growth factor 2, vitamin K, valsartan (an angiotensin II antagonist), and interleukin (IL) 3, 4, 6, and 13 [66,67]. Generally, periostin is expressed at a low level in human tissues but can be rapidly upregulated by various pathophysiological signals [67].

Periostin has been linked to allergy and inflammation as type 2 immunity cytokines interleukins IL-4, IL-5, and IL-13 are central to the pathogenesis of many allergic inflammatory diseases. As IL-4 and IL-13 bind to their receptors, they upregulate the expression of periostin directly or indirectly [68]. Therefore, high levels of periostin can be observed in bronchial asthma, chronic rhinosinusitis, atopic dermatitis, allergic conjunctivitis, ulcerative colitis and Crohn's disease, rheumatoid arthritis and ankylosing spondylitis, eosinophil-associated gastrointestinal disorders, including eosinophilic esophagitis [66,68].

Periostin has defined functions in osteology, tissue repair and oncology. Increased periostin level is observed in non-small cell lung carcinoma, breast cancer, ovarian cancer and thymoma [66,68,69].

Several eye diseases, such as diabetic retinopathy, age-related macular degeneration, glaucoma, pterygia and corneal dystrophy coincide with the induction of IL-4 and/or IL-13, which can alter the normal physiological interactions among fibroblasts, macrophages, and ECM protein in the eye and the level of periostin [70].

It has recently been proven that periostin is aberrantly expressed in various forms of chronic kidney disease, and its expression correlates with the degree of interstitial fibrosis and the

decline in renal function. While in polycystic kidney disease, periostin is secreted by the cyst epithelial cells and accumulates within the extracellular matrix adjacent to the cysts. It conduces to rapid cyst growth and contributes to structural changes in the kidneys, including interstitial fibrosis [71].

According to a recent review, periostin may play a potential role in the pathophysiology of cardiovascular disease [72]. Studies prove that periostin is secreted into ischemic tissue after acute myocardial infarction and has an essential role in the repair process [73,74]. Additionally, the upregulated expression of TGF- β and periostin in RAAS (renin–angiotensin–aldosterone) system is correlated with the degree of atrial fibrosis in patients with AF [75].

The neuroprotective and neurogenic effects of exogenous periostin have been demonstrated on both in vitro and in vivo IS models [76]. Periostin significantly enhances neural stem cell proliferation and differentiation after hypoxic-ischemic injury [77] and can enhance the neurite outgrowth activity of the surrounding neurons [78]. Upregulation of periostin was also reported in a cerebrovascular clinical setting and in neuronal injury due to head trauma. Dong et al. found that serum periostin concentration on admission was an independent predictor for 30-day mortality and overall survival after head trauma [79]. Ji et al. provided evidence that periostin concentrations of the sera from ICH patients were highly correlated with hematoma volume and baseline NIHSS scores, and serum periostin emerged as an independent predictor for 6-month unfavorable outcome after acute ICH [80]. Furthermore, serum periostin concentrations resembled hematoma volume and NIHSS score in terms of the predictive value assessed by AUCs (area under the ROC curve) for a 6-month unfavorable outcome [80]. Another study reported that in patients with aSAH, a higher admission serum level of periostin was correlated with unfavorable 90-day outcome, worse admission neurological status, larger hemorrhage volume and more frequent development of delayed cerebral ischemia [81]. He et al. have shown that increased serum periostin levels after IS might have been associated with NIHSS scores and more extensive stroke volume in patients with LAAS stroke [82].

Periostin is involved in several clinical studies, as it was identified in many pathological conditions. It has been proven that periostin can be used as a predictive and prognostic biomarker. However, more research is needed to fully elucidate the roles of periostin in the pathophysiology of diseases and to fully understand its utility for clinical decision-making.

III. Aneurysmal subarachnoid hemorrhage (aSAH)

3.1. Definition and epidemiology of aSAH

The hemorrhagic subtype of stroke, although less common than IS and TIA, still has a significant public health impact due to higher mortality and morbidity, and represents an exceptionally high disease-specific burden [2,30]. The Stroke Council of AHA/ASA defined it as „bleeding into the subarachnoid space, between the arachnoid membrane and the pia mater of the brain or spinal cord” [2].

The incidence of aneurysmal SAH (aSAH) varies widely depending on geographic location, age, and sex [30]. The overall incidence of SAH is estimated to be 9/100,000 people/year but changes significantly by region, with doubled rates in Japan and Finland, and far lower rates in South and Central America [30,83,84]. The median age of onset of the first SAH is 50–60 years. The gender distribution varied with age. At young ages, the occurrence was higher in men, while the predominance of women is only apparent in the fifth decade [83,84]. The incidence of SAH has probably decreased slightly over the past 45 years, although to a lesser extent than that of stroke in general [83].

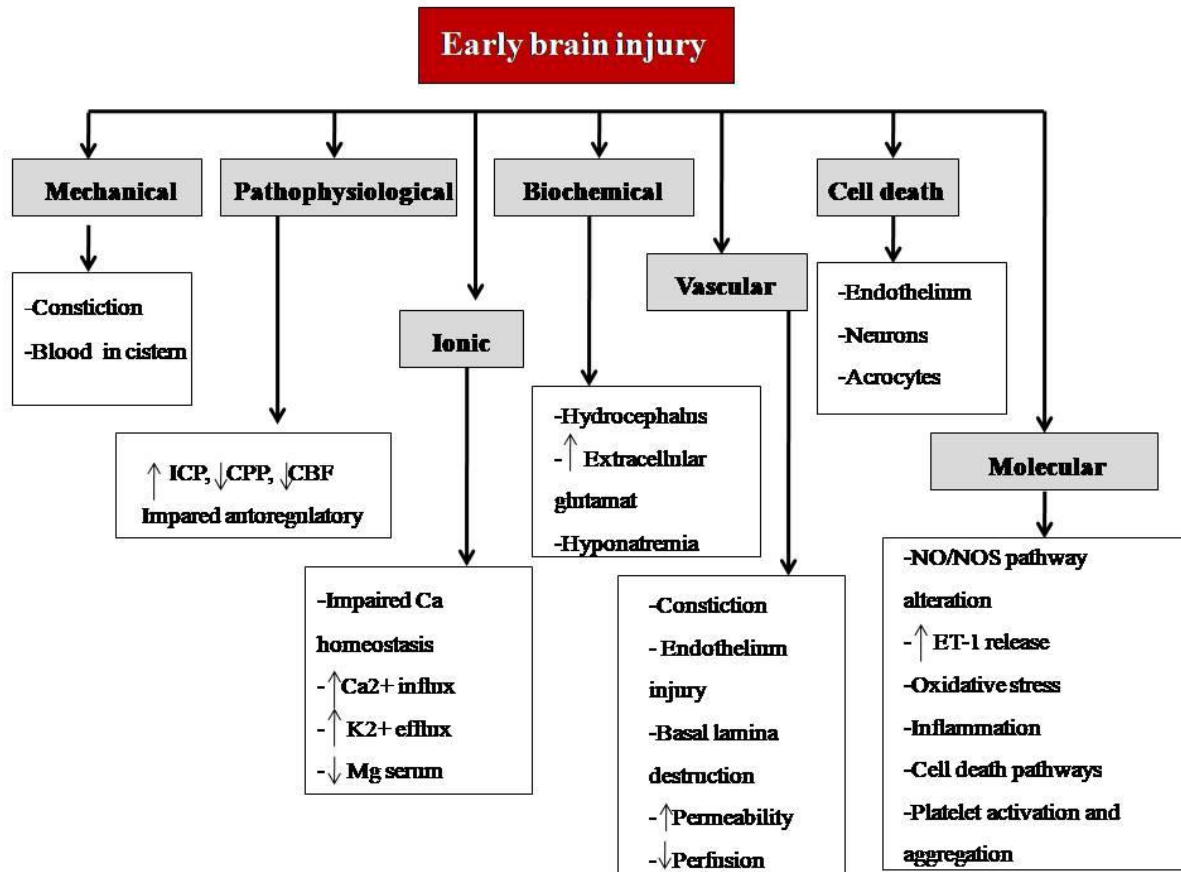
3.2. Etiology and pathogenesis of aSAH

SAH can be divided into traumatic and non-traumatic subgroups. Non-traumatic SAHs are mainly caused by ruptured saccular aneurysms in 75%-80% of cases. Other causes include arteriovenous malformations (20%), intracranial artery dissections, vasculitis, cerebral venous sinus thrombosis, tumors, mycotic aneurysms, bleeding diatheses, substance abuse, reversible cerebral vasoconstriction syndrome and cerebral amyloid angiopathy [2,85].

The pathogenesis of aneurysm formation is multifactorial. Oxidative stress and inflammation may play an important role in cerebral aneurysm formation, progression and rupture [86,87]. Endothelial dysfunction is an early step in aneurysm formation followed by vascular smooth muscle cell phenotypic modulation, extracellular matrix remodeling and cell death [86]. When an aneurysm ruptures, blood pours into the subarachnoid space leading to a sudden increase in intracranial pressure (ICP), jeopardizing cerebral perfusion pressure (CPP), and leading to global ischemia and early brain injury (EBI). EBI is the product of pathological mechanisms triggered in the brain during the first 72 hours after SAH and starts just after the aneurysmal rupture [88,89]. It is characterized by microcirculation constriction, microthrombosis,

disruption of the BBB, cytotoxic and vasogenic cerebral edema, and neuronal and endothelial cell death (Figure 5) [88,90].

Figure 5. Major changes during the development of EBI after SAH



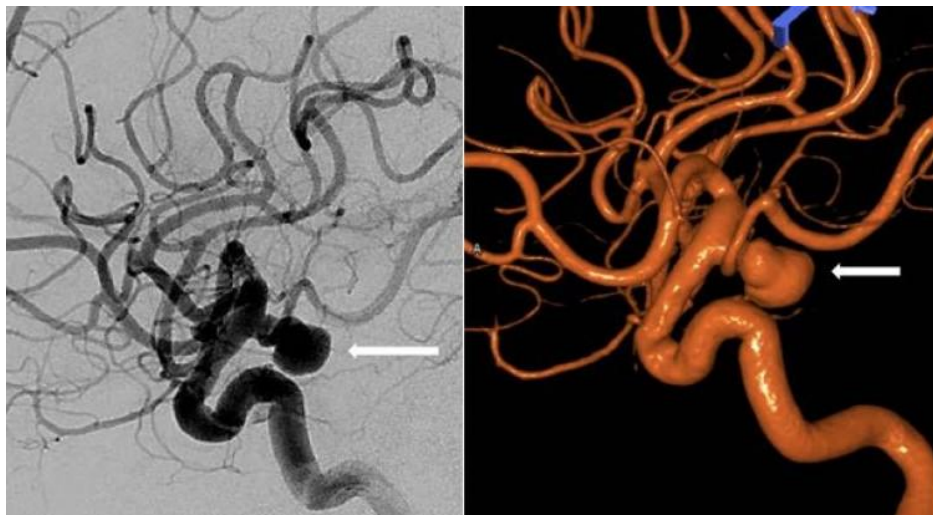
Abbreviations: SAH, subarachnoid hemorrhage; EBI, early brain injury; ICP, intracranial pressure, CPP, cerebral perfusion pressure; CBF, cerebral blood flow, Ca, calcium ion; K, potassium ion; Mg, magnesium ion; ET-1, endothelin-1. *Source:* reference [88-90]

The transient global ischemia triggers sympathetic nervous system activation, leading to systemic complications including neurogenic pulmonary edema, cardiac dysfunction and arrhythmia. Within days after SAH, systemic inflammation may develop besides homeostasis disorders like CSW (cerebral salt-wasting syndrome), SIADH syndrome (syndrome of inappropriate antidiuretic hormone release), or diabetes insipidus with polyuria. The blood lysis in the subarachnoid space can cause an obstruction in the cerebrospinal fluid (CSF) flow

resulting in hydrocephalus. Furthermore, the blood breakdowns lead to the irritation of the meninges generating meningismus [90].

Intracranial aneurysms are present in approximately 2% to 5% of the population and typically can be found at the bifurcations of the major vessels around the circle of Willis [85]. Common sites of intracranial aneurysms include the ICA, the anterior communicating artery (ACom), the MCA, the posterior communicating artery (PCom), the posterior cerebral artery (PCA), the basilar artery and the vertebral artery (**Figure 6.**) [85,91].

Figure 6. Lateral view of ruptured left PCom artery aneurysm (arrow) on a cerebral angiogram



Source: Baylor College of Medicine: Brain Aneurysms

Several risk factors may play an important role in the formation, growth and rupture of aneurysms. Familial preponderance, hypertension, smoking, alcohol abuse, inflammation, connective tissue diseases such as Ehlers-Danlos syndrome, autosomal dominant polycystic kidney disease may contribute, while hormone replacement therapy among women, hypercholesterolemia, and diabetes mellitus may reduce this risk [84,86,87].

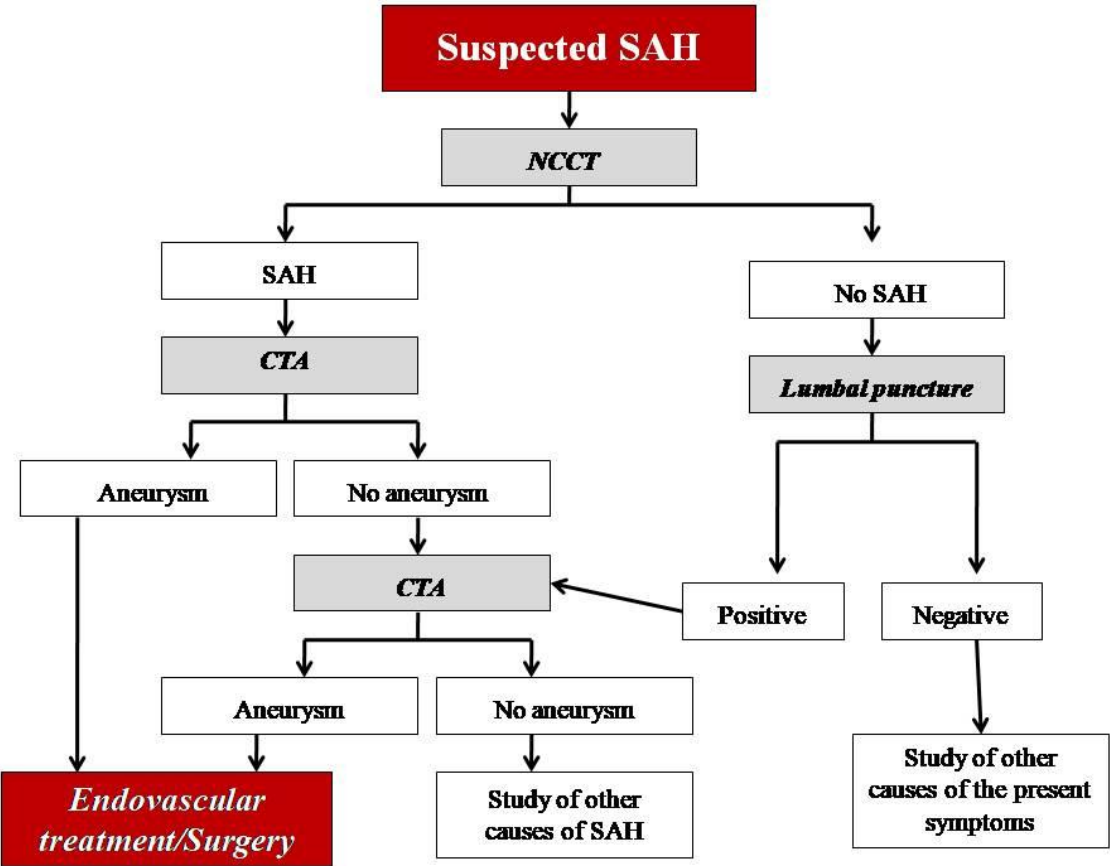
3.3. Diagnostic approach and treatment of aSAH

The classic presentation of patients with aSAH is a sudden-onset, severe headache, which intensity peaks in an hour and is usually described as the worst headache ever felt [92,93]. Around 10%-40% of patients report a history of a sudden and severe headache called sentinel headache, occurring days to weeks prior to aneurysm rupture. Behind the sentinel episode, there is either minor hemorrhage or physical changes within the aneurysm wall (acute dissection, thrombosis or expansion). This episode increases the likelihood of death or disability four-fold [93]. Commonly associated symptoms of SAH include loss of consciousness (53%), nausea, vomiting (77%), meningism (35%), ocular bleeding and diverse focal neurological deficits (10%), including ophthalmoplegia, hemiparesis, aphasia and neglect [91,92,93]. Unruptured intracranial aneurysms are being detected increasingly due to improved quality and higher frequency of cranial imaging in clinical practice. Most remain asymptomatic, but in some cases, they can cause neurologic symptoms [94].

The diagnosis of SAH is based not only on symptoms but on imaging techniques (**Figure 7**). Modern CT technology provides a sensitive method to detect subarachnoid blood in the early phase after SAH. Therefore, if SAH is clinically suspected, a cranial CT should be performed to confirm the diagnosis. Head NCCT is the primary means of the diagnosis of SAH [2,91]. The sensitivity of modern head CT for detecting SAH is nearly 100% in the first six hours after SAH, then decreases to 93% in 24 hours, then to 60% on the fifth day [92]. In case of non-diagnostic head CT and/or MRI but SAH is suspected anamnestically or clinically, a lumbar puncture has to be performed 6-12 hours after the onset of symptoms. Waterclear CSF excludes SAH in the last 2-3 weeks [84]. On the other hand, elevated opening pressure during puncture and elevated red blood cell count (RBC) in CSF are classic signs of SAH. The differentiation between artificial bleeding and SAH can be made by sedimentation. In case of artificial bleeding RBCs are going to sediment [91]. Although it is still recommended by current guidelines, this approach is now a matter of debate. Some claim that since the incidence of SAH is low and it can be difficult to distinguish between SAH and puncture-related trauma therefore lumbar puncture is no longer of great value [93]. Cerebral panangiography continues to be the gold standard for the detection, demonstration and localization of the source of hemorrhage. CTA has been reported to have a sensitivity and specificity of 0.77-0.97 and 0.87-1.00, respectively for the detection of intracranial aneurysms [84]. Digital Subtraction Angiography (DSA) is a preferred diagnostic modality, with a reported sensitivity of 99%. Both 2D-DSA and 3D-DSA enable the detection of vascular

malformations and endovascular treatment initiation at the same time. DSA is performed frequently in patients with negative CTA findings. Studies demonstrated that DSA successfully identified vascular pathology in 4%–14% of patients with negative CTA findings [95].

Figure 7. Diagnostic approach and treatment of aSAH.



Abbreviations: NCCT, non-contrast CT; SAH, subarachnoid hemorrhage; CTA, CT angiography. *Source:* reference [84,91-93,95]

After diagnostic steps and stabilization of vital parameters, patients with SAH should be transported to a high-volume center with neurocritical care unit and a background of expert neurosurgical, neurointerventional and neurointensive care [84]. During continuous observation, monitoring the level of consciousness (Glasgow Coma Scale, GCS), focal deficits and temperature frequently at least in the first 7 days after SAH, is important. Fluid balance, blood pressure and ECG (electrocardiogram) should be monitored continuously, as well as ICP if necessary. Patient management includes headache, hyperglycemia, fever, high or low blood pressure, thromboprophylaxis and antiepileptic treatment (**Table 6**) [84,96].

Table 6. Recommendations for the care of patients with aneurysmal SAH

Monitoring	<ul style="list-style-type: none"> • Intensive continuous observation at least until occlusion of the aneurysm • Continuous ECG monitoring • Start with GCS, focal deficits, blood pressure and temperature at least every hour
Blood pressure	<ul style="list-style-type: none"> • Stop antihypertensive medication that the patient was using – • Do not treat hypertension unless it is extreme; limits for extreme blood pressures should be set on an individual basis, taking into account age of the patient, pre-SAH blood pressures and cardiac history; systolic blood pressure should be kept below 180 mm Hg, only until coiling or clipping of ruptured aneurysm, to reduce risk for rebleeding
Fluids and electrolytes	<ul style="list-style-type: none"> • Intravenous line mandatory • Insert an indwelling urinary catheter • Start with 3 liter/day (isotonic saline, 0.9%), and adjust infusion for oral intake • Aim for normovolaemia also in case of hyponatremia and compensate for fever • Monitor electrolytes, glucose and white blood cell count at least every other day
Pain	<ul style="list-style-type: none"> • Start with paracetamol (acetaminophen) 500 mg every 3–4 h; avoid aspirin before aneurysm occlusion • For severe pain, use codeine, tramadol (suppository or i.v.) or, as a last resort, piritramide (i.m. or i.v.)
Prevention of deep vein thrombosis and pulmonary embolism	<ul style="list-style-type: none"> • Compression stockings and intermittent compression by pneumatic devices in high-risk patients

Abbreviations: ECG, electrocardiogram; SAH, subarachnoid hemorrhage; GCS, Glasgow Coma Scale. *Source:* reference [84,96]

In the early days of cerebral aneurysm treatment, surgery was the only approach. Starting with proximal ligation (trapping) of vessels, such as the carotid artery, followed by wrapping the aneurysm with muscle tissue to reinforce the aneurysm wall to prevent rebleeding. Nowadays, surgical treatment is based on clip occlusion, in which a clip is placed across the neck of the aneurysm. The endovascular coiling system was introduced later [84]. During this procedure, a catheter is inserted into an artery, which is routinely the femoral artery or in selected cases the radial artery. Platinum coils are inserted into the aneurysm obliterating the aneurysmal sac. To compare both therapeutic approaches, clipping and coiling, a randomized controlled trial, the ISAT (International Subarachnoid Aneurysm Trial) was made [97]. Patients with ruptured intracranial aneurysms and low-grade SAH were randomly assigned to neurosurgical clipping or endovascular coiling. According to the results, endovascular coiling is preferred over clipping, considering a higher rate of good functional outcome even after 7 years of follow-up. However, the occurrence of rebleeding is low, but is more common after endovascular coiling than after surgical clipping. New techniques including stent-assisted coiling, balloon-assisted coiling, flow diverters and disruptors, as well as new embolic material including liquids offer promising results in the treatment of aneurysms. Decisions regarding the timing and choice of therapy for patients with ruptured intracranial aneurysms are ideally made by a team of experienced specialists. Before the procedure, the neurologic grade and clinical status of the patient, the availability of expertise in surgical and endovascular techniques, as well as the anatomic characteristics of the aneurysm should be taken into consideration (**Figure 7**) [84,97].

3.4. Classification of aSAH

Grading systems have been developed for the initial assessment of SAH patients. A widely used scale is Hunt and Hess, which is composed of the level of consciousness (graded into drowsiness, stupor and deep coma), headache (minimal, moderate and severe), neck stiffness (slight nuchal rigidity vs. nuchal rigidity) and focal neurological deficits (mild, moderate and severe hemiparesis) [98]. However, due to the unclear definition of neurological status, this scale is not completely reliable. The World Federation of Neurological Surgeons (WFNS) Committee proposed a grading scale of five levels, essentially based on GCS [99]. The cut-off points are based on consensus and not on formal analysis. The PAASH (Prognosis on Admission of Aneurysmal Subarachnoid Haemorrhage) grading scale is also based on GCS, but the cut-off points between the categories were selected by calculating at which point 2

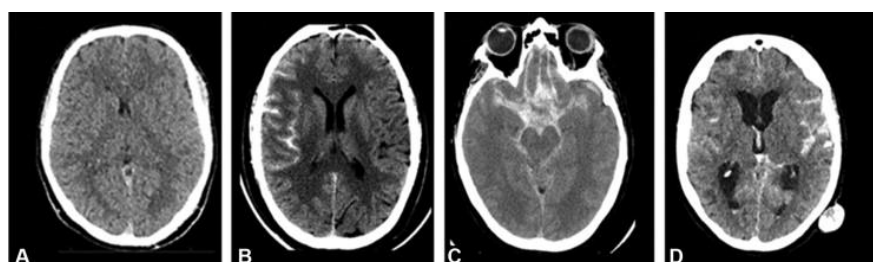
consecutive categories corresponded to a statistically significant different outcome at 6 months [100]. This scale has good internal and external validity regarding clinical outcome. These grading systems, listed above, are shown in **Table 7**. The modified Fisher score system (mFisher) classifies the severity based on native CT scan. The localization, the bleeding volume and the ventricular involvement are taken into account (**Figure 8**) [101].

Table 7. Grading systems in SAH

Grade	Hunt and Hess scale	WFNS scale	PAAHS scale
I.	Asymptomatic, or minimal headache and slight nuchal rigidity	GCS 15	GCS 15
II.	Moderate to severe headache, nuchal rigidity, no neurological deficit other than cranial nerve palsy	GCS 13-14 without focal deficit	GCS 11-14
III.	Drowsiness, confusion or mild focal deficit	GCS 13-14 with focal deficit	GCS 8-10
IV.	Stupor, moderate to severe hemiparesis, possibly early decerebrate rigidity, and vegetative disturbances	GCS 7-12	GCS 4-7
V.	Deep coma, decerebrate rigidity, moribund appearance	GCS 3-5	GCS 3

Abbreviations: SAH, subarachnoid hemorrhage; WFNS, World Federation of Neurological Surgeons; GCS, Glasgow Coma scale; PAAHS, Prognosis on Admission of Aneurysmal Subarachnoid Haemorrhage *Source:* reference [98-101]

Figure 8. modified Fisher score in SAH



Source: M. Edjlali, C. Rodriguez-Régent, J. Hodel et al. Subarachnoid hemorrhage in ten questions. *Diagn. and Interventional Imaging.* 2015, 96, 7–8, 657-666, Figure 2

Note:

A. Grade 0: no SAH, no ventricular hemorrhage.

B. Grade 1: minimal SAH, no ventricular hemorrhage in the 2 lateral ventricles.

C. Grade 3: large SAH. No ventricular hemorrhage in the two lateral ventricles.

D. Grade 4: large SAH ventricular hemorrhage in both lateral ventricles.

3.5. Complications after aSAH and outcome

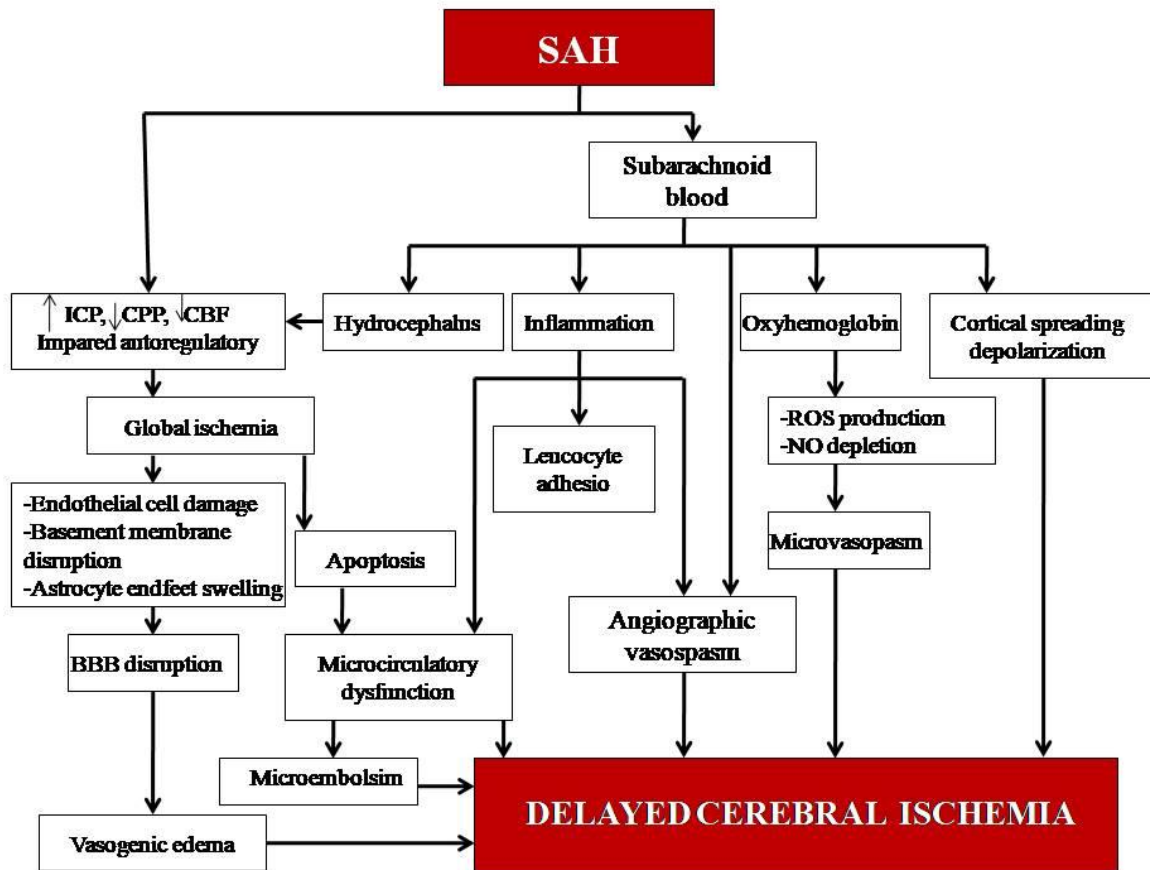
SAH is a relevant health problem with a mortality rate of about 60% in 6 months [84]. The prognosis for patients with aSAH is influenced by multiple factors. The neurological condition, particularly the level of consciousness, age, history of hypertension, heavy alcohol consumption, cigarette smoking, aneurysm site and size, and the amount of extravasated blood seen on CT scans are related to the outcome after SAH [84]. Medical complications such as rebleeding, hydrocephalus, cerebral vasospasm (CV), increased ICP, seizures and delayed cerebral ischemia (DCI) contribute significantly to the long-term functional outcome of the disease [84,96,102].

Rebleeding is a devastating consequence of aSAH, accounting for significant morbidity and mortality that occurs in 8% to 23% of patients [9]. The incidence of rebleeding is 90% in the first 6 hours after the initial hemorrhage and 7%-22% in the first three days. Ultra-early rebleeding (in the first 24 hours) occurs with an incidence of 15% and a mortality rate of 70% [92]. Patients with low-grade SAH, large aneurysm, sentinel bleeding, longer time to surgery, and those undergoing catheter angiography have a higher risk of rebleeding which manifests as a worsening or acute headache or change in mental status [9,92].

Other than rebleeding, CV is the leading cause of morbidity and mortality following aSAH [102]. The exact cause of vessel narrowing is unclear, but oxyhemoglobin release, ROS production, inflammation and decreased NO levels are involved [103]. Vasospasm can be determined on a clinical, radiographic, Doppler or angiographic basis. Angiographic vasospasm was defined as moderate-to-severe arterial narrowing on DSA not attributable to atherosclerosis, catheter-induced spasms, or vessel hypoplasia, as determined by a neuroradiologist [104]. It may occur in up to 70% of patients, typically between 5 and 14 days after the onset of SAH [102]. The relationship between angiographic spasm and clinical symptoms can be inconsistent [104]. Symptomatic vasospasm occurs in 20%-40% of patients with SAH and is typically associated with clinical deterioration. This is a subjective diagnosis and can be limited in poor-grade cases [104]. TCD vasospasm was defined as a mean flow velocity in any vessel > 120 cm/sec [104]. It is commonly used, although its positive and negative predictive values for angiographic spasm of the MCA are adequate, its sensitivity to detect angiographic vasospasm of the anterior cerebral artery and distal cerebral vasculature is poor. Furthermore, the relationship between TCD abnormalities and clinical worsening is unreliable [104]. The prevention and treatment of CV is difficult, as it appears to be a multifactorial process [102].

The prognosis for patients with aSAH is heavily influenced by the development of DCI which occurs in up to 30% of patients after SAH, usually within the first two weeks after the symptom onset [96,102]. It is defined as the occurrence of any focal neurological impairment (hemiparesis, apraxia, aphasia, hemianopia or neglect) or decrease of at least two points on the GCS, that lasts at least one hour, was not apparent immediately after aneurysm occlusion and cannot be attributed to other causes (hydrocephalus, infection, electrolyte disturbance or seizure) [105]. Also defined as symptomatic vasospasm and/or infarction attributable to vasospasm [104]. Several factors influence the development of DCI, such as vascular dysfunction, the elevation of ICP, cerebral edema, microthrombosis, autoregulatory failure, neuroinflammation, disruption of the BBB, cell death, oxidative stress, and cortical spreading depolarization (**Figure 9**) [103,106]. This series of events is part of EBI (**Figure 5**) [88,89]. DCI occurs mostly due to vasospasm, however, vasospasm is not considered the only leading factor of DCI as impaired cerebral autoregulation also plays a role [107]. According to studies, about 20% of SAH patients develop DCI without evidence of CV and only 30% of patients with CV actually suffer from DCI [108]. The clinical diagnosis of DCI in conscious or sedated patients is particularly difficult as it is almost impossible to assess consciousness in a sedated patient [109]. A recent study found that Hunt and Hess scale has the optimal sensitivity and specificity to distinguish between patients who developed DCI and clinically stable patients. Additionally, Fisher scale is a sensitive and specific predictor of DCI, respectively the presence and site of an aneurysm may raise the risk of DCI [107]. TCD and angiography are commonly used to diagnose vasospasm [104,110]. In a very recent study, an early mild, TCD-based vasospasm severity threshold had a high negative predictive value for DCI [111]. To this day adequate and effective therapy for DCI has not been resolved. Some drugs may reduce arterial spasm but not DCI, while others may reduce DCI and poor outcomes, but have no effect on vasospasm [112]. The only evidence-based strategy for the prevention and treatment of DCI is nimodipine, which can prevent and reverse spasms of small vessels but has no effect on vasospasm of larger vessels [103,112]. Endovascular strategies have been used for radiographic vasospasm, including balloon angioplasty and placement of intracranial stents [112]. The risk of DCI is mainly correlated with the amount of intraventricular blood on the initial neuroimaging. The risk is also higher in patients with poor neurological status after resuscitation [96].

Figure 7. DCI after SAH



Abbreviations: SAH, subarachnoid hemorrhage; DCI, delayed cerebral ischemia; ICP, intracranial pressure, CPP, cerebral perfusion pressure; CBF, cerebral blood flow. *Source:* reference [103,106]

Hydrocephalus can occur in acute and chronic stages, in up to 50% of patients after SAH. It is thought to be caused by obstruction of CSF flow by blood products, adhesions or by a reduction of CSF absorption at the arachnoid granulations. Progressive deterioration in the level of consciousness and ocular signs of elevated ICP (blurred vision, double vision, visual field loss) may raise the concern of hydrocephalus. In this case, an early head CT scan should be performed. Management of elevated ICP includes immediate lumbar puncture, CSF diversion with an external ventricular drain or lumbar drainage, osmotic therapy and diuresis, hemicraniectomy or long-term management with ventriculoperitoneal shunt insertion [92,113].

High ICP is also a frequent complication. Brain edema, intraparenchymal hemorrhage, hydrocephalus, or rebleeding can lead to elevated intracranial pressure. As a treatment,

barbiturate sedation, analgesia, hyperosmolar therapy, cerebrospinal fluid drainage and in refractory cases, decompressive craniectomy or hypothermia are recommended [92,96].

Acute epileptic seizures hyponatremia, cardiac and pulmonary complications, fever and thrombosis can occur after aSAH. Preventive and adequate therapy for these conditions is crucial in terms of outcome and mortality [96].

3.6. Biomarkers in aSAH

Several markers have been studied for the prediction of functional outcome in the context of aSAH. The high variability in the temporal patterns of inflammation-related proteins indicates the complexity of the inflammatory response following aSAH.

Fractalkine/CX3C chemokine ligand 1 (CX3CL1) is a chemokine expressed by neurons in the CNS and also is involved in the anti-cancer function of lymphocytes [114,115]. CX3CL1 signals through its unique receptor called CX3CR1. Fractalkine plays an important role in the cancer process as stimulates cancer cell proliferation and participates in angiogenesis, apoptosis resistance, cancer cell migration and recruitment of cells to a cancer niche. Its increased level in tumors improve the prognosis for cancer patients but in some type of cancers, it is associated with a poorer prognosis [114]. CX3CL1 is involved in the adhesion and recruitment of immune system cells. Its expression is elevated in CD4⁺ and CD8⁺ T cells in exposure to IL-2, and in blood vessels by proinflammatory cytokines like interferon- γ (IFN- γ), tumor necrosis factor- α (TNF- α) and IL-1 β [114]. CX3CL1 shows high expression in neurons, microglia, astrocytes and vascular endothelial cells. CX3CL1 was successfully analyzed in human CSF after aSAH with an increasing trend in concentration with a late peak on day 10 [116]. CX3CL1 can exist either as a static membrane-bound glycoprotein that mediates cell adhesion or as a soluble isoform with chemotactic features. The properties of both isoforms are mediated by a specific G-protein coupled, seven-transmembrane domain receptor (CX3CR1). The reciprocal interaction between the microglial chemokine receptor and the neuronal ligand CX3CL1 allows effective communication between neurons and microglial cells and thus plays a key role in coordinating many aspects of brain function [115]. Fractalkin acts as a regulator of microglia activation in response to brain injury or inflammation and may have a dual function of being neuroprotective and anti-inflammatory in a variety of hypoxic and excitotoxic in vitro and in vivo models, while proinflammatory and contributing to neuronal damage in others [117,118]. A study by Zanier ER et al. suggested

that CX3CL1: CX3CR1 signaling exacerbates the toxic cascades at early time-points whereas it is needed for long-term recovery in traumatic brain injury (TBI) [119]. CX3CL1 expression is upregulated in intact neurons within the penumbra while both CX3CL1 and CX3CR1 expression are upregulated in infarcted brains in experimental stroke models in rats [120]. Another study shows that exogenous CX3CL1 reduced ischemia-induced cerebral infarct size and neurological deficits in rats and these microglia-mediated CX3CL1-induced neuroprotective effects were long-lasting, being observed up to 50 days after pMCAO (permanent MCA occlusion) in rats [121]. High expression of CX3CL1 is also found in the kidneys, lungs and bones.

Monocyte chemoattractant protein (MCP) -1, -2 and -3 form a subfamily of the chemotactic cytokines or β -chemokines [122,123]. MCPs are produced by a variety of cells on stimulation with cytokines such as IL-1, TNF- α , IFN- γ and also bacterial and viral products or mitogens [124]. MCP-1, -2 and -3 have been found to induce directional migration of various cell types, including neutrophils, monocytes, T lymphocytes, basophils, eosinophils, or fibroblasts [123,125]. MCP-1 levels are enhanced during inflammation and infection, which are characterized by leukocyte infiltration. MCP-1 binds to its receptor and thus activates the signaling pathways which regulate the migration of cells. By influencing the activity of the NF- κ B pathway, Akt signaling pathway, ERK pathway and several others, affect the development and progression of diseases [122,124]. MCP-1 plays a crucial role in the pathogenesis of numerous disease conditions either directly or indirectly like novel corona virus, cancers, neuroinflammatory diseases, brain pathologies, bone and joint disorders, respiratory infections, endothelial dysfunction and cardiovascular diseases [122,123]. It is known that serum MCP-1 concentrations correlated with vasospasm in patients with SAH, whereas the serum MCP-1 levels did not correlate with DCI. Concentrations of MCP-1 in the CSF proved to be significantly higher in patients with angiographically demonstrated vasospasm [126].

IFN- γ -inducible protein 10 also called IP-10 is a chemokine secreted by various cell types such as neutrophils, endothelial cells, keratinocytes, fibroblasts, dendritic cells, astrocytes and hepatocytes and involved in trafficking immune cells to inflammatory sites [127,128]. IP-10 has a transient burst of accumulation in the CNS during experimental autoimmune encephalitis (EAE), highlighting that astrocyte-derived IP-10 is a potential chemoattractant for inflammatory cells during EAE [129]. IP-10 and MCP-1 lead to the accumulation of activated T cells and monocytes in the CSF compartment in the early stage of viral meningitis

[130]. CSF levels of iron and heme are associated with an inflammatory response (plasma levels of macrophage inflammatory protein (MIP)-1b and IP-10) within the human brain after a hemorrhagic event, suggesting a causal relationship [131].

IL-4 is regulate among others many aspects of allergic inflammation and plays an important role in regulating the responses of lymphocytes, myeloid cells, and non-hematopoietic cells [132]. Al-Tamimi et al. observed significantly higher levels of IL-4 in CSF in patients with delayed ischemic neurological deficits, with peak-levels on Day 5 [133]. Early intracerebral injection of IL-4 potentially promotes neuro-functional recovery, probably by enhancing the activation of M2 (protective) phenotype microglia and inhibiting the M1 (injurious/toxic) phenotype activation in patients with intracerebral hemorrhage [134].

IL-1b is a potent pro-inflammatory cytokine that has an essential role in responses to infection and injury but also exacerbates damage during chronic disease and acute tissue injury. It is produced and secreted by a variety of cell types [135]. Microglial IL-1b levels increase after ICH, as microglial activation is thought to be one of the characteristics of brain inflammation [136]. More importantly, a recent study by Asare et al. showed that a decrease in IL-1b increases the risk of stroke, and a mild increase in IL-1b is protective against stroke [137].

Fibroblast growth factor (FGF)-2 suppresses autophagy levels and therefore may reduce neuronal apoptosis following SAH, providing a neuroprotective role, at least partially, by activating the PI3K/Akt pathway [141,13]. Recently, triggering by receptor expressed on myeloid cell 2 (TREM2) was identified as a regulator of both IP-10 and FGF-2 among others. TREM2 is involved in the activation of IP-10, MIP-1a, and IL-8, while it inhibits FGF-2, and thus it plays a role in enhancing the microglial function, suggesting that therapeutic strategies that seek to activate TREM2 may not only enhance phagocytosis but also inhibit apoptosis [140].

C-C motif chemokine 11 (CCL11), also called eotaxin-1 known for its role in chemoattracting eosinophils, promoting degranulation, and releasing eosinophil cationic proteins. It operates through the receptor CCR3, which acts on Th2 lymphocytes, basophils, mast cells, and eosinophils [141,142]. Eotaxin plays an important role in a variety of pathological conditions including allergy, coronary heart disease, inflammatory bowel disease and the formation of atherosclerosis. It is overexpressed in endothelium and vascular smooth muscle cells in human atheroma, as it promotes endothelial cell migration in vitro, as well as angiogenesis and endothelial cell sprouting from the artery [142]. An elevated level of CCL11 was found in

several animal models of neuroinflammation, including traumatic brain injury and Alzheimer's disease and linked to decreased neurogenesis in mice [143]. A high concentration of eotaxin was found in the lumen of human cerebral aneurysms compared to femoral aneurysms [144]. Additionally, a study discovered that low CCL11 was significantly predictive of worse stroke severity (NIHSS) at discharge from the hospital. Furthermore, after controlling for initial stroke severity, low CCL11 levels also predicted negative functional outcomes at both 3 and 12 months after stroke. The biology behind the association between low acute eotaxin levels and long-term functional outcomes remains unknown [143].

Decreased level of fms-like tyrosine kinase-3 ligand (FLT-3L) was observed in severe stroke [145], while MIP-1b plays an unknown role in the prognosis of stroke [146].

The exact role of the inflammation-related proteins is not easy to establish, especially considering the fact that many of these substances may play both a detrimental and a beneficial role in the course of diseases. Still seems to be useful biomarkers.

IV. Aims

4.1. Ischemic stroke

We aimed to measure serum periostin levels in the hyperacute phase of ischemic stroke in order to reveal its predictive power in identifying patients with poor collateral network.

- (1) How does serum periostin level correlate with 90-day outcome?
- (2) How ASPECT score and NIHSS correlate with systemic concentration of periostin?
- (3) How associate the periostin level with ASPECT score < 6 calculated on admission CT scan?

4.2. Aneurysmal subarachnoid hemorrhage

As a single biomarker study is not suitable for the complex characterization of the mechanisms underlying DCI, we aimed to create a biomarker profile to investigate the relationship of biomarkers to DCI and the functional outcome and their relationship to each other.

- (1) Are MCP-3 and CX3CL1 levels associating with the occurrence of DCI?
- (2) Are IP-10, MCP-3, and MIP-1b levels correlating with Day 30 adverse outcome?
- (3) Is the serum level of IL-4 significantly higher in TCD-positive patients than in TCD-negative ones?

V. Methods

5.1. Ischemic stroke

5.1.1. Study design

This was a prospective observational study from a tertiary stroke treatment center in Pecs, Hungary. During the period between July 2019 and April 2021, a total of 122 patients with acute ischemic stroke within the first 6 hours after onset were prospectively enrolled. Acute IS was diagnosed according to WHO criteria [1]. As controls, we recruited fifteen age- and sex-matched healthy individuals. The following inclusion criteria were applied: (i) first-ever ischemic stroke, (ii) admission within 6 h after the index event. Exclusion criteria were as follows: (i) <18 years; (ii) previous ischemic or hemorrhagic stroke; (iii) premorbid modified Rankin score (mRS) > 1; (iv) active malignant or autoimmune disease; (v) immunosuppressive therapy; (vi) acute or chronic infection at study enrollment; (vii) severe hepatic or renal insufficiency; (viii) and pregnancy. All procedures were performed in accordance with ethical guidelines of the 1975 Declaration of Helsinki. The study was approved by the Hungarian Medical Research Council. Written informed consent was given by each patient or their representatives before enrollment into the study.

5.1.2. Clinical protocol

Stroke severity was assessed using GCS and NIHSS scores. The early ischemic changes were evaluated by ASPECT score calculated on admission using cranial NCCT scan by a certified neuroradiologist who was blinded to the patients' clinical information. The unfavorable outcome was defined as an mRS score > 2 at 90 days after IS. Venous blood samples were collected on admission to the stroke unit immediately after NCCT scan, but not later than 6 h after symptom onset. The patients received the standard stroke care: (i) within 4.5 hours, if there were no contraindications, they received IVrtPA; if the suspicion of large vessel occlusion arose (NIHSS > 8), CT angiography was performed; if a large vessel occlusion was confirmed (MCA—M1, ICA or basilar artery), thrombectomy was also performed after thrombolysis (ii; EVT + IVrtPA) or without systemic thrombolysis (iii; EVT alone). Patients with an ASPECT score < 6 on admission were considered to have a poor collateral network [60].

5.1.3. Sampling and laboratory analysis

The blood samples were immediately centrifuged at 3500 r/min for 15 min and aliquots of the samples were immediately stored at $-80\text{ }^{\circ}\text{C}$ before assay. Biomarker concentrations were measured by investigators blinded to the clinical outcome and neuroimaging findings. The serum periostin level was determined by the workers in the Department of Immunology and Biotechnology, University of Pecs, using ELISA-based kits manufactured by Shanghai YL Biotech Co., Shanghai, China. Samples were all processed by the same laboratory technician using the same equipment and blinded to all clinical data. The detection limit for the assay was 0.251 ng/L.

5.1.4. Statistical analysis

Data were evaluated using SPSS (version 11.5; IBM, Armonk, NY, USA). Categorical data were summarized by means of absolute and relative frequencies (counts and percentages). The Kolmogorov–Smirnov test was applied to check for normality. The chi-square test for categorical data and Student’s t-test as well as Mann–Whitney test for continuous data were used for the analysis of demographic and clinical factors. Non-normally distributed data are presented as median and interquartile range. Correlation analysis was performed by calculating Spearman’s correlation coefficient(r). To find an independent predictor of ASPECT <6 , a binary logistic regression was used. ROC (receiver operating characteristic) curve analysis was performed to evaluate the predictive values of serum periostin concentrations for 90-day unfavorable outcome. Subsequently, the AUC (area under the curve) and the corresponding 95% CI were calculated. In a combined logistic-regression model, we estimated the additive benefit of periostin concentrations to NIHSS scores. A p -value <0.05 was considered statistically significant.

5.2. Aneurysmal subarachnoid hemorrhage

5.2.1. Study design

This was a prospective observational study from a tertiary stroke treatment center in Pecs, Hungary. All patients ≥ 18 years of age with a newly diagnosed aSAH admitted to our hospital between November 2018 and December 2021 were offered enrollment into this study. Exclusion criteria were: traumatic SAH, pregnancy, hospital admission later than 24 h after ictus, no aneurysm treatment, absence of a signed consent form, underlying SARS-CoV-2 infection, and systemic diseases (chronic neurological disease, tumors, liver and/or renal insufficiency, and chronic lung disease). Written informed consent was obtained from each patient or their legal representative. All included patients underwent CTA or MRA before admission and conventional cerebral angiography after admission and received treatment according to clinical treatment guidelines. Following the diagnosis of aSAH, according to our hospital standards, the aneurysm was treated endovascularly within 24 hours. In all cases, the patient spent at least 12–14 days in the neurointensive care unit, so that expected complications (e.g., DCI) could be detected in time. DCI was screened by using TCD from admission every day of hospital care. If DCI was suspected, MRI and catheter angiography were performed to confirm macrovascular vasospasm and DCI. If vasospasm was confirmed, intra-arterial nimodipine was administered.

5.2.2. Clinical protocol

For each patient, data on demographics (age, sex) were collected. Basic comorbidities (hypertension, diabetes mellitus, and smoking) were identified. Aneurysm location and admission laboratory parameters (creatinine, C-reactive protein (CRP), neutrophile-lymphocyte ratio (NLR)) were collected according to hospital records. Further, the severity of aSAH was assessed using WFNS grade and mFisher scale, taking into consideration the amount of blood in the initial CT scan. The presence of mechanical ventilation, the need for decompressive craniectomy, and extra ventricular or lumbar drainage were recorded. TCD spasm indicated TCD positivity (TCD+) was diagnosed by daily transcranial Doppler measurements and defined as a peak-value increase by >50 cm/s/24 h compared with the previous result or a mean value >120 cm/s in one of the main supply branches [107]. Angiographic vasospasm was defined as moderate-to-severe arterial narrowing on DSA not

attributable to atherosclerosis, catheter-induced spasm, or vessel hypoplasia, as determined by a neuroradiologist [101]. We used the widespread, consensus definition of DCI [101]. The definition of infection was symptoms of infection with fever, elevated CRP and/or procalcitonin, and a positive diagnostic test such as chest X-ray or urine test. The clinical endpoints were DCI and unfavorable outcome (mRS \geq 3) after 30 days after aSAH.

5.2.3. Sampling and laboratory analysis

Samples were collected from the patients at two-time points: (i) 24 h after ictus (Day 1) and (ii) 5–7 days after ictus and were stored at -80 °C until measurement. The biomarkers measured in our study were selected according to different criteria: (i) previously their role was investigated in animal models of ischemic stroke or SAH; (ii) its role in the case of SAH has already been investigated, but the studies mainly focused on its level in the CSF; (iii) its pathophysiological role was primarily investigated in human IS and in SAH. Serum concentrations of CCL11, FGF-2, FLT-3L, CX3CL1, IL-1b, IL-4, IP-10, MCP-3 and MIP-1b were determined using a customized MILLIPLEX Human Cytokine/Chemokine/Growth Factor Panel A multiplex assay (HCYTA-60K, Merck KGaA, Darmstadt, Germany) according to the manufacturer's protocol. Briefly, 25 μ L of each serum sample, standard and control, was added to the appropriate wells of 96-well plates provided with the kit together with 25 μ L of assay buffer and 25 μ L of the mixture of fluorescent-coded magnetic beads, each of which was coated with a specific capture antibody. After overnight incubation at 2–8 °C for each analyte to be captured by the beads and three rounds of washing, 25 μ L of biotinylated detection antibody was introduced for an hour at room temperature. The reaction mixture was then incubated for 30 min with 25 μ L Streptavidin–phycoerythrin conjugate, the reporter molecule, to complete the reaction on the surface of each bead. Following washing the plate three times it was run on the Luminex MAGPIX instrument (Luminex Corporation, Austin, TX, USA); each individual bead was identified and the result of its bioassay was quantified based on fluorescent reporter signals. Data were analyzed using the Belysa Immunoassay Curve Fitting Software (Merck KGaA, Darmstadt, Germany) in accordance with the manufacturer's instructions. Samples were all processed by the same laboratory technician using the same equipment and blinded to all clinical data.

5.2.4. Statistical analysis

SPSS 19.0 (SPSS Inc., Chicago, IL, USA) and Graph Pad Prism 9 software (GraphPad Software, San Diego, CA, USA) was used for the statistical analysis of data. The categorical variables are presented as frequency and percentage. The continuous variables are presented as mean \pm standard deviation or median (percentile 25–75). The comparison of data between two groups, the significance of inter-group differences were assessed using the chi-square test or Fisher exact test for categorical data as well as the Student t-test or Mann–Whitney U test for continuous variables. Bivariate correlations were analyzed by Spearman’s correlation coefficient. Because a high number of correlations are possible among the 9 cytokines, a hard threshold of 0.50 was used to exclude correlations below this value and to focus only on strong correlations. A binary logistic regression model was used to identify independent predictors with respect to DCI status. All p-values lower than 0.05 were considered statistically significant.

VI. Results

6.1. Ischemic stroke

6.1.1. Clinical characteristics

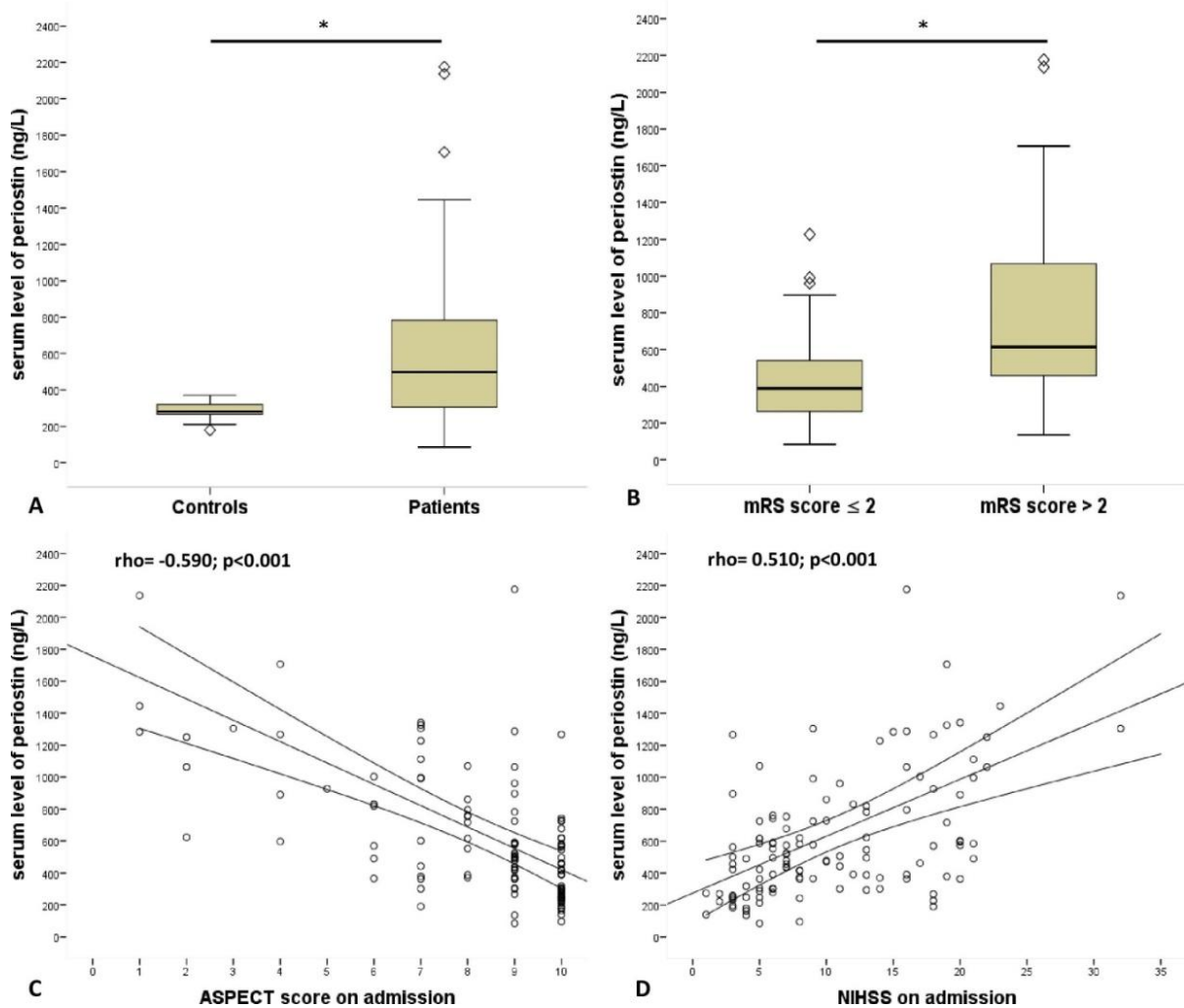
This cross-sectional study enrolled 122 patients with first-ever acute ischemic stroke. **Table 8** shows clinical profiles of patient groups based on their best mRS scores at 3 months as the primary outcome measure. The median age of the patients was 71 years (interquartile range: 63–79, min-max. values: 30–91) and 39.3% were female. Fifteen healthy volunteers served as age-matched normal controls. The median age of controls was 66 (interquartile range (IQR): 55–73, range 46–82), and 46.7% were female. The age and sex differences between patients and controls were non-significant. Regarding comorbidities, 100 patients (82%) had hypertension, 35 patients (29%) had diabetes, and 34 patients (27.9%) presented with AF. The median admission NIHSS score was 8 (IQR: 5–16, min-max: 1–32), and the median systolic and diastolic blood pressure on admission was 150 mmHg (IQR: 130–170, range: 90–240) and 84 mmHg (IQR: 80–93.5, range: 48–118). The median ASPECT score was 9 (IQR: 7–10, min-max: 1–10). In total, 29 patients (24%) underwent EVT, 51 (42%) received intravenous systemic rtPA treatment, and 17 (14%) underwent a combined EVT + IVrtPA treatment. A total of 25 patients (20.5%) were not eligible either for EVT or for IVrtPA; therefore, they received conservative treatment. The median serum level of periostin was 498.4 ng/L (IQR, 305–783) in patients with IS, and 280.4 ng/L (IQR, 259–332) in healthy controls ($p < 0.001$, **Figure 10A**).

Table 8. Baseline characteristics of the study population.

Characteristics	Total (n=122)	Favorable* outcome (n=59)	Unfavorable* outcome (n=63)	p=value
Age, y, median (IQR)	71 (63-79)	71 (62-77)	73 (64-79)	0.127
Male, n (%)	74 (61)	35 (59)	39 (62)	0.770
Hypertension, n (%)	100 (82)	48 (81.4)	52 (82.5)	0.865
Diabetes, n (%)	35 (29)	17 (29)	18 (29)	0.976
Smoking, n (%)	52 (3)	19 (32)	33 (52)	0.024*
Atrial fibrillation, n (%)	34 (28)	7 (12)	27 (43)	<0.001*
GCS, median (IQR)	15 (12-15)	15 (15)	14 (11-15)	<0.001*
NIHSS , median (IQR)	8 (5-16)	6 (4-8)	13 (8-19)	<0.001*
SBP, median (IQR), Hgmm	150 (130-170)	148 (130-170)	160 (138-180)	0.237
DBP, median (IQR), Hgmm	84 (80-94)	82 (80-90)	86 (80-100)	0.463
ASPECTS, median (IQR)	9 (7-10)	10 (9-10)	8 (6-9)	<0.001*
WBC, median (IQR), G/L	8.4 (6.9-10.7)	7.7 (9-10)	8.8 (7-11)	0.264
NLR, median (IQR)	2.9 (2-5.6)	2.5 (1.7)	3.6 (2.5-7.3)	0.002*
platelet, median (IQR), G/L	242 (188-306)	245 (196-300)	238 (185-305)	0.625
creatinine, median (IQR), µmol/L	86 (73-102)	83 (70-97)	87 (74-104)	0.411
glucose , median (IQR), mmol/L	7.2 (6.2-8.9)	6.8 (5.9-8.1)	7.8 (6.8-9)	0.004*
CRP, median (IQR), mg/L	3.7 (1.4-9.5)	2.6 (1.4-5.4)	5.1 (1.7-16)	0.042*
Thrombectomy, n (%)	29 (23.8)	14 (23.7)	15 (23.8)	0.856
Intravenous tPA, n (%)	51 (41.8)	28 (47.5)	23 (36.5)	0.190
Thrombectomy plus intravenous tPA, n (%)	17 (13.9)	6 (10.2)	11 (17.5)	0.260
Conservative, n (%)	25 (20.5)	11 (18.6)	14 (22.2)	0.658
serum level of periostin, median (IQR), ng/L	462 (297-735)	390 (260-563)	615 (443-1070)	<0.001*

Abbreviations: GCS, Glasgow coma scale; NIHSS, National Institutes of Health Stroke Scale; SBP, systolic blood pressure; DBP, diastolic blood pressure; ASPECTS, Alberta stroke programme early CT score; WBC, white blood cell; NLR, neutrophil-lymphocyte ratio; CRP, C-reactive protein; tPA, tissue plasminogen activator; * at Day 90 follow-up. *Note:* Continuous variables are expressed as medians (interquartile ranges). Categorical values are given as frequencies (percentages).

Figure 10. Comparison of serum periostin level (A) among patients with stroke and controls, (B) between patients with favorable outcome (mRS \leq 2) vs. unfavorable outcome (mRS $>$ 2) on Day 90 follow-up. Correlation of admission serum periostin level with (C) ASPECT score measured on admission and (D) NIHSS score recorded on admission.



Abbreviations: ASPECT, Alberta stroke programme early CT score; mRS, modified Rankin score; NIHSS, National Institutes of Health Stroke Scale. *Note:* Serum periostin level was measured at 24 hours after stroke onset. *p-value < 0.001. Statistical analysis was performed with Mann-Whitney U-test (A,B) and using Spearman rank correlation (C,D).

6.1.2. Admission periostin level, comorbidities and outcome

The admission serum periostin concentration was significantly higher in those patients who later had an unfavorable 90-day outcome compared to patients with favorable outcome (**Figure 10B** and **Table 8**). Moreover, the admission concentration of serum periostin showed an inverse correlation with ASPECT score (**Figure 10C**), while it was positively correlated with the admission NIHSS score (**Figure 10D**). In multivariate analysis, we found positive associations between admission level of periostin and AF, admission white blood cell (WBC) count, NLR, creatinine, CRP, and glucose level (**Table 9**). In contrast, serum periostin level was negatively associated with GCS and ASPECT score, both measured at admission.

Table 9. Spearman correlation between admission clinical parameters and serum periostin level measured at 24 hours after admission.

Variable	Spearman correlation coefficient (r)	p-value
Atrial fibrillation	0.335	< 0.001
Systolic blood pressure	0.068	0.459
Dyastolic blood pressure	0.119	0.193
Glasgow Coma Scale	-0.308	< 0.001
ASPECT score	-0.590	< 0.001
White blood cell count, G/L	0.239	0.01
Neutrophil-lymphocyte ratio	0.328	< 0.001
Creatinine, µmol/L	0.277	0.003
C-reactive protein, mg/L	0.285	0.002
Glucose, mmol/L	0.257	0.007
Platelet, G/L	-0.059	0.534
Carbamide, mmol/L	0.245	0.01

Abbreviations: ASPECT, Alberta stroke programme early CT score. *Note:* Coefficient (r) values > 0 indicate a positive association; values < 0 indicate a negative association. Statistically significant values are given in bold.

6.1.3. Variables associated with poor collaterals

ASPECT score < 6 indicating patients with poor collaterals on admission were positively associated with admission GCS in univariate analysis. In contrast, diabetes, AF, admission NIHSS, periostin level, NLR, CRP as well as creatinine levels were inversely associated with ASPECT score < 6 calculated in univariate analysis. Age and sex were not shown correlation with ASPECT < 6. Although GCS, NIHSS, AF, CRP, diabetes, creatinine and NLR were adjusted in a binary logistic regression model, serum periostin level remained a significant predictor for ASPECT < 6 status on admission (OR, 5.911; CI, 0.990–0.999; p = 0.015, **Table 10**). Next, another binary logistic regression analysis was performed to explore independent predictors of the outcome: NIHSS on admission and atrial fibrillation were independently associated with a favorable 90-day outcome (mRS0–2). Based on ROC (receiver operating characteristic) analysis, both NIHSS score (AUC, 0.817; 95% CI, 0.743–0.892, cutoff: 8.5, sensitivity: 75%, specificity: 78%, p < 0.001) and admission serum concentration of periostin (AUC, 0.757; 95%CI, 0.672–0.841, cutoff: 466.7 ng/L, sensitivity: 75 %, specificity: 65%, p < 0.001) showed similar sensitivity and specificity in the prediction of unfavorable 3-month outcome. In contrast, the combination of these two variables had significantly greater predictive power (AUC, 0.842; 95% CI, 0.773–0.911, p < 0.001) (**Figure 11**). The serum concentration of periostin with a cut-off value of ≥ 594.5 independently predicted admission ASPECT < 6 reflecting the poor collateral status with a sensitivity of 84.2% and specificity of 72%.

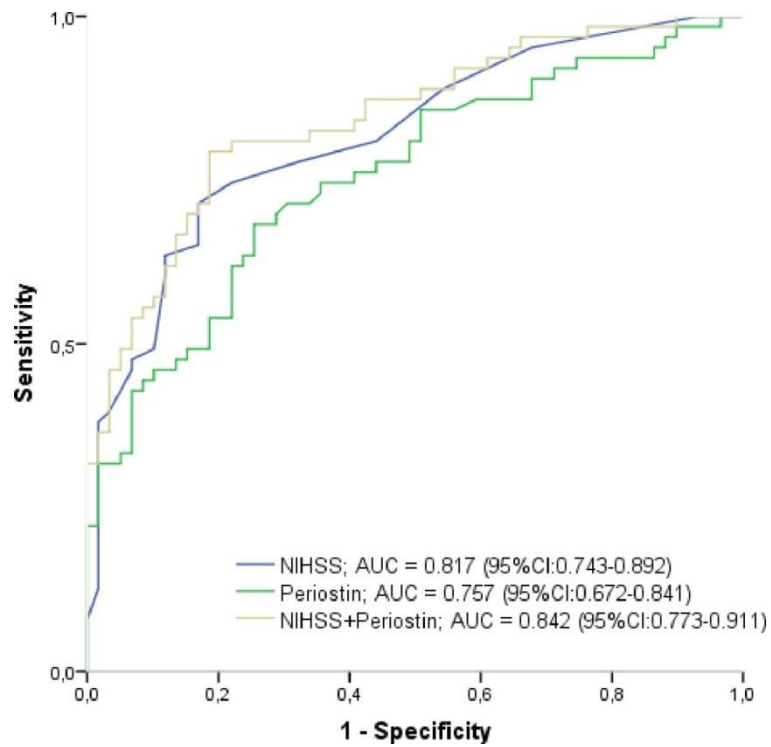
Table 10. Binary logistic regression analysis of predictors for admission ASPECT score <6 in patients with acute ischemic stroke.

	Odds ratio	95% CI	P-value
periostin	15.532	0.995-0.998	<0.001
Model 1	6.339	0.995-0.999	0.012
Model 2	5.917	0.993-0.999	0.015
Model 3	5.911	0.990-0.999	0.015

Abbreviations: CI, confidence interval.

Note: Model 1 included Glasgow Coma Scale and National Institute of Health Stroke Scale. Model 2 included variables in model 1 plus atrial fibrillation and admission level of C-reactive protein. Model 3 included variables in model 2 plus diabetes, admission serum level of creatinine and admission neutrophil-lymphocyte ratio.

Figure 11. Receiver operating characteristic curve analysis of prognostic predictive ability of serum NIHSS score on admission, serum level of periostin on admission and the combination of NIHSS score and periostin for 3-month unfavorable outcome in patients with acute ischemic stroke.



Abbreviations: AUC, area under the curve; CI, confidence interval; NIHSS, National Institute of Health Stroke Scale

6.2. Aneurysmal subarachnoid hemorrhage

6.2.1. Clinical characteristics

One hundred and twelve patients with aSAH (**Table 11**) were included in this study. Patients were enrolled between November 2018 and December 2021. All (100%) of the aneurysms were secured by coiling. Patients had a mean age of 57 (SD13) and 62% were female. Of them, 38 patients with aSAH (34%) presented to the emergency department with a WFNS Grade I. Almost half of the patients had a history of arterial hypertension (43.8%) and 11% had a history of smoking. Nearly one-third of the patients had DCI (29.1%) during their in-hospital stay. A description of these aSAH patients is shown in **Table 11**.

Table 11. Patients characteristics.

Number of patients with aneurysmal SAH, n=112		
Age	(years, mean±SD)	57±13
Female	(N,%)	69 (61.6)
Hypertension	(N,%)	49 (43.8)
Diabetes mellitus	(N,%)	11 (9.8)
Smoking	(N,%)	12 (10.7)
Aneurysm location		
– Internal carotid artery	(N,%)	16 (14.3)
– Middle cerebral artery	(N,%)	22 (19.6)
– Anterior communicating artery	(N,%)	31 (27.7)
– Posterior communicating artery	(N,%)	13 (11.6)
– Anterior cerebral artery	(N,%)	14 (12.5)
– Vertebrobasilar	(N,%)	16 (14.3)
WFNS		
– 1	(N,%)	38 (33.9)
– 2	(N,%)	24 (21.4)
– 3	(N,%)	8 (7.1)
– 4	(N,%)	14 (12.5)
– 5	(N,%)	28 (25)
modified Fischer grade		
– 1	(N,%)	1 (0.9)
– 2	(N,%)	18 (16.1)
– 3	(N,%)	57 (50.9)
– 4	(N,%)	36 (32.1)
Glasgow coma scale, on admission	median, IQR	13 (6-15)
Neutrophile-lymphocyte ratio, on admission	median, IQR	5.9 (4-10)
C-reactive protein, on admission, mg/L	median, IQR	13 (4-61)
Creatinine, on admission, µmol/L	median, IQR	61 (50-72)
Extraventricular drainage	(N,%)	53 (47.3)
Infection, CSF	(N,%)	7 (6.3)
Infection, systemic	(N,%)	18 (16.1)
Infection, CSF+systemic	(N,%)	5 (4.5)
Mechanical ventilation	(N,%)	50 (44.6)
Decompressive craniotomy	(N,%)	14 (12.5)
Lumbar drainage	(N,%)	14 (12.5)
Delayed cerebral ischemia	(N,%)	32 (29.1)
Angiographic vasospasm	(N,%)	28 (28.3)
Transcranial Doppler positivity	(N,%)	41 (41.8)
Ischaemic laesion on MRI	(N,%)	16 (15.8)
Favorable outcome on Day 30 (mRS=0-2)	(N,%)	58 (51.8)
In-hospital death	(N,%)	15 (13.4)

Abbreviations: SAH, subarachnoid hemorrhage; WFNS, World Federation of Neurological Societies Score; MRI, magnetic resonance imaging; CSF, cerebrospinal fluid. *Note:* The categorical variables are displayed presented as frequency (%) and the continuous variables are displayed presented as mean ± standard deviation (SD) or median with interquartile range (IQR).

6.2.2. Cytokines associated with DCI and functional outcome

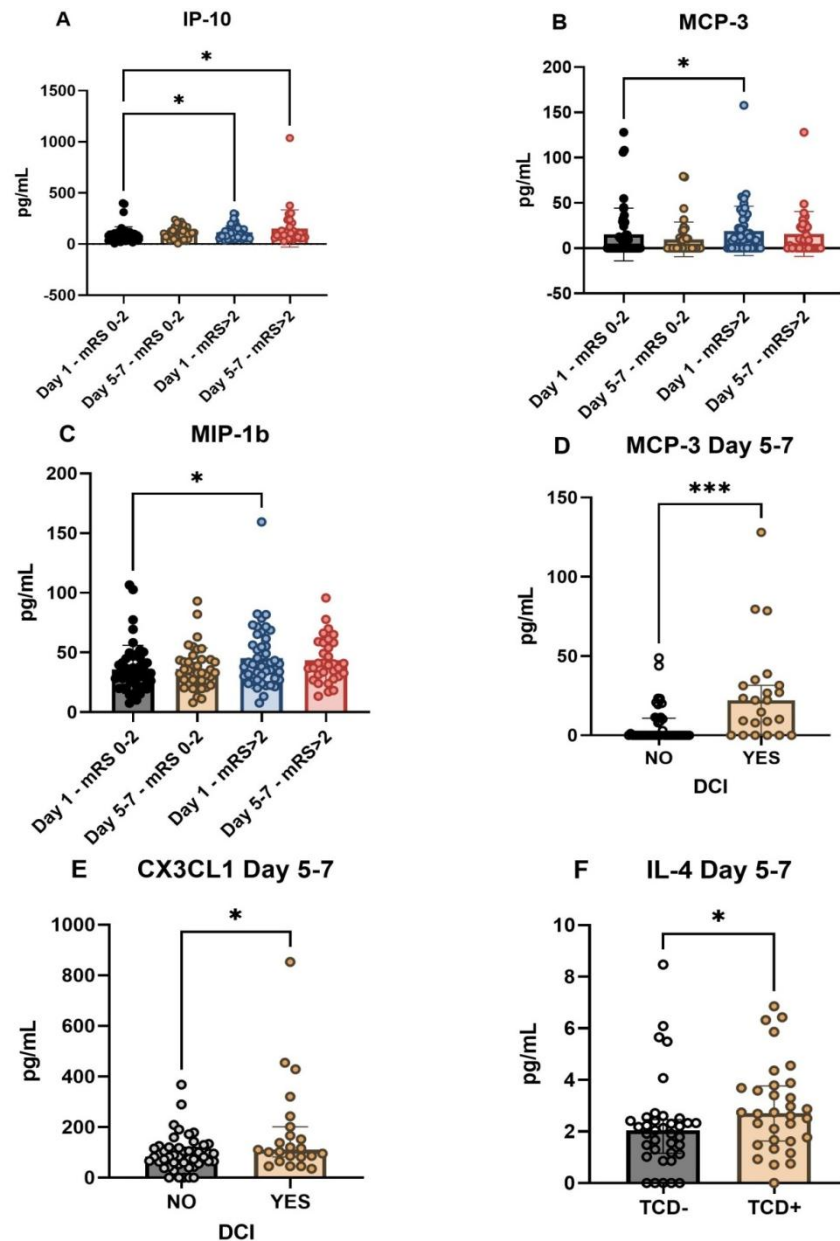
None of the cytokines tested on Day 1 were associated with DCI, whereas only cytokines measured on Day 1 (IP-10, MCP-3, MIP-1b) were associated with functional outcome (**Table 12**). CX3CL1 and MCP-3 measured on Days 5–7 were significantly higher in patients with DCI compared to those without DCI (CX3CL1: Day 5–7, without DCI: 82.6 pg/mL, IQR: 58–119 vs. Day 5–7, with DCI: 110.5 (82–201), $p = 0.036$ and MCP-3: Day 5–7, without DCI: 0 (0–11) vs. Day 5–7, with DCI: 22 (0–32), $p < 0.001$, **Figure 12**). Serum IP-10 levels in patients with poor outcomes were significantly higher than in patients with favorable outcomes at both time points (Day 1, favorable outcome: 74.7 pg/mL, IQR: 43–97 vs. Day 1, unfavorable outcome: 100, 68–146, $p = 0.005$ and Day 1, favorable outcome: 74.7 pg/mL, IQR: 43–97 vs. Day 5–7, unfavorable outcome: 98.8, 65–157, $p = 0.004$). For MCP-3 and MIP-1b, the serum concentrations measured on Day 1 showed significantly higher levels in patients with unfavorable outcome compared with the group with favorable Day 30 outcome (MCP-3: Day 1, favorable: 0 pg/mL, IQR: 0–15 vs. Day 1, unfavorable: 11.8, 0–25, $p = 0.045$ and MIP-1b: Day 1, favorable: 31.8 pg/mL, 23–42 vs. Day 1, unfavorable: 40, 28–56, $p = 0.025$, **Figure 12**).

Table 12. . Cytokines associated with DCI during hospitalization and functional outcome on Day 30.

Cytokines	DCI during hospitalization		mRS score at Day 30	
	DCI - ($n=78$ [71%]) vs. DCI + ($n=32$ [29%])		Unfavorable outcome (mRS \geq 3, $n=54$ [48.2%]) vs. Favorable outcome (mRS \leq 2, $n=58$ [51.8%])	
	Day 1	Day 5-7	Day 1	Day 5-7
Eotaxin	-	-	-	-
FGF-2	-	-	-	-
FLT-3L	-	-	-	-
CX3CL1	-	H*	-	-
IL-1b	-	-	-	-
IL-4	-	-	-	-
IP-10	-	-	H*	-
MCP-3	-	H**	H*	-
MIP-1b	-	-	H*	-
Total	0	2	3	0

Abbreviations: DCI, delayed cerebral ischemia; mRS, modified-Rankin scale; FGF-2, fibroblast growth factor-2; FLT-3L, Fms-related tyrosine kinase 3 ligand; CX3CL1, chemokine ligand 1, also known as fractalkine; IL-1b, interleukin-1b; IL-4, interleukin-4; IP-10, interferon gamma-induced protein 10, also known as C-X-C motif chemokine ligand 10 (CXCL10); MCP-3, Monocyte chemoattractant protein-3; MIP-1b, macrophage inflammatory protein 1-beta; H, high level; * $p < 0.05$; ** $p < 0.001$.

Figure 12. Characteristics of serum biomarker levels in different clinical subgroups in patients with aSAH. Correlation of the functional outcome with the investigated biomarkers, in the case of IP-10 (A), MCP-3 (B) and MIP-1b (C). Correlation of MCP-3 (D) and CX3CL1 (E) measured at T2 with DCI. Association of IL-4 (F) with TCD positivity.



Abbreviations: DCI, delayed cerebral ischemia; aSAH, aneurysmal subarachnoid hemorrhage; TCD, transcranial Doppler ultrasound; CX3CL1, chemokine ligand 1, also known as fractalkine; IL-4, interleukin-4; IP-10, interferon gamma-induced protein 10, also known as C-X-C motif chemokine ligand 10 (CXCL10); MCP-3, Monocyte chemoattractant protein-3; MIP-1b, macrophage inflammatory protein 1-beta. *Note:* The functional outcome was examined 30 days after admission and characterized on the modified Rankin scale (mRS). Biomarker sampling times: Day 1, 24 h after aSAH, Day 5–7, 5–7 days after aSAH. * denotes $p < 0.05$, *** denotes $p < 0.001$.

In order to clarify how the increase of MCP-3 and CX3CL1 seen in DCI is related to the time of DCI, we performed an additional analysis. The average time of onset of DCI in our cohort was 6 ± 3.2 days (mean \pm SD). We grouped the DCI cases based on the sampling dates: the cases before T2 were in Group A, while the cases after T2 were in Group B, **Table 13**.

Table 13. The association of MCP-3 and CX3CL1 levels measured at T2 with the time of DCI detection.

	No DCI (N=78)	Group A DCI prior toT2 (N=7)	Group B DCI followingT2 N=25)	p-value (between A-B)
MCP-3 T2, pg/mL, median (IQR)	0 (0-11)	22 (8-27)	18 (0-32)	0.857
CX3CL1 T2, pg/mL, median (IQR)	83 (58-119)	116 (103-138)	106 (65-243)	0.691

Abbreviations: DCI, delayed cerebral ischemia; MCP-3, Monocyte chemotactic protein-3; CX3CL1, chemokine ligand 1, also known as fractalkine. *Note:* T1, serum sample at Day 1 following aSAH; T2, serum sample at Days 5-7 following aSAH.

6.2.3. Clinical variables associated with DCI and Day 30 functional outcome

We found no significant association between admission WFNS and Fischer scores and the development of DCI in aSAH patients. Similarly, there was no association between demographic (female, age) and clinical risk factors (hypertension, diabetes, smoking) and the emergence of DCI during hospital stay (**Table 14**). The admission GCS score was significantly lower in the DCI group than in the non-DCI group (DCI: 9, IQR: 5–14 vs. no DCI: 14, 10–15, $p = 0.02$). Decompressive craniectomy was required more frequently in the DCI group, but there was no difference between the two groups in terms of EVD use. Other factors related to DCI and Day 30 functional outcome are shown in **Table 14-15**. We found that regardless of whether the patient had an infection or not during hospitalization, the serum level of MCP-3 was significantly higher in the DCI group than in the non-DCI group. In contrast, de CX3CL1 concentration measured at T2 did not show a significant difference in the two groups of DCI, regardless of the presence of an infection (**Table 16**).

Table 14. . Comparison of clinical and biochemical characteristics between patients with and without DCI in patients with aneurysmal subarachnoid hemorrhage.

Variable	DCI		p-value
	DCI (n = 32)	No-DCI (n = 78)	
Age (years, mean±SD)	54.8±11	57.9±14	0.223
Female, N (%)	17 (53)	50 (64)	0.284
Hypertension, n (%)	11 (34.4)	37 (47.4)	0.210
Diabetes mellitus, n (%)	3 (9.4)	8 (10.3)	0.889
Smoking, n (%)	2 (6.3)	10 (12.8)	0.315
WFNS, median (IQR)	3 (1–5)	2 (1–4)	0.412
modified Fischer grade, median (IQR)	3 (2–4)	3 (2–4)	1.000
Glasgow coma scale, median (IQR)	9 (5–14)	14 (10–15)	0.02
Neutrophile-lymphocyte ratio, median (IQR)	7 (5–10)	5 (3–11)	0.092
C-reactive protein, median (IQR)	24 (5–75)	9.5 (3–43)	0.104
Creatinine, median (IQR)	61 (50–72)	60 (50–72)	0.744
Extraventricular drainage, n (%)	18 (56.3)	33 (42.3)	0.183
Mechanical ventilation, n (%)	19 (59.4)	29 (37.2)	0.033
Decompressive craniotomy, n (%)	8 (25)	5 (6.4)	0.006
Angiographic vasospasm, n (%)	27 (84.4)	1 (1.5)	<0.001
Transcranial Doppler positivity, N (%)	30 (96.8)	11 (16.4)	<0.001
Ischemic lesion on MRI, N (%)	16 (50)	0 (0)	<0.001

Abbreviations: IQR, interquartile range; DCI, delayed cerebral ischemia; WFNS, World Federation of Neurological Surgeons; MRI, magnetic resonance imaging. *Note:* The categorical variables are presented as frequency and percentage, and the continuous variables are presented as mean ± standard deviation or median (percentile 25–75). The significances of inter-group differences were assessed using chi-square test or Fisher exact test for categorical data as well as Student t test or Mann–Whitney U test for continuous variables.

Table 15. Comparison of clinical and biochemical characteristics between patients with unfavorable vs. favorable outcome (Day 30) in patients with aneurysmal subarachnoid hemorrhage.

Variable	Functional Outcome at Day 30		p-Value
	Unfavorable (n = 54)	Favorable (n = 58)	
Age (years, mean±SD)	61.8 ± 12	52.6 ± 12	<0.001
Female, N (%)	29 (53.7)	40 (69)	0.097
Hypertension, n (%)	28 (51.9)	21 (36.2)	0.095
Diabetes, n (%)	10 (18.5)	1 (1.7)	0.003
Smoking, n (%)	4 (7.4)	8 (13.8)	0.275
WFNS, median (IQR)	4 (3–5)	1 (1–2)	<0.001
modified Fischer grade, median (IQR)	4 (3–4)	2 (1–3)	<0.001
Glasgow coma scale, median (IQR)	6 (3–12)	14 (13–15)	<0.001
Neutrophile-lymphocyte ratio, median (IQR)	7 (4–12)	5.3 (3–8)	0.054
C-reactive protein, median (IQR)	41 (9–89)	6.8 (3–17)	<0.001
Creatinine, median (IQR)	63 (50–76)	59 (50–67)	0.122
Extraventricular drainage, n (%)	41 (75.9)	12 (20.7)	<0.001
Mechanical ventilation, n (%)	43 (79.6)	7 (12.1)	<0.001
Decompressive craniotomy, n (%)	11 (20.4)	3 (5.2)	0.015
Angiographic vasospasm, n (%)	22 (52.4)	6 (10.5)	<0.001
Transcranial Doppler positivity, N (%)	23 (54.8)	18 (32.1)	0.025
Ischemic lesion on MRI, N (%)	16 (35.6)	0 (0)	<0.001

Abbreviations: IQR, interquartile range; DCI, delayed cerebral ischemia; WFNS, World Federation of Neurological Surgeons; MRI, magnetic resonance imaging. *Note:* Favorable outcome = modified Rankin score 0–2, unfavorable = 3–6. The categorical variables are presented as frequency and percentage, and the continuous variables are presented as mean ± standard deviation or median (percentile 25–75). The significances of inter-group differences were assessed using chi-square test or Fisher exact test for categorical data as well as Student t test or Mann–Whitney U test for continuous variables.

Table 16. Correlation between the occurrence of infection the appearance of DCI and biomarker values in aSAH patients.

	No Infection			Infection during Hospitalization		
	No DCI	DCI	p-Value	No DCI	DCI	p-Value
MCP-3 T2, pg/mL, median (IQR)	0 (0–11)	12 (0–32)	0.025	0 (0–8)	23 (9–27)	0.004
CX3CL1 T2, pg/mL, median (IQR)	82 (53–118)	102 (46–201)	0.221	94 (60–179)	116 (95–166)	0.152

Abbreviations: IQR, interquartile range; DCI, delayed cerebral ischemia; MCP-3, Monocyte chemotactic protein-3; CX3CL1, chemokine ligand 1, also known as fractalkine. *Note:* T2, serum sample at Day 5–7 after aSAH.

6.2.4. Correlations between biomarkers in aSAH patients

Correlations for all measured serum biomarkers at both measurement time points were examined. The Spearman r coefficient of correlation between all these parameters is presented as a heat-map in **Figure 13**. The heat-map confirmed a positive and strong correlation between IL-1b and FGF-2, CX3CL1 and MCP-3, as well as between MCP-3 and FGF-2 at T1 time point. For biomarkers measured at T2, only the correlation between MCP-3 and CX3CL1 remained strong. For more correlations see **Figure 13**.

Figure 13. . Correlation between different serum biomarkers in patients with aSAH.

	Eotaxin T1	FGF-2 T1	FLT-3L T1	CX3CL1 T1	IL-1b T1	IL-4 T1	IP-10 T1	MCP-3 T1	MIP-1b T1	Eotaxin T2	FGF-2 T2	FLT-3L T2	CX3CL1 T2	IL-1b T2	IL-4 T2	IP-10 T2	MCP-3 T2	MIP-1b T2
Eotaxin T1	1,000	0,233	0,237	0,060	0,233	0,153	0,095	0,116	0,185	0,654	0,278	0,118	0,144	0,233	0,220	-0,122	0,208	0,039
FGF-2 T1	0,233	1,000	0,295	0,461	0,694	0,346	-0,086	0,524	0,151	0,259	0,724	0,367	0,257	0,580	0,219	-0,337	0,247	-0,116
FLT-3L T1	0,237	0,295	1,000	0,241	0,268	0,330	0,193	0,226	0,218	0,323	0,197	0,607	0,075	0,342	0,036	0,021	0,088	0,052
CX3CL1 T1	0,060	0,461	0,241	1,000	0,356	0,516	0,239	0,778	0,242	0,069	0,174	0,013	0,857	0,226	0,352	0,226	0,424	0,145
IL-1b T1	0,233	0,694	0,268	0,356	1,000	0,276	0,039	0,438	0,239	0,224	0,530	0,214	0,206	0,833	0,200	-0,181	0,210	0,102
IL-4 T1	0,153	0,346	0,330	0,516	0,276	1,000	0,261	0,435	0,235	0,163	0,134	0,084	0,395	0,180	0,694	0,064	0,223	0,121
IP-10 T1	0,095	-0,086	0,193	0,239	0,039	0,261	1,000	0,216	0,411	-0,184	-0,243	-0,071	0,085	-0,126	0,046	0,519	-0,076	0,371
MCP-3 T1	0,116	0,524	0,226	0,778	0,438	0,435	0,216	1,000	0,210	0,054	0,298	0,044	0,615	0,260	0,348	0,002	0,687	0,128
MIP-1b T1	0,185	0,151	0,218	0,242	0,239	0,235	0,411	0,210	1,000	0,038	0,017	0,055	0,073	0,140	0,013	0,177	-0,039	0,643
Eotaxin T2	0,654	0,259	0,323	0,069	0,224	0,163	-0,184	0,054	0,038	1,000	0,194	0,242	0,095	0,037	0,196	-0,112	0,053	-0,058
FGF-2 T2	0,278	0,724	0,197	0,174	0,530	0,134	-0,243	0,298	0,017	0,194	1,000	0,182	0,415	0,486	0,247	-0,413	0,445	-0,121
FLT-3L T2	0,118	0,367	0,607	0,013	0,214	0,084	-0,071	0,044	0,055	0,242	0,182	1,000	-0,019	0,203	0,071	0,044	0,018	0,149
CX3CL1 T2	0,144	0,257	0,075	0,857	0,206	0,395	0,085	0,615	0,073	0,095	0,415	-0,019	1,000	0,237	0,443	0,133	0,637	-0,022
IL-1b T2	0,233	0,580	0,342	0,226	0,833	0,180	-0,126	0,260	0,140	0,037	0,486	0,203	0,237	1,000	0,248	-0,213	0,325	0,035
IL-4 T2	0,220	0,219	0,036	0,352	0,200	0,694	0,046	0,348	0,013	0,196	0,247	0,071	0,443	0,248	1,000	0,008	0,430	0,107
IP-10 T2	-0,122	-0,337	0,021	0,226	-0,181	0,064	0,519	0,002	0,177	-0,112	-0,413	0,044	0,133	-0,213	0,008	1,000	-0,134	0,328
MCP-3 T2	0,208	0,247	0,088	0,424	0,210	0,223	-0,076	0,687	-0,039	0,053	0,445	0,018	0,637	0,325	0,430	-0,134	1,000	-0,096
MIP-1b T2	0,039	-0,116	0,052	0,145	0,102	0,121	0,371	0,128	0,643	-0,058	-0,121	0,149	-0,022	0,035	0,107	0,328	-0,096	1,000

Abbreviations: FGF-2, fibroblast growth factor-2; FLT-3L, Fms-related tyrosine kinase 3 ligand; CX3CL1, chemokine ligand 1, also known as fractalkine; IL-1b, interleukin-1b; IL-4, interleukin-4; IP-10, interferon gamma-induced protein 10, also known as C-X-C motif chemokine ligand 10 (CXCL10); MCP-3, Monocyte chemotactic protein-3; MIP-1b, macrophage inflammatory protein 1-beta; aSAH, aneurysmal subarachnoid hemorrhage.

Note: red indicates that the two parameters were positively correlated, and blue indicates that the two parameters were negatively correlated; the darker the color, the stronger the correlation. T1, serum sample at Day 1 after aSAH; T2, serum sample at Day 5–7 after aSAH. Statistical method: Spearman.

The binary logistic regression analysis identified serum Day 5–7 MCP-3 levels as an independent predictor for DCI status, **Table 17**. Serum level of FGF-2 showed a strong negative correlation with serum level of IP-10 in patients with favorable outcome, while this correlation disappeared in the case of the group with an unfavorable outcome (**Figure 14**).

Table 17. Binary logistic regression model of independent predictors of DCI status after aSAH.

	B	Wald	Sig.	Exp(B)
MCP-3 T2	0.045	5.221	0.022	1.046
GCS on admission	-0.031	-0.062	0.803	0.97
Mechanical Ventilation	-0.954	0.638	0.424	0.385
Sex	-0.974	2.496	0.114	0.378
Age	-0.026	1.062	0.303	0.974
Constant	1.593	0.922	0.337	4.917

Abbreviations: GCS, Glasgow coma scale; aSAH, aneurysmal subarachnoid hemorrhage; MCP-3, Monocyte chemotactic protein-3; DCI, delayed cerebral ischemia. *Note:* T2, sample time: Day 5–7 after aSAH.

Figure 14. Correlation between serum biomarkers in different clinical subgroups (A): favorable, n = 58; (B): unfavorable, n = 58).

A	FGF-2 T1	CX3CL1 T1	IL-1b T1	IP-10 T1	MCP-3 T1	FGF-2 T2	CX3CL1 T2	IL-1b T2	IP-10 T2	MCP-3 T2
FGF-2 T1	1,000	0,523	0,684	-0,253	0,613	0,867	0,306	0,467	-0,420	0,320
CX3CL1 T1	0,523	1,000	0,369	0,137	0,730	0,121	0,872	0,195	0,049	0,564
IL-1b T1	0,684	0,369	1,000	-0,126	0,481	0,569	0,216	0,849	-0,345	0,211
IP-10 T1	-0,253	0,137	-0,126	1,000	0,090	-0,570	-0,034	-0,260	0,485	-0,158
MCP-3 T1	0,613	0,730	0,481	0,090	1,000	0,124	0,461	0,179	-0,165	0,729
FGF-2 T2	0,867	0,121	0,569	-0,570	0,124	1,000	0,480	0,495	-0,517	0,475
CX3CL1 T2	0,306	0,872	0,216	-0,034	0,461	0,480	1,000	0,235	0,011	0,697
IL-1b T2	0,467	0,195	0,849	-0,260	0,179	0,495	0,235	1,000	-0,366	0,295
IP-10 T2	-0,420	0,049	-0,345	0,485	-0,165	-0,517	0,011	-0,366	1,000	-0,164
MCP-3 T2	0,320	0,564	0,211	-0,158	0,729	0,475	0,697	0,295	-0,164	1,000

B	FGF-2 T1	CX3CL1 T1	IL-1b T1	IP-10 T1	MCP-3 T1	FGF-2 T2	CX3CL1 T2	IL-1b T2	IP-10 T2	MCP-3 T2
FGF-2 T1	1,000	0,409	0,722	0,068	0,465	0,708	0,260	0,712	-0,210	0,242
CX3CL1 T1	0,409	1,000	0,346	0,345	0,841	0,247	0,866	0,337	0,293	0,350
IL-1b T1	0,722	0,346	1,000	0,194	0,388	0,559	0,215	0,817	0,042	0,250
IP-10 T1	0,068	0,345	0,194	1,000	0,236	-0,006	0,194	-0,017	0,579	-0,115
MCP-3 T1	0,465	0,841	0,388	0,236	1,000	0,464	0,781	0,431	0,150	0,648
FGF-2 T2	0,708	0,247	0,559	-0,006	0,464	1,000	0,326	0,532	-0,300	0,374
CX3CL1 T2	0,260	0,866	0,215	0,194	0,781	0,326	1,000	0,291	0,246	0,559
IL-1b T2	0,712	0,337	0,817	-0,017	0,431	0,532	0,291	1,000	-0,050	0,396
IP-10 T2	-0,210	0,293	0,042	0,579	0,150	-0,300	0,246	-0,050	1,000	-0,108
MCP-3 T2	0,242	0,350	0,250	-0,115	0,648	0,374	0,559	0,396	-0,108	1,000

Abbreviations: T1, serum sample at Day 1 after aSAH; T2, serum sample at Day 5–7 after aSAH. FGF-2, fibroblast growth factor-2; FLT-3L, Fms-related tyrosine kinase 3 ligand; CX3CL1, chemokine ligand 1, also known as fractalkine; IL-1b, interleukin-1b; IL-4, interleukin4; IP-10, interferon gamma-induced protein 10, also known as C-X-C motif chemokine ligand 10 (CXCL10); MCP-3, Monocyte chemotactic protein-3; MIP-1b, macrophage inflammatory protein 1-beta.

Note: Unfavorable, mRS = 3–6 on Day 30; favorable, mRS = 0–2 on Day 30. Red indicates that the two parameters were positively correlated, and blue indicates that the two parameters were negatively correlated. The darker the color, the stronger the correlation. Statistical method: Spearman.

VII. Discussion

7.1. Ischemic stroke

In a previous study, increased serum periostin levels were observed at 6 days and beyond at 4 weeks post-ischemia and were positively correlated with severity in terms of infarct volume and neurological deficit, but not with functional outcome in patients with large-artery atherosclerotic stroke [82]. Interestingly, the periostin level measured on the first day showed no difference compared to the values measured in the control group. In contrast, in our study, serum periostin levels measured in the hyperacute phase of IS were increased compared to healthy controls. Importantly, our study population shows several differences: (i) in etiology, as almost one-third of the total study population and 43% of the unfavorable outcome subgroup presented with atrial fibrillation on admission; (ii) inflammatory status, as CRP and NLR were higher in patients with poor 90-day outcome; and (iv) metabolic status, as plasma glucose level was significantly elevated among patients with poor outcome. In accordance with He et al. [82], serum concentration of periostin showed a strong correlation with NIHSS in our cohort. Additionally, we also find the relationship between the systemic concentration of periostin measured in the acute phase of stroke and ASPECT score a valid assessment of the collateral circulation of the ischemic brain. Taken together, these may suggest that matricellular proteins (e.g., apelin, oncostatin M, and periostin) regulating myogenesis/angiogenesis and vessel formation during regeneration processes [147] may have an impact on the collateral circulation determining the salvageable penumbral brain tissue [148].

Based on the aforementioned clinical studies, periostin emerged as a novel prognostic marker in assessing the long-term outcome of diseases with severe neurological damage. However, there is a great need to find markers estimating the cerebral collaterals upon developing an acute ischemic insult. Periostin as a prehospital point-of-care marker might have the potential to provide information about the prior collateral status and the expected outcome, contributing to early diagnostics and the clinical decision-making of the stroke care team. In our study, we found that serum periostin concentration is an independent predictor of ASPECT < 6 calculated on admission, and this finding indicates that periostin could reflect the extent of early brain injury in the hyperacute stage of ischemic stroke. According to the ESMINT (European Stroke Organisation—European Society for Minimally Invasive Neurological Therapy) Guidelines on Mechanical Thrombectomy in Acute Ischemic Stroke [149], patients

with acute IS with large vessel occlusion should be treated with MT plus the best medical management up to approximately 7 h 18 min after stroke onset, without the need for perfusion imaging-based selection if patients have ASPECTS ≥ 6 and moderate-to-good collateral circulation. Since many studies [49,55,63-65] prove that ASPECT score is a sensitive marker of the ischemic core, and thus indirectly of the collateral network, its close correlation with periostin can act as an important diagnostic tool. Considering this, periostin as a surrogate marker measured within 6 h after acute stroke might contribute to establishing the indication of mechanical thrombectomy in the lack of advanced neuroimaging.

However, the source of elevated periostin is not yet clear. Periostin is generally present at low levels in most adult tissues but is highly expressed at sites of injury or inflammation and in tumors of adult organisms. Current evidence demonstrates that periostin actively contributes to tissue injury, inflammation, fibrosis and tumor progression [150]. Therefore, these extracerebral sources should be excluded prior to any therapeutic decisions. Given the acute increase in periostin level in our study in patients with poor outcome and ASPECT < 6 , it is possible that the acute breakdown of the blood–brain barrier and leakage into circulation may be a significant source. Liu et al. demonstrated that periostin was upregulated in the cerebral cortex after experimental SAH in mice and was responsible for early brain injury, which was possibly mediated by p38/ERK/MMP-9 signaling pathways [151]. Furthermore, in our cohort, CRP, NLR, and WBC showed a close correlation with admission periostin levels, indicating a possible link between the early immune response and post-ischemic brain injury. CRP and NLR have recently been reported as potential novel biomarkers of the baseline inflammatory process and could serve as outstanding predictors in patients with ischemic stroke [152]. Elevated levels of CRP after stroke have been related to poor functional outcome and mortality [153]. Our study also found a strong positive association between AF and the admission level of periostin. As a matricellular protein, periostin has been proven to play an important role in fibrogenesis [154,155]. Wu et al. [75] and evidence from a recent review [72] suggest that the source of periostin, in addition to brain tissue damage that enters the systemic circulation through damage to the blood–brain barrier, may also be of myocardial origin.

Summarizing, initial periostin level may serve as a surrogate prognostic marker for hyperacute IS reflecting stroke severity, long-term outcome, and patient's eligibility for intervention.

However, our study has several limitations. First, data about the changes of circulating periostin concentrations during the progression of ischemic stroke were not reported. Periostin kinetics could provide important information regarding the evolution of stroke. Second, only NCCT and CTA were performed on admission, while MR would have been more suitable to determine the size of early infarction. As CTA-based collateral score calculation was not performed in all cases, we were not able to include it in our study. Third, various isoforms of periostin have been described in humans [76]; the ELISA kit used in our study detects all periostin isoforms present in the circulation and was not capable to differentiate between them. Fourth, we did not measure other conventional markers of both brain and heart tissue damage such as S100B or troponin, so it is unclear whether the measured periostin level is entirely of cerebral origin [156]. In addition, the relatively small number of cases in our study limits the generalizability of the study results. Therefore, further studies are warranted to explore the real specificity of periostin in early brain damage due to ischemia. As the pathophysiology, prognosis and clinical features of acute small vessel IS are different from other types of cerebral infarcts, an anethiology-based intergroup comparison of the systemic concentration of periostin would be worthwhile in the future [157].

In conclusion, there is an urgent need to find reliable markers reflecting the collateral circulation in patients with acute IS either predicting the extension of early brain damage or supporting decision-making in cases where opportunities for advanced neuroimaging are limited. Reasonably, the concept of endothelial dysfunction as well as other vascular features related to cerebrovascular insults might have to be redefined as we learn more about multiple proteins (e.g., matricellular proteins) secreted by endothelial cells besides NO [158,159]. Overall, periostin may be a useful laboratory marker to identify patients with a poor collateral network and consequently with a more extensive core, especially when advanced neuroradiological procedures, e.g., CT perfusion, are not available.

7.2. Aneurysmal subarachnoid hemorrhage

CX3CL1 also called fractalkin has a direct effect on microglia and has the ability to induce the release of soluble factors that orchestrate a neuroprotective response [118]. CX3CL1 and its receptor are involved in a complex network of both paracrine and autocrine interactions between neurons and glia and have a role in microglia polarization [160]. In the acute phase following SAH, the microglia mainly appear to be activated into their M1 (pro-inflammatory) phenotype, while the M2 (anti-inflammatory) phenotype is more prevalent in the subacute and delayed phases [160]. In the early phase of IS, the microglia initially demonstrate the M2-dominated activation which gradually changes into the M1 phenotype in peri-infarct regions. It seems that ischemic neurons lead microglial polarization more toward the M1 phenotype [161]. There is also evidence that while inhibiting inflammatory cytokines contributes to the protective activity of CX3CL1, it also reduces microglial activation, keeping these cells in a “switched off” state [121]. In rodent models, the intracerebroventricular administration of exogenous CX3CL1 provides a long-lasting neuroprotective effect against cerebral ischemia [162]. In our study, CX3CL1 levels on Day 5–7 were significantly higher in DCI patients, which also coincides with the time of microglia polarization of M2 phenotype. The CX3CL1/CX3CR1 axis may play a protective role after SAH by attenuating microglial activation [163]; thus, the elevated levels of CX3CL1 in the late phase of aSAH may also contribute to the pathogenesis of DCI through its effect on microglia.

Two possible mechanisms arise in aSAH: (i) high levels of CX3CL1 may indicate protective mechanisms; (ii) this increase is inadequate to avoid DCI. Based on our findings, a delayed elevation of CX3CL1 in patients with DCI rather suggests an overexpression of CX3CL1 as an adaptive mechanism, and not the insufficient CX3CL1 expression contributing per se to DCI development. In contrast, in patients without DCI, the level of secondary ischemic damage does not reach the necessary threshold required for the induction of CX3CL1 expression.

In rat models, MCP-1 was found to have a significantly increased expression in the major cerebral arteries during CV [164]. It was demonstrated earlier that MCP-1 concentration measured in the CSF of SAH patients increased between day 1 and 5, peaking at day 3, followed by a gradual decrease thereafter [165]. In rat brains at twelve hours following ischemia, a marked increase of MCP-1 mRNA was observed, which was sustained in the ischemic cortex up to 5 days post-ischemic injury [166]. In our study, MCP-3 concentrations were significantly higher on Day 5–7 in patients with DCI compared with those without DCI,

regardless the presence of hospital-acquired infection. An increasing trend with a late peak at day 10 of MCP-3 was observed in CSF after SAH in humans [116]. This late peak reflects a more delayed activation post-SAH that may indicate an involvement of MCP-3 in the healing processes or the development of late complications such as late vasospasm and DCI.

In our cohort, both Day 5–7 serum MCP-3 and CX3CL1 levels were significantly higher in DCI patients, suggesting that high MCP-3 levels indicate marked inflammatory activity, which is part of the pathogenesis of DCI. At the same time, we did not find a statistically significant difference between the serum MCP-3 and CX3CL1 levels (both measured at the T2 time point) measured in patients who developed DCI before and after T2 sampling. Based on this, it cannot be clearly determined whether the increase in the detected markers is a consequence or a cause.

In terms of functional outcome, we found that early (Day 1) high levels of IP-10, MCP-3, and MIP-1b were correlated with Day 30 adverse outcome. Lower concentration of IP-10 at 24 h after aSAH was independently associated with DCI [167] and its concentrations increased significantly during the first 5 days after SAH and may play a role in the development of delayed ischemic neurological deficits through simultaneous activation of monocytes and lymphocytes [165]. Considering the fact that both IP-10 and MCP-3 peak only late in the course of SAH [116], and both have a potent chemoattractant for inflammatory cells, the association of their early high levels with poor outcome, as we found in our study, suggests a prominent role of inflammation in the pathophysiology of early aSAH.

During our investigations, we found that the serum level of IL-4 measured on Day 5–7 was significantly higher in TCD-positive patients than in TCD-negative ones. Our study supports the assumption that patients with DCI and a putatively larger inflammatory response mount an even greater compensatory anti-inflammatory response reflected by IL4 elevation. However, since the serum IL-4 level showed a correlation with TCD positivity and not with DCI, the increase in velocity detected with TCD in the arteries is a part of the development of DCI, but not the sole mechanism. Based on the above evidence, we can state that the significantly higher IL-4 level detected in TCD-positive patients shows the pathophysiological role of IL-4 in the development of vasospasm, which may be the basis of DCI.

On correlation analysis, although FGF-2 did not show a direct correlation with the outcome or the occurrence of DCI, a strong negative correlation was observed with IP-10 which was found to be associated with functional outcome. This novel association between IP-10 as a

marker influencing the post-aSAH outcome and FGF-2 suggests independent pathological pathways in the neuroinflammatory response after aSAH. Moreover, it also raises questions that require further studies to clarify the role of the FGF-2/FGFRs neurotrophic system in aSAH.

Our study has several limitations. Biomarker samples were only taken at two time points after aSAH, which limits the precise analysis of the long-term kinetics of the markers. The relatively lower number of cases also reduces the generalizability of our study. One of the reasons for this is that unfortunately, due to the medical emergency caused by COVID-19, long-term monitoring of patients in our institution was not possible in all cases due to limited access to medical personnel. This significantly limited the number of patients who could be screened. Sampling at two-time points is insufficient to provide further information on whether the observed increase in markers is a consequence or a cause.

VIII. Conclusion

The overall aim of this thesis was to explore the clinical utility of biomarkers potentially associated with acute IS and aSAH.

As a novelty, we investigated the matricellular protein periostin in humans in the hyperacute phase of acute IS. The major findings were the following:

- (i) Serum periostin level measured in the hyperacute phase of IS was significantly higher in patients with IS compared to healthy controls.
- (ii) The admission serum periostin level was significantly higher in patients with unfavorable outcome at 90-day follow-up.
- (iii) ASPECT score reflecting the collateral circulation was negatively, while NIHSS indicated the severity of IS was positively correlated with the systemic concentration of periostin.
- (iv) Periostin level measured on admission was independently associated with ASPECT score < 6 calculated on admission CT scan. Thus, serum periostin level at the time of admission may indirectly indicate the quality of the collateral network in the acute phase of IS.

We were also able to show that:

- (v) MCP-3 and CX3CL1 levels measured at 5–7 days (T2) after aSAH were significantly higher in patients with DCI compared to those without DCI.
- (vi) Early (Day 1) high levels of IP-10, MCP-3, and MIP-1b were correlated with Day 30 adverse outcome.
- (vii) Serum level of Il-4 measured on Day 5–7 was significantly higher in TCD-positive patients than in TCD-negative ones.

- (viii) Strong positive correlation was observed between IL-1b and FGF-2, a CX3CL1 and MCP-3, as well as between MCP-3 and FGF-2 on Day 1. On Day 5-7, the correlation only remained strong between MCP-3 and CX3CL1.
- (ix) Serum level of FGF-2 showed a strong negative correlation with serum level of IP-10 in patients with favorable 30-Day outcome.

Periostin may be a useful laboratory marker to identify patients with a poor collateral network. If randomized controlled studies with a higher number of cases confirm our results, measuring periostin serum levels could be developed into a point-of-care diagnostic test, which facilitates the prehospital selection of patients suitable for neurointervention. Additionally, as our results suggest, several biomarkers are associated with DCI, but their pathophysiological role remains unknown. Some of the markers found in our study may hold promise in predicting disease and could be potential therapeutic targets for personalized treatment strategies in the future.

IX. Own findings

1. The systemic matricellular protein periostin is an early prognostic marker in patients with IS.
2. The serum periostin level at the time of admission may indirectly indicate the quality of the collateral network in the acute phase of IS.
3. Early elevation in serum concentration of IP-10, MCP-3, and MIP-1b shows association with 30-day poor outcome in patients with aSAH.
4. MCP-3 and CX3CL1 levels measured at 5–7 post-SAH days predict DCI.

X. List of publications and presentations

List of publications

Spantler D., Molnar T., Simon D., Berki T., Buki A., Schwarcz A., Csecsei P. Biomarker associations in delayed cerebral ischemia after aneurysmal subarachnoid hemorrhage, *Int. J. of Molecular Sciences*, 2022, 23, 8789. <https://doi.org/10.3390/ijms23158789>

IF: 6,208

Spantler D., Csecsei P., Borocz K., Berki T., Zavori L., Schwarcz A., Lenzser G., Molnar T. Serum Periostin May Help to Identify Patients with Poor Collaterals in the Hyperacute Phase of Ischemic Stroke. *Diagnostics* 2022, 12, 1942. <https://doi.org/10.3390/diagnostics12081942>

IF: 3,992

List of presentations

Osijek student congress (OSCON) 2022

Presentation title: Comparison of external ventricular drain related infections before vs during the COVID-19 Pandemic

Magyar Aneszteziológiai és Intenzív Terápiás Társaság (MAITT) congress 2023

Presentation title: Periostin és a kollaterális hálózat kapcsolata ischaemiás stroke hiperakut fázisában (MAITT Szabad előadások I. díj)

MedPECS congress 2023

Presentation title: Association between serum periostin level and poor collaterals in the hyperacute phase of ischemic stroke

XI. Acknowledgement

I would like to express my gratitude to my supervisors Tihamér Molnár and Péter Csécsei for their useful advice, professional support and guidance.

I am grateful to Erzsébet Ezer and the employees of the Intensive Care Unit at the Department of Neurosurgery.

I would like to thank the Department of Immunology and Biotechnology for measuring biomarker levels.

XII. References

1. Warlow C.P. Epidemiology of stroke. *Lancet* 1998, 352, 3,1–4.
2. Sacco R.L., Kasner S.E., Broderick J.P. et al. An Updated Definition of Stroke for the 21st Century, A Statement for Healthcare Professionals From the American Heart Association/American Stroke Association. *Stroke* 2013, 44, 2064–2089. <https://doi.org/10.1161/STR.0b013e318296aeca>
3. Donkor E.S. Stroke in the 21st Century: A Snapshot of the Burden, Epidemiology, and Quality of Life. *Stroke Research and Treatment* 2018. <https://doi.org/10.1155/2018/3238165>
4. McKay J., Mensah G.A., Mendis S., Greenlund K. The Atlas of Heart Disease and Stroke. *WHO* 2004.
5. Payne G.H., Fang J., Fogle C.C. et al. Stroke Awareness: Surveillance, Educational Campaigns, and Public Health Practice. *Journal Public Health Management Practice* 2010, 16(4), 345–358. <https://doi.org/10.1097/PHH.0b013e3181c8cb79>
6. Metias M.M., Eisenberg N., Clemente M.D. et al. Public health campaigns and their effect on stroke knowledge in a high-risk urban population: A five-year study. *Vascular* 2017, 0,1-7. . <https://doi.org/10.1177/1708538117691879>
7. Xing L., Jing L., Tian Y. et al. High prevalence of stroke and uncontrolled associated risk factors are major public health challenges in rural northeast China: A population-based study. *International Journal of Stroke* 2019, 0, 1-13. <https://doi.org/10.1177/1747493019851280>
8. Maida C.D., Norrito R.L., Daidone M. et al. Neuroinflammatory Mechanisms in Ischemic Stroke: Focus on Cardioembolic Stroke, Background, and Therapeutic Approaches. *International Journal of Molecular Sciences* 2020, 21, 6454. <https://doi.org/10.3390/ijms21186454>
9. Kuriakose D., Xiao Z. Pathophysiology and Treatment of Stroke: Present Status and Future Perspectives. *International Journal of Molecular Sciences* 2020, 21, 7609. <https://doi.org/10.3390/ijms21207609>
10. Morotti A., Poli L., Costa P. Acute Stroke. *Seminars in Neurology* 2019, 39, 61-72. <https://doi.org/10.1055/s-0038-1676992>.
11. World Health Organization, Prevention of Cardiovascular Disease: Guidelines for Assessment and Management of Cardiovascular Risk. 2007. http://apps.who.int/iris/bitstream/10665/43685/1/9789241547178_eng.pdf.
12. Feigin V.L., Norrving B., George M.G., et al. Prevention of stroke: A strategic global imperative. *Nature Reviews Neurology* 2016, 12(9), 501– 512. <https://doi.org/10.1038/nrneurol.2016.107>

13. Owolabi M.O., Ugoya S., Platz T. Racial disparity in stroke risk factors: The Berlin-Ibadan experience; A retrospective study. *Acta Neurologica Scandinavica* 2009, 119(2), 81–87. <https://doi.org/10.1111/j.1600-0404.2008.01077.x>
14. Tolhurst R., Rowlands I. Stroke: long-term management. *Clinical Pharmacist* 2011, 3(7), 209–212.
15. Salter K.L., Moses M.B., Foley N.C., et al. Health-related quality of life after stroke: What are we measuring? *International Journal of Rehabilitation Research* 2008, 31(2), 111–117. <https://doi.org/10.1097/MRR.0b013e3282fc0f33>
16. Yin S., Njai R., Barker L. et al. Summarizing health-related quality of life (HRQOL): development and testing of a one-factor model. *Population Health Metrics* 2016, 14, 22. <https://doi.org/10.1186/s12963-016-0091-3>.
17. Hopman W.M., Verner J., Quality of life during and after inpatient stroke rehabilitation. *Stroke* 2003, 34(3), 801–805. <https://doi.org/10.1161/01.STR.0000057978.15397.6F>
18. Hackett M.L., Duncan J.R., Anderson C.S., et al. Health-related quality of life among long-term survivors of stroke: Results from the Auckland stroke study, 1991-1992. *Stroke* 2000, 31(2), 440–447. <https://doi.org/10.1161/01.str.31.2.440>
19. Clarke P., Marshall V., Black S.E., et al. Wellbeing after stroke in Canadian seniors: Findings from the Canadian Study of Health and Aging. *Stroke* 2002, 33(4), 1016–1021. <https://doi.org/10.1161/01.str.0000013066.24300.f9>
20. Lai S.M., Studenski S., Duncan P.W., et al. Persisting consequences of stroke measured by the stroke impact scale. *Stroke* 2002, 33(7), 1840–1844. <https://doi.org/10.1161/01.str.0000019289.15440.f2>
21. NIH Definitions Working Group. (2000). Biomarkers and surrogate endpoints in clinical research: Definitions and conceptual model. *Biomarkers and Surrogate Endpoints* (pp. 1-9)
22. FitzGerald G. A. Measure for measure: Biomarker standards and transparency. *Science Translational Medicine* 2016, 8, 343fs10. <https://doi.org/10.1126/scitranslmed.aaf8590>
23. Bloom J.C. Biomarkers in clinical drug development: definitions and disciplines. In *Biomarkers in Clinical Drug Development*. Bloom JC, Dean RA. eds. 1st ed. Marcel Dekker, New York, 2003,132: p 1–10.
24. Rumbus Z., Matics R., Hegyi P., et al. Fever Is Associated with Reduced, Hypothermia with Increased Mortality in Septic Patients: A Meta-Analysis of Clinical Trials. *PLoS One* 2017, 12(1): e0170152. <https://doi.org/10.1371/journal.pone.0170152>
25. Aronson J.K., Ferner R.E. Biomarkers—A General Review. *Current Protocols in Pharmacology* 2017, 9.23.1–9.23.17. <https://doi.org/10.1002/cpph.19>
26. Anderson D.C., Kodukula K. Biomarkers in Pharmacology and Drug Discovery. *Biochemical Pharmacology* 2013. <http://dx.doi.org/10.1016/j.bcp.2013.08.026>

27. Biomarkers Definitions Working Group: Biomarkers and surrogate endpoints: preferred definitions and conceptual framework. *Clinical Pharmacology and Therapeutics* 2001, 69, 89. <https://doi.org/10.1067/mcp.2001.113989>
28. Szalmas PA. BIOMARKER KUTATÁSOK ONKOLÓGIAI, IMMUNPATOMECHANIZMUSÚ ÉS CSONTANYAGCSERE KÓRKÉPEKBEN, *MTA Doktori Értekezés* 2015.
29. Saini V., Guada L., Yavagal D.R. Global Epidemiology of Stroke and Access to Acute Ischemic Stroke Interventions. *Neurology* 2021, 16, 97:S6-S16. <https://doi.org/10.1212/WNL.0000000000012781>.
30. Etminan N., Chang H.S., Hackenberg K. et al. Worldwide Incidence of Aneurysmal Subarachnoid Hemorrhage According to Region, Time Period, Blood Pressure, and Smoking Prevalence in the Population. *JAMA Neurology* 2019, 76(5), 588–597. <https://doi.org/10.1001/jamaneurol.2019.0006>
31. O'Donnell M.J., Denis X., Liu L. et al. Risk factors for ischaemic and intracerebral haemorrhagic stroke in 22 countries (the INTERSTROKE study): a case-control study, *Lancet* 2010, 376(9735), 112–123. [https://doi.org/10.1016/S0140-6736\(10\)60834-3](https://doi.org/10.1016/S0140-6736(10)60834-3)
32. Sarfo F.S., Ovbiagele B., Gebregziabher M. et al. Stroke Among Young West Africans. *Stroke* 2018, 49(5), 1116–1122. <https://doi.org/10.1161/STROKEAHA.118.020783>
33. Adams Jr H.P., Bendixen B.H., Kappelle L.J., et al. Classification of subtype of acute ischemic stroke. Definitions for use in a multicenter clinical trial. TOAST. Trial of Org 10172 in Acute Stroke Treatment. *Stroke* 1993, 24, 35–41. <https://doi.org/10.1161/01.str.24.1.35>
34. Kim H., Kim J.T., Lee J.S., et al. Stroke of Other Determined Etiology: Results From the Nationwide Multicenter Stroke Registry. *Stroke* 2022, 53, 2597–2606. <https://doi.org/10.1161/STROKEAHA.121.037582>
35. Herpich F., Rincon F. Management of Acute Ischemic Stroke. *Clinical Care Medicine* 2020, 48, 11. <https://doi.org/10.1097/CCM.0000000000004597>
36. Bhatia K., Bhagavan S., Bains N. et al. Current endovascular treatment of acute ischemic stroke. *Missouri Medicine* 2020, 117(5), 480-499.
37. Jadhav A.P., Desai S.M., Liebeskind D.S. et al. Neuroimaging of Acute Stroke, *Neurologic Clinics* 2020, 38, 185–199. <https://doi.org/10.1016/j.ncl.2019.09.004>
38. Turc G., Tsivgoulis G., Audebert H.J. et al. European Stroke Organisation (ESO)–European Society for Minimally Invasive Neurological Therapy (ESMINT) expedited recommendation on indication for intravenous thrombolysis before mechanical thrombectomy in patients with acute ischemic stroke and anterior circulation large vessel occlusion. *Journal of NeuroInterventional Surgery* 2022, 14, 209–227. <https://doi.org/10.1136/neurintsurg-2021-018589>

39. Abou-Chebl A., Bajzer C.T., Krieger D.W. et al. Multimodal therapy for the treatment of severe ischemic stroke combining GPIIb/IIIa antagonists and angioplasty after failure of thrombolysis. *Stroke* 2005, 36, 2286–2288. <https://doi.org/10.1161/01.STR.0000179043.73314.4f>
40. Qureshi A.I., Harris-Lane P., Kirmani J.F. et al. Intra-arterial reteplase and intravenous abciximab in patients with acute ischemic stroke: An open-label, dose-ranging, phase I study. *Neurosurgery* 2006, 59, 789–796; discussion 796–787. <https://doi.org/10.1227/01.NEU.0000232862.06246.3D>
41. Khatri P., Hill M.D., Palesch Y.Y. et al. Methodology of the Interventional Management of Stroke (IMS) III Trial. *International Journal of Stroke* 2008, 3(2), 130–137. <https://doi.org/10.1111/j.1747-4949.2008.00151.x>
42. Chen J., Sun D., Liu M. et al. Therapy for Acute Ischemic Stroke: 1332 Consecutive Cases. *Scientific Reports* 2018, 8, 9489.
43. Hao Z., Liu M., Counsell C. et al. Fibrinogen depleting agents for acute ischaemic stroke. *Cochrane Database Systematic Reviews* 2012, 14(3):CD000091. <https://doi.org/10.1002/14651858.CD000091.pub2>
44. Levy D.E., Trammel J., Wasiewski W.W. For the Ancrod Stroke Program (ASP) Study Team. Ancrod for acute ischemic stroke: A new dosing regimen derived from analysis of prior ancrod stroke studies. *Journal of Stroke and Cerebrovascular Diseases* 2009, 18, 23–27. <https://doi.org/10.1016/j.jstrokecerebrovasdis.2008.07.009>
45. Higashida R.T., Furlan A.J., Roberts H. et al. Technology Assessment Committee of the American Society of Interventional and Therapeutic Neuroradiology; Technology Assessment Committee of the Society of Interventional Radiology: Trial design and reporting standards for intra-arterial cerebral thrombolysis for acute ischemic stroke. *Stroke* 2003, 34(8),e109–137. <https://doi.org/10.1161/01.STR.0000082721.62796.09>
46. Powers W.J., Derdeyn C.P., Biller J. et al. American Heart Association/American Stroke Association Focused Update of the 2013 Guidelines for the Early Management of Patients With Acute Ischemic Stroke Regarding Endovascular Treatment: A Guideline for Healthcare Professionals From the American Heart Association/American Stroke Association. *Stroke* 2015, 46(10), 3020-35. <https://doi.org/10.1161/STR.0000000000000074>
47. Goyal M., Menon B.K., van Zwam W.H. et al. Endovascular thrombectomy after large-vessel ischaemic stroke: a meta-analysis of individual patient data from five randomised trials. *Lancet* 2016, 387(10029), 1723-31. [https://doi.org/10.1016/S0140-6736\(16\)00163-X](https://doi.org/10.1016/S0140-6736(16)00163-X)
48. Albers G.W., Marks M.P., Kemp S. et al. DEFUSE 3 Investigators: Thrombectomy for stroke at 6 to 16 hours with selection by perfusion imaging. *New England Journal of Medicine* 2018, 378,708–718. <https://doi.org/10.1056/NEJMoa1713973>

49. Nogueira R.G., Jadhav A.P., Haussen D.C. et al. Thrombectomy 6 to 24 hours after stroke with a mismatch between deficit and infarct. *New England Journal of Medicine* 2018, 378, 11–21. <https://doi.org/10.1056/NEJMoa1706442>
50. Powers W.J., Rabinstein A.A., Ackerson T. et al. Guidelines for the Early Management of Patients With Acute Ischemic Stroke: 2019 Update to the 2018 Guidelines for the Early Management of Acute Ischemic Stroke: A Guideline for Healthcare Professionals From the American Heart Association/American Stroke Association. *Stroke* 2019, 50(12), 344-418. <https://doi.org/10.1161/STR.0000000000000211>
51. Pexman J.H.W., Barber P.A., Hill M.D. et al. Use of the Alberta stroke program early CT score (ASPECTS) for assessing CT scans in patients with acute stroke. *American Journal of Neuroradiology* 2001, 22, 1534-42.
52. Leira E., K. Muir K.. EXTEND trial. *Stroke* 2019, 50, 2637–2639. <https://doi.org/10.1161/STROKEAHA.119.026249>
53. Silver B., Arnold M. Implications of the WAKE-UP Trial. *Stroke* 2018, 49, 3115–3117. <https://doi.org/10.1161/STROKEAHA.118.022436>
54. Winship I.R. Cerebral Collaterals and Collateral Therapeutics for Acute Ischemic Stroke. *Microcirculation* 2015, 22(3), 228-36. <https://doi.org/10.1111/micc.12177>.
55. Nannoni S., Sirimarco G., Cereda C.W. et al. Determining factors of better leptomeningeal collaterals: a study of 857 consecutive acute ischemic stroke patients. *Journal of Neurology* 2019, 266(3), 582-588. <https://doi.org/10.1007/s00415-018-09170-3>
56. Grunwald I.Q., Kulikovski J., Reith W. et al. Collateral Automation for Triage in Stroke: Evaluating Automated Scoring of Collaterals in Acute Stroke on Computed Tomography Scans. *Cerebrovascular Diseases* 2019, 47, 217–222. <https://doi.org/10.1159/000500076>
57. Christoforidis G.A., Karakasis C., Mohammad Y. et al. Predictors of hemorrhage following intra-arterial thrombolysis for acute ischemic stroke: the role of pial collateral formation. *American Journal of Neuroradiology* 2009, 30, 165–70. <https://doi.org/10.3174/ajnr.A1276>
58. Christoforidis G.A., Mohammad Y., Kehagias D. et al. Angiographic assessment of pial collaterals as a prognostic indicator following intra-arterial thrombolysis for acute ischemic stroke. *American Journal of Neuroradiology* 2005, 26,1789–97.
59. Miteff F., Levi C.R., Bateman G.A. et al. The independent predictive utility of computed tomography angiographic collateral status in acute ischaemic stroke. *Brain* 2009, 132, 2231–8. <https://doi.org/10.1093/brain /awp155>
60. Vagal A., Menon B.K., Foster L.D. et al. Association Between CT angiogram collaterals and CT perfusion in the interventional management of stroke III trial. *Stroke* 2016, 47(2), 535–538. <https://doi.org/10.1161/STROKEAHA.115.011461>

61. Bang O.Y., Saver J.L., Kim S.J. et al. Collateral flow predicts response to endovascular therapy for acute ischemic stroke. *Stroke* 2011, 42(3), 693–699. <https://doi.org/10.1161/STROKEAHA.110.595256>
62. Dundamadappa S., Iyer K., Agrawal A. et al. Multiphase CT Angiography: A Useful Technique in Acute Stroke Imaging—Collaterals and Beyond. *American Journal of Neuroradiology* 2021, 42, 221–27. <http://dx.doi.org/10.3174/ajnr.A6889>
63. Dehkharghani S., Bammer R., Straka M. et al. Performance of CT ASPECTS and Collateral Score in Risk Stratification: Can Target Perfusion Profiles Be Predicted without Perfusion Imaging? *American Journal of Neuroradiology* 2016, 37, 1399–1404. <https://doi.org/10.3174/ajnr.A4727>
64. Seker F., Potreck A., Möhlenbruch M. et al. Comparison of four different collateral scores in acute ischemic stroke by CT angiography. *Journal of Neurointerventional Surgery* 2016, 8, 1116–1118. <https://doi.org/10.1136/neurintsurg-2015-012101>
65. Raza S.A., Barreira C.M., Rodrigues G.M. et al. Prognostic importance of CT ASPECTS and CT perfusion measures of infarction in anterior emergent large vessel occlusions. *Journal of Neurointerventional Surgery* 2019, 11, 670–674. <https://doi.org/10.1136/neurintsurg-2018-014461>
66. Izuhara K., Conway S.J., Moore B.B. et al. Roles of Periostin in Respiratory Disorders. *American Journal of Respiratory and Critical Care Medicine* 2016, 193, 949–956. <https://doi.org/10.1164/rccm.201510-2032PP>
67. Conway S.J., Izuhara K., Kudo Y. et al. A. The role of periostin in tissue remodeling across health and disease. *Cellular and Molecular Life Sciences* 2014, 71, 1279–1288. <https://doi.org/10.1007/s00018-013-1494-y>
68. Sonnenberg-Riethmacher E., Mieke M., Riethmacher D. Periostin in Allergy and Inflammation. *Frontiers in Immunology* 2021, 12, 722170. <https://doi.org/10.3389/fimmu.2021.722170>
69. Ma H., Wang J., Zhao X. et al. Periostin Promotes Colorectal Tumorigenesis through Integrin-FAK-Src Pathway-Mediated YAP/TAZ Activation. *Cell Reports* 2020, 30, 793–806. <https://doi.org/10.1016/j.celrep.2019.12.075>
70. Yoshida S., Umeno Y., Haruta M. Periostin in Eye Diseases. *Advances in Experimental Medicine and Biology* 2019, 1132, 113–124. https://doi.org/10.1007/978-981-13-6657-4_12
71. Wallace D.P. Periostin in the Kidney. *Advances in Experimental Medicine and Biology* 2019, 1132, 99–112. https://doi.org/10.1007/978-981-13-6657-4_11
72. Azharuddin M., Adil M., Ghosh P. et al. Periostin as a novel biomarker of cardiovascular disease: A systematic evidence landscape of preclinical and clinical studies. *Journal of Evidence Based Medicine* 2019, 12, 325–336. <https://doi.org/10.1111/jebm.12368>

73. Kühn B., Del Monte F., Hajjar R.J. et al. Periostin induces proliferation of differentiated cardiomyocytes and promotes cardiac repair. *Nature Medicine* 2007, 13, 962–969. <https://doi.org/10.1038/nm1619>
74. Dorn G.W.. Periostin and myocardial repair, regeneration, and recovery. *New England Journal of Medicine* 2007, 357, 1552–1554. <https://doi.org/10.1056/NEJMcibr074816>
75. Wu H., Xie J., Li G.N. et al. Possible involvement of TGF- β /periostin in fibrosis of right atrial appendages in patients with atrial fibrillation. *International Journal of Clinical and Experimental Pathology* 2015, 8, 6859–6869
76. Shimamura M., Taniyama Y., Katsuragi N. et al. Role of central nervous system periostin in cerebral ischemia. *Stroke* 2012, 43, 1108–1114. <https://doi.org/10.1161/STROKEAHA.111.636662>
77. Ma S.M., Chen L.X., Lin Y.F. et al. Periostin Promotes Neural Stem Cell Proliferation and Differentiation following Hypoxic-Ischemic Injury. *PLoS ONE* 2015, 10, e0123585. <https://doi.org/10.1371/journal.pone.0123585>
78. Matsunaga E., Namb, S., Oka M. et al. Periostin, a neurite outgrowth-promoting factor, is expressed at high levels in the primate cerebral cortex. *Development, Growth and Differentiation* 2015, 57, 200–208. <https://doi.org/10.1111/dgd.12194>
79. Dong X.Q., Yu W.H., Du Q. et al. Serum periostin concentrations and outcomes after severe traumatic brain injury. *Clinica Chimica Acta* 2017, 471, 298–303. <https://doi.org/10.1016/j.cca.2017.06.020>
80. Ji W.J., Chou X.M., Wu G.Q. et al. Association between serum periostin concentrations and outcome after acute spontaneous intracerebral hemorrhage. *Clinica Chimica Acta* 2017, 474, 23–27. <https://doi.org/10.1016/j.cca.2017.09.002>
81. Luo W., Wang H., Hu J. Increased concentration of serum periostin is associated with poor outcome of patients with aneurysmal subarachnoid hemorrhage. *Journal of Clinical Laboratory Analysis* 2018, 32, e22389. <https://doi.org/10.1002/jcla.22389>
82. He X., Bao Y., Shen Y. et al. Longitudinal evaluation of serum periostin levels in patients after large-artery atherosclerotic stroke: A prospective observational study. *Scientific Reports* 2018, 8, 11729. <https://doi.org/10.1038/s41598-018-30121-5>
83. de Rooij N.K., Linn F.H.H., van der Plas J.A. et al. Incidence of subarachnoid haemorrhage: a systematic review with emphasis on region, age, gender and time trends. *Journal of Neurology, Neurosurgery and Psychiatry* 2007, 78, 1365–1372. <https://doi.org/10.1136/jnnp.2007.117655>
84. Steiner T., Juvela S., Unterberg A. et al. European Stroke Organization Guidelines for the Management of Intracranial Aneurysms and Subarachnoid Haemorrhage. *Cerebrovascular Diseases* 2013, 35, 93–112. <https://doi.org/10.1159/000346087>

85. Wang Y., Emeto T.I., Lee J. et al. Mouse Models of Intracranial Aneurysm. *Brain Pathology* 2015, 25, 237–247. <https://doi.org/10.1111/bpa.12175>
86. Starke R.M., Chalouhi N., Ali M.S. et al. The Role of Oxidative Stress in Cerebral Aneurysm Formation and Rupture. *Current Neurovascular Research* 2013, 10(3), 247–255. <https://doi.org/10.2174/15672026113109990003>.
87. Chalouhi N., Points L., Pierce G.L. et al. Localized Increase of Chemokines in the Lumen of Human Cerebral Aneurysms. *Stroke* 2013, 44(9). <https://doi.org/10.1161/STROKEAHA.113.002361>.
88. Sehba F.A., Pluta R.M., Zhang J.H. Metamorphosis of Subarachnoid Hemorrhage Research: From Delayed Vasospasm to Early Brain Injury. *Molecular Neurobiology* 2011, 43, 27–40. <https://doi.org/10.1007/s12035-010-8155-z>
89. Macdonald R.L. Delayed neurological deterioration after subarachnoid haemorrhage. *Nature Reviews Neurology* 2014, 10, 44–58. <https://doi.org/10.1038/nrneuro.2013.246>.
90. Oliveira Manoel A, Goffi A., Marotta T.R. et al. The critical care management of poorgrade subarachnoid haemorrhage. *Critical Care* 2016, 20, 21. <https://doi.org/10.1186/s13054-016-1193-9>
91. Long B., Koyfman A., Runyon M.S. Subarachnoid Hemorrhage: Updates in Diagnosis and Management. *Emergency Medicine Clinics of North America* 2017, 35(4), 803-824. <https://doi.org/10.1016/j.emc.2017.07.001>
92. Manoel A.L., Turkel-Parrella D., Duggal A. et al. Managing aneurysmal subarachnoid hemorrhage: it takes a team. *Cleveland Clinic Journal of Medicine* 2015, 82(3),177-92. <https://doi.org/10.3949/ccjm.82a.14021>
93. Lawton M.T., Vates G.E. Subarachnoid Hemorrhage. *New England Journal of Medicine* 2017, 377(3), 257-66. <https://doi.org/10.1056/NEJMcp1605827>
94. Brown R.D., Broderick J.P. Unruptured intracranial aneurysms: epidemiology, natural history, management options, and familial screening. *Lancet* 2014, 13(4), 393-404. [https://doi.org/10.1016/S1474-4422\(14\)70015-8](https://doi.org/10.1016/S1474-4422(14)70015-8)
95. Heit J.J., Pastena X.G.T., Nogueira X.R.G. et al. Cerebral Angiography for Evaluation of Patients with CT Angiogram-Negative Subarachnoid Hemorrhage: An 11-Year Experience. *American Journal of Neuroradiology* 2016, 37, 297–304. <http://dx.doi.org/10.3174/ajnr.A4503>
96. Rouanet C., Sampaio Silva G. Aneurysmal subarachnoid hemorrhage: current concepts and updates. *Arquivos Neuro-Psiquiatria* 2019, 77(11). <https://doi.org/10.1590/0004-282X20190112>
97. Molyneux A.J., Kerr R.S., Yu L.M. et al. International subarachnoid aneurysm trial (ISAT) of neurosurgical clipping versus endovascular coiling in 2143 patients with ruptured intracranial aneurysms: a randomised comparison of effects on survival, dependency, seizures, rebleeding,

- subgroups, and aneurysm occlusion. *Lancet* 2005, 366(9488), 809-17.
[https://doi.org/10.1016/S0140-6736\(05\)67214-5](https://doi.org/10.1016/S0140-6736(05)67214-5)
98. Hunt W.E., Hess R.M. Surgical risk as related to time of intervention in the repair of intracranial aneurysms. *Journal of Neurosurgery* 1968, 28, 14–20.
<https://doi.org/10.3171/jns.1968.28.1.0014>
99. World Federation of Neurological Surgeons Committee: Report of World Federation of Neurological Surgeons Committee on a Universal Subarachnoid Hemorrhage Grading Scale. *Journal of Neurosurgery* 1988, 68, 985–986. <https://doi.org/10.3171/jns.1988.68.6.0985>
100. Takagi K., Tamura A., Nakagomi T. et al. How should a subarachnoid hemorrhage grading scale be determined? A combinatorial approach based solely on the Glasgow Coma Scale. *Journal of Neurosurgery* 1999, 90, 680–687.
<https://doi.org/10.3171/jns.1999.90.4.0680>
101. Frontera J.A., Claassen J., Schmidt J.M. et al. Prediction of symptomatic vasospasm after subarachnoid hemorrhage: the modified fisher scale. *Neurosurgery* 2006, 59(1), 21-7.
<https://doi.org/10.1227/01.NEU.0000218821.34014.1B>
102. Velat G.J., Kimball M.M., Mocco J. et al. Vasospasm after Aneurysmal Subarachnoid Hemorrhage: Review of Randomized Controlled Trials and Meta-Analyses in the Literature. *World Neurosurgery* 2011, 76, 446–454. <https://doi.org/10.1016/j.wneu.2011.02.030>
103. Flynn L., Andrews P. Advances in the understanding of delayed cerebral ischaemia after aneurysmal subarachnoid haemorrhage. *F1000 Faculty Reviews* 2015, 4, 1200.
<https://doi.org/10.12688/f1000research.6635.1>
104. Frontera J.A., Fernandez A., Schmidt J.M. et al. Defining vasospasm after subarachnoid hemorrhage: What is the most clinically relevant definition? *Stroke* 2009, 40, 1963–1968. <https://doi.org/10.1161/STROKEAHA.108.544700>
105. Vergouwen M.D.I., Vermeulen M., van Gijn J. et al. Definition of delayed cerebral ischemia after aneurysmal subarachnoid hemorrhage as an outcome event in clinical trials and observational studies: Proposal of a Multidisciplinary Research Group. *Stroke* 2010, 41(10), 2391-5. <https://doi.org/10.1161/STROKEAHA.110.589275>
106. Dodd W.S., Laurent D., Dumont A.S. et al. Pathophysiology of Delayed Cerebral Ischemia after Subarachnoid Hemorrhage: A Review. *Journal of American Heart Association* 2021, 10, e021845. <https://doi.org/10.1161/JAHA.121.021845>
107. Abdel-Tawab M., Hasan A.A., Ahmed M.A. et al. Prognostic factors of delayed cerebral ischemia after subarachnoid hemorrhage including CT perfusion: A prospective cohort study. *Egypt Journal of Radiology and Nuclear Medicine* 2020, 51, 61.
108. Alaraj A., Charbel F.T., Amin-Hanjani S. Peri-operative measures for treatment and prevention of cerebral vasospasm following subarachnoid hemorrhage. *Neurological Research* 2009, 31, 651–659. <https://doi.org/10.1179/174313209X382395>

109. Bacigaluppi S., Zona G., Secci F. et al. Diagnosis of cerebral vasospasm and risk of delayed cerebral ischemia related to aneurysmal subarachnoid haemorrhage: an overview of available tools. *Neurosurgery Review* 2015, 38, 603–618. <https://doi.org/10.1007/s10143-015-0617-3>
110. Grosset D.G., Straiton J., du Trevou M. et al. Prediction of Symptomatic Vasospasm After Subarachnoid Hemorrhage by Rapidly Increasing Transcranial Doppler Velocity and Cerebral Blood Flow Changes. *Stroke* 1992, 23, 674–679. <https://doi.org/10.1161/01.STR.23.5.674>
111. Snider S.B., Migdady I., LaRose S.L. et al. Transcranial Doppler-Measured Vasospasm Severity is Associated with Delayed Cerebral Infarction after Subarachnoid Hemorrhage. *Neurocritical Care* 2022, 36, 815–821. <https://doi.org/10.1007/s12028-021-01382-2>
112. Koenig H.M., Chen J., Sieg E.P. Delayed Cerebral Ischemia: Is Prevention Better than Treatment? *Journal of Neurosurgical Anesthesiology* 2021, 33, 191–192. <https://doi.org/10.1097/ANA.0000000000000773>
113. Douglas M.R., Daniel M., Lagord C. et al. High CSF transforming growth factor beta levels after subarachnoid haemorrhage: association with chronic communicating hydrocephalus. *Journal of Neurology, Neurosurgery and Psychiatry* 2009, 80(5), 545-50. <https://doi.org/10.1136/jnnp.2008.155671>.
114. Korbecki J, Siminska D., Kojder K. et al. Fractalkine/CX3CL1 in Neoplastic Processes. *International Journal of Molecular Sciences* 2020, 21, 3723. <https://doi.org/10.3390/ijms21103723>
115. Pawelec P., Ziemka-Nalecz M., Sypecka J. et al. The Impact of the CX3CL1/CX3CR1 Axis in Neurological Disorders. *Cells* 2020, 9, 2277. <https://doi.org/10.3390/cells9102277>
116. Vlachogiannis P., Hillered L., Enblad P. et al. Temporal patterns of inflammation-related proteins measured in the cerebrospinal fluid of patients with aneurysmal subarachnoid hemorrhage using multiplex Proximity Extension Assay technology. *PLoS ONE* 2022, 17, e0263460. <https://doi.org/10.1371/journal.pone.0263460>
117. Rancan M., Bye N., Otto V.I. et al. The Chemokine Fractalkine in Patients with Severe Traumatic Brain Injury and a Mouse Model of Closed Head Injury. *Journal of Cerebral Blood Flow and Metabolism* 2004, 24, 1110–1118. <https://doi.org/10.1097/01.WCB.0000133470.91843.72>
118. Lauro C., Catalano M., Trettel F. et al. Fractalkine in the nervous system: Neuroprotective or neurotoxic molecule? *Annals of New York Academy of Sciences* 2015, 1351, 141–148. <https://doi.org/10.1111/nyas.12805>

119. Zanier E.R., Marchesi F., Ortolano F. et al. Fractalkine Receptor Deficiency Is Associated with Early Protection but Late Worsening of Outcome following Brain Trauma in Mice. *Journal of Neurotrauma* 2016, 33, 1060–1072. <https://doi.org/10.1089/neu.2015.4041>
120. Tarozzo G., Campanella M., Ghiani M. et al. Expression of fractalkine and its receptor, CX3CR1, in response to ischaemia-reperfusion brain injury in the rat. *European Journal of Neuroscience*. 2002, 15, 1663–1668. <https://doi.org/10.1046/j.1460-9568.2002.02007.x>.
121. Cipriani R., Villa P., Chece G. et al. CX3CL1 Is Neuroprotective in Permanent Focal Cerebral Ischemia in Rodents. *Journal of Neuroscience* 2011, 31, 16327–16335. <https://doi.org/10.1523/JNEUROSCI.3611-11.2011>
122. Singh S., Anshita D., Ravichandiran V. MCP-1: Function, regulation, and involvement in disease. *International Immunopharmacology* 2021, 101, 107598. <https://doi.org/10.1016/j.intimp.2021.107598>
123. Taub D.D., Proost P., Murphy W.J. et al. Monocyte Chemotactic Protein-1 (MCP-1), -2, and -3 Are Chemotactic for Human T Lymphocytes. *Journal of Clinical Investigation* 1995, 95, 1370-1376.
124. Proost P., Wuyts A., van Damme J. Human monocyte chemotactic proteins-2 and -3: structural and functional comparison with MCP-1. *Journal of Leukocyte Biology* 1996, 59, 166-74. <https://doi.org/10.1002/jlb.59.1.67>
125. Dahinden C.A., Geiser T., Brunner T. et al. Monocyte chemotactic protein 3 is a most effective basophil- and eosinophil-activating chemokine. *Journal of Experimental Medicine* 1994, 179, 751–756. <https://doi.org/10.1084/jem.179.2.751>
126. Kim G.H., Kellner C.P., Hahn D.K. et al. Monocyte chemoattractant protein-1 predicts outcome and vasospasm following aneurysmal subarachnoid hemorrhage. *Journal of Neurosurgery* 2008, 109, 38–43. <https://doi.org/10.3171/JNS/2008/109/7/0038>.
127. Lei J., Yin X., Shang H. et al. IP-10 is highly involved in HIV infection, *Cytokine* 2019, 115, 97-103. <https://doi.org/10.1016/j.cyto.2018.11.018>
128. Ruffilli I., Ferrari S.M., Colaci M. et al. IP-10 in Autoimmune Thyroiditis. *Hormone and Metabolic Research* 2014, 46(09), 597-602. <https://doi.org/10.1055/s-0034-1382053>
129. Ransohoff R.M., Hamilton T.A., Tani M. et al.. Astrocyte expression of mRNA encoding cytokines IP-10 and JE/MCP-1 in experimental autoimmune encephalomyelitis. *FASEB Journal* 1993, 7, 592–600. <https://doi.org/10.1096/fasebj.7.6.8472896>.
130. Lahrtz F., Piali L., Nadal D. et al. Chemotactic activity on mononuclear cells in the cerebrospinal fluid of patients with viral meningitis is mediated by interferon- γ inducible protein-10 and monocyte chemotactic protein-1. *European Journal of Immunology* 1997, 27, 2484–2489. <https://doi.org/10.1002/eji.1830271004>

131. Rigny C., Turon R., De Freitas G. et al. Hemoglobin metabolism by-products are associated with an inflammatory response in patients with hemorrhagic stroke. Subprodutos do metabolismo da hemoglobina se associam com resposta inflamatória em pacientes com acidente vascular cerebral hemorrágico. *Revista Brasileira de Terapia Intensiva* 2018, 30, 21–27. <https://doi.org/10.5935/0103-507x.20180003>
132. Junttila I.S. Tuning the Cytokine Responses: An Update on interleukin (IL)-4 and IL-13 Receptor Complexes. *Frontiers in Immunology* 2018, 9, 888. <https://doi.org/10.3389/fimmu.2018.00888>
133. Al-Tamimi Y.Z., Bhargava D., Orsi N.M. et al. Compartmentalisation of the inflammatory response following aneurysmal subarachnoid haemorrhage. *Cytokine* 2019, 123, 154778. <https://doi.org/10.1016/j.cyto.2019.154778>
134. Eyang J., Eding S., Ehuang W. et al. Interleukin-4 Ameliorates the Functional Recovery of Intracerebral Hemorrhage through the Alternative Activation of Microglia/Macrophage. *Frontiers Neuroscience* 2016, 10, 61. <https://doi.org/10.3389/fnins.2016.00061>
135. Lopez-Castejon G., Brough D. Understanding the mechanism of IL-1 β secretion. *Cytokine and Growth Factor Reviews* 2011, 22(4), 189–195. <https://doi.org/10.1016/j.cytogfr.2011.10.001>
136. Weng X., Tan Y., Chu X. et al. N-methyl-D-aspartic acid receptor 1 (NMDAR1) aggravates secondary inflammatory damage induced by hemin-NLRP3 pathway after intracerebral hemorrhage. *Chinese Journal of Traumatology* 2015, 18, 254-258. <http://dx.doi.org/10.1016/j.cjtee.2015.11.010>
137. Asare K., Gee B.E., Stiles J.K. et al. Plasma interleukin-1beta concentration is associated with stroke in sickle cell disease. *Cytokine* 2010, 49, 39-44. <https://doi.org/10.1016/j.cyto.2009.10.002>
138. Wang Y., Pan X.F., Liu G.D. et al. FGF-2 suppresses neuronal autophagy by regulating the PI3K/Akt pathway in subarachnoid hemorrhage. *Brain Research Bulletin* 2021, 173, 132–140. <https://doi.org/10.1016/j.brainresbull.2021.05.017>.
139. Okada T., Enkhjargal B., Travis Z.D. et al. FGF-2 Attenuates Neuronal Apoptosis via FGFR3/PI3k/Akt Signaling Pathway after Subarachnoid Hemorrhage. *Molecular Neurobiology* 2019, 56, 8203–8219. <https://doi.org/10.1007/s12035-019-01668-9>
140. Akhter R., Shao Y., Formica S. et al. TREM2 alters the phagocytic, apoptotic and inflammatory response to A β 42 in HMC3 cells. *Molecular Immunology* 2021, 131, 171–179. <https://doi.org/10.1016/j.molimm.2020.12.035>
141. Lieschke S., Zechmeister B., Haupt M. et al. CCL11 Differentially Affects Post-Stroke Brain Injury and Neuroregeneration in Mice Depending on Age. *Cells* 2020, 9, 66. <https://doi.org/10.3390/cells9010066>





142. Liang C., Ni G., Ma J. et al. Impact of Tag Single Nucleotide Polymorphisms (SNPs) in CCL11 Gene on Risk of Subtypes of Ischemic Stroke in Xinjiang Han Populations. *Medical Science Monitor* 2017, 23, 4291-4298. <https://doi.org/10.12659/MSM.905942>
143. Roy-O'Reilly M., Ritzel R.M., Conway S.E. et al. CCL11 (Eotaxin-1) Levels Predict Long-Term Functional Outcomes in Patients Following Ischemic Stroke. *Translational Stroke Research* 2017, 8(6), 578–584. <https://doi.org/10.1007/s12975-017-0545-3>
144. Chalouhi N., Points L., Pierce G.L. et al. Localized Increase of Chemokines in the Lumen of Human Cerebral Aneurysms. *Stroke* 2013, 44(9). <https://doi.org/10.1161/STROKEAHA.113.002361>.
145. Li X., Lin S., Chen X. et al. The Prognostic Value of Serum Cytokines in Patients with Acute Ischemic Stroke. *Aging and disease* 2019, 10(3), 544-556. <http://dx.doi.org/10.14336/AD.2018.0820>
146. Garcia-Berrosoco T., Giralt D., Bustamante A. et al. Role of beta-defensin 2 and interleukin-4 receptor as stroke outcome biomarkers. International Society for Neurochemistry. *Journal of Neurochemistry* 2014, 129, 463–472. <https://doi.org/10.1111/jnc.12649>.
147. Latroche C., Weiss-Gayet M., Muller L. et al. Coupling between Myogenesis and Angiogenesis during Skeletal Muscle Regeneration Is Stimulated by Restorative Macrophages. *Stem Cell Reports* 2017, 9, 2018–2033. <https://doi.org/10.1016/j.stemcr>
148. Jiang W., Hu W., Ye L. et al. Contribution of Apelin-17 to Collateral Circulation Following Cerebral Ischemic Stroke. *Translational Stroke Research* 2019, 10, 298–307. <https://doi.org/10.1007/s12975-018-0638-7>
149. Turc G., Bhogal P., Fischer U. et al. European Stroke Organisation (ESO)—European Society for Minimally Invasive Neurological Therapy (ESMINT) Guidelines on Mechanical Thrombectomy in Acute Ischemic Stroke. *Journal of NeuroInterventional Surgery* 2019, 11, 535–538. <https://doi.org/10.1136/neurintsurg-2018-014569>
150. Liu A.Y., Zheng H., Ouyang G. Periostin, a multifunctional matricellular protein in inflammatory and tumor microenvironments. *Matrix Biology* 2014, 37, 150–156. <https://doi.org/10.1016/j.matbio.2014.04.007>
151. Liu L., Kawakita F., Fujimoto M. et al. Role of Periostin in Early Brain Injury After Subarachnoid Hemorrhage in Mice. *Stroke* 2017, 48, 1108–1111. <https://doi.org/10.1161/STROKEAHA.117.016629>
152. (Lux D., Alakbarzade V., Bridge L. et al. The association of neutrophillymphocyte ratio and lymphocyte-monocyte ratio with 3-month clinical outcome after mechanical thrombectomy following stroke. *Journal of Neuroinflammation* 2020, 17, 60. <https://doi.org/10.1186/s12974-020-01739-y>

153. Molnar T., Papp V., Banati M. et al. Relationship between C-reactive protein and early activation of leukocytes indicated by leukocyte antisedimentation rate (LAR) in patients with acute cerebrovascular events. *Clinical Hemorheology and Microcirculation* 2010, 44, 183–192. <https://doi.org/10.3233/CH-2010-1273>.
154. Mael-Ainin M., Abed A., Conway S.J. et al. Inhibition of periostin expression protects against the development of renal inflammation and fibrosis. *Journal of American Society of Nephrology* 2014, 25, 1724–1736. <https://doi.org/10.1681/ASN.2013060664>
155. Liu W., Zi M., Tsui H. et al. A novel immunomodulator, FTY-720 reverses existing cardiac hypertrophy and fibrosis from pressure overload by targeting NFAT (nuclear factor of activated T-cells) signaling and periostin. *Circulation Heart Failure* 2013, 6, 833–844. <https://doi.org/10.1161/CIRCHEARTFAILURE.112.000123>
156. Csecsei P., Pusch G., Ezer E. et al Relationship between Cardiac Troponin and Thrombo Inflammatory Molecules in Prediction of Outcome after Acute Ischemic Stroke. *Journal of Stroke and Cerebrovascular Diseases* 2018, 27, 951–956. <https://doi.org/10.1016/j.jstrokecerebrovasdis.2017.10.040>
157. Rudilosso S., Rodríguez-Vázquez A., Urra X. et al. The Potential Impact of Neuroimaging and Translational Research on the Clinical Management of Lacunar Stroke. *International Journal of Molecular Sciences* 2022, 23, 1497. <https://doi.org/10.3390/ijms23031497>
158. Segers V.F.M., Brutsaert D.L., De Keulenaer G.W. Cardiac Remodeling: Endothelial Cells Have More to Say Than Just NO. *Frontiers in Physiology* 2018, 9, 382. <https://doi.org/10.3389/fphys.2018.00382>
159. Schranz D., Molnar T., Erdo-Bonyar S. et al. Increased level of LIGHT/TNFSF14 is associated with survival in aneurysmal subarachnoid hemorrhage. *Acta Neurologica Scandinavica* 2021, 143, 530–537. <https://doi.org/10.1111/ane.13394>
160. Zheng Z.V., Wong K.C.G. Microglial activation and polarization after subarachnoid hemorrhage. *Neurology, Neuroimmunology and Neuroinflammation* 2019, 6, 1. <https://doi.org/10.20517/2347-8659.2018.52>
161. Wang G., Zhang J., Hu X. et al. Microglia/Macrophage Polarization Dynamics in White Matter after Traumatic Brain Injury. *Journal of Cerebral Blood Flow and Metabolism* 2013, 33(12), 1864–1874. <https://doi.org/10.1038/jcbfm.2013.146>
162. Pawelec P., Ziemka-Nalecz M., Sypecka J. et al The Impact of the CX3CL1/CX3CR1 Axis in Neurological Disorders. *Cells* 2020, 9, 2277. <https://doi.org/10.3390/cells9102277>
163. Chen X., Jiang M., Li H. et al. CX3CL1/CX3CR1 axis attenuates early brain injury via promoting the delivery of exosomal microRNA-124 from neuron to microglia after subarachnoid hemorrhage. *Journal of Neuroinflammation* 2020, 17(1), 209. <https://doi.org/10.1186/s12974-020-01882-6>

164. Lu H., Shi J.-X., Chen H.-L. et al. Expression of monocyte chemoattractant protein-1 in the cerebral artery after experimental subarachnoid hemorrhage. *Brain Research* 2009, 1262, 73–80. <https://doi.org/10.1016/j.brainres.2009.01.017>
165. Niwa A., Osuka K., Nakura T. et al. Interleukin-6, MCP-1, IP-10, and MIG are sequentially expressed in cerebrospinal fluid after subarachnoid hemorrhage. *Journal of Neuroinflammation* 2016, 13, 217. <https://doi.org/10.1186/s12974-016-0675-7>
166. Wang X., Li X., Yaish-Ohad S. et al. Molecular cloning and expression of the rat monocyte chemotactic protein-3 gene: A possible role in stroke. *Molecular Brain Research* 1999, 71, 304–312. [https://doi.org/10.1016/s0169-328x\(99\)00203-x](https://doi.org/10.1016/s0169-328x(99)00203-x)
167. Ahn S.H., Savarraj J., Parsha K. et al. Inflammation in delayed ischemia and functional outcomes after subarachnoid hemorrhage. *Journal of Neuroinflammation* 2019, 16, 1–10. <https://doi.org/10.1186/s12974-019-1578-1>.

Article

Serum Periostin May Help to Identify Patients with Poor Collaterals in the Hyperacute Phase of Ischemic Stroke

Dora Spantler¹, Peter Csecsei^{2,*}, Katalin Borocz³, Tímea Berki³, Laszlo Zavori⁴, Attila Schwarcz², Gabor Lenzser² and Tihamer Molnar¹

¹ Department of Anaesthesiology and Intensive Care and Department of Neurosurgery, Medical School, University of Pecs, 7624 Pecs, Hungary

² Department of Neurosurgery, Medical School, University of Pecs, 7624 Pecs, Hungary

³ Department of Immunology and Biotechnology, Medical School, University of Pecs, 7624 Pecs, Hungary

⁴ Salisbury NHS Foundation Trust, Salisbury SP2 8BJ, UK

* Correspondence: csecseipeti@yahoo.com; Tel.: +36-72535832

Abstract: Background: Periostin is a glycoprotein that mediates cell functions in the extracellular matrix and appears to be a promising biomarker in neurological damage, such as ischemic stroke (IS). We aimed to measure serum periostin levels in the hyperacute phase of ischemic stroke to explore its predictive power in identification of patients with poor collaterals (ASPECT < 6). Methods: We prospectively enrolled 122 patients with acute ischemic stroke within the first 6 h after onset. The early ischemic changes were evaluated by calculating ASPECT score on admission using a native CT scan. An unfavorable outcome was defined as the modified Rankin Scale (mRS) > 2 at 90 days follow-up. Blood samples were collected on admission immediately after CT scan and periostin serum concentrations were determined by ELISA. Results: The admission concentration of serum periostin was significantly higher in patients with unfavorable outcome than in patients with favorable outcome (615 ng/L, IQR: 443–1070 vs. 390 ng/L, 260–563, $p < 0.001$). In a binary logistic regression model, serum periostin level was a significant predictor for ASPECT < 6 status on admission, within 6 h after stroke onset (OR, 5.911; CI, 0.990–0.999; $p = 0.015$). Conclusion: Admission periostin levels can help to identify patients who are not suitable for neurointervention, especially if advanced neuroimaging is not available.

Keywords: hyperacute ischemic stroke; periostin; ASPECT; collaterals



Citation: Spantler, D.; Csecsei, P.; Borocz, K.; Berki, T.; Zavori, L.; Schwarcz, A.; Lenzser, G.; Molnar, T. Serum Periostin May Help to Identify Patients with Poor Collaterals in the Hyperacute Phase of Ischemic Stroke. *Diagnostics* **2022**, *12*, 1942. <https://doi.org/10.3390/diagnostics12081942>

Academic Editor: Ludmilla Morozova-Roche

Received: 21 July 2022

Accepted: 10 August 2022

Published: 11 August 2022

Publisher's Note: MDPI stays neutral with regard to jurisdictional claims in published maps and institutional affiliations.



Copyright: © 2022 by the authors. Licensee MDPI, Basel, Switzerland. This article is an open access article distributed under the terms and conditions of the Creative Commons Attribution (CC BY) license (<https://creativecommons.org/licenses/by/4.0/>).

1. Introduction

Ischemic stroke (IS) accounts for approximately 80% of all stroke cases and causes a tremendous burden on health resources and families [1]. Inflammation plays a pivotal role in the pathogenesis of IS exerting both beneficial and detrimental effects. The activation of resident cells, such as microglia, astrocytes, and endothelial cells, is neuroprotective and promotes brain regeneration and recovery, whilst the recruitment of immune cells expressing inflammatory mediators and leading to blood–brain barrier (BBB) disruption results in neuronal death, brain edema, and hemorrhagic transformation [2].

Periostin is a 93-kDa secreted N-glycoprotein that mediates cell-matrix interactions and cell functions in the extracellular matrix [3] and has been identified in many pathological conditions such as cardiovascular diseases, tumors, and airway inflammation [4–6]. Generally, periostin is expressed at low level in human tissues but can be rapidly upregulated by various pathophysiological signals [7]. Previous studies have revealed that periostin is rapidly secreted into ischemic tissue after acute myocardial infarction and has an essential role in the repair process [5,8]. Additionally, the neuroprotective and neurogenic effects of exogenous periostin have been demonstrated on both in vitro and in vivo IS models [9]. In patients with aneurysmal subarachnoid hemorrhage, a higher admission serum level of periostin was correlated with unfavorable 90-day outcome, worse admission neurological

status, larger hemorrhage volume and more frequent development of delayed cerebral ischemia [10]. He et al. have shown that increased serum periostin levels after IS might have been associated with higher National Institute of Health Stroke Scale (NIHSS) scores and more extensive stroke volume in patients with large-artery atherosclerotic stroke [11]. Several studies have proven that the ASPECT score is a simple and effective tool for assessing the collateral system by helping to estimate the core-penumbra ratio and thus the extent of the collateral network [12–15]. Based on the analysis of a large stroke register database, we know that better collaterals were associated with lower core volumes and higher ASPECT score, but not with higher penumbra volumes [16]. This suggests a major role of collaterals in early tissue loss. All the clinical studies that serve as the basis for the treatment of acute ischemic stroke lasting longer than 6 h [16,17] used core-based selection when conducting the study. Until now, there has not been a single clinically applicable serum biomarker that would indicate the core volume with high specificity and sensitivity and thus playing a role in clinical decision-making.

In the present study, we aimed to measure serum periostin levels at admission in patients with acute ischemic stroke and investigate whether it has predictive value or decision-making power in very early ischemic stroke by helping to estimate core volume.

2. Materials and Methods

2.1. Participants

This was a prospective observational study from a tertiary stroke treatment center in Pecs, Hungary. During the period between July 2019 and April 2021, a total of 122 patients with acute ischemic stroke within the first 6 h after onset were prospectively enrolled. Acute ischemic stroke was diagnosed according to WHO criteria [9]. As controls, we recruited fifteen age- and sex-matched healthy individuals. The following inclusion criteria were applied: (i) first-ever ischemic stroke, (ii) admission within 6 h after the index event. Exclusion criteria were as follows: (i) <18 years; (ii) previous ischemic or hemorrhagic stroke; (iii) pre-morbid modified Rankin score (mRS) > 1; (iv) active malignant or autoimmune disease; (v) immunosuppressive therapy; (vi) acute or chronic infection at study enrollment; (vii) severe hepatic or renal insufficiency; (viii) pregnancy. A flow chart of the study is shown in Figure 1. All procedures were performed in accordance with ethical guidelines of the 1975 Declaration of Helsinki. The study was approved by the Hungarian Medical Research Council. Written informed consent was given by each patient or their representatives before enrollment into the study.

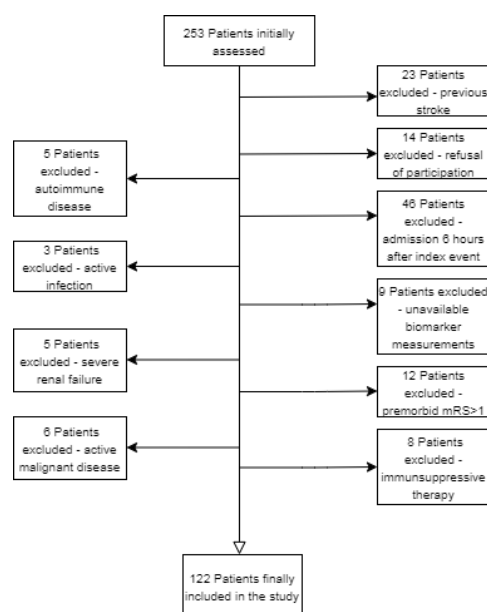


Figure 1. Flow chart illustrating excluded and included patients with acute ischemic stroke.

2.2. Clinical Protocol

Stroke severity was assessed using Glasgow Coma Scale (GCS) and NIHSS scores. The early ischemic changes were evaluated by ASPECT score calculated on admission using native cranial CT (NCCT) scan by a certified neuroradiologist who was blinded to the patients' clinical information. Unfavorable outcome was defined as an mRS score > 2 at 90 days after IS. Venous blood samples were collected on admission to stroke unit immediately after NCCT scan, but not later than 6 h after symptom onset. The patients received the standard stroke care: (i) within 4.5 h, if there were no contraindications, they received intravenous systemic recombinant tissue plasminogen activator (rtPA); if the possibility of large vessel occlusion arose (NIHSS > 8), CT angiography was performed; if a large vessel occlusion was confirmed (middle cerebral artery—M1, internal carotid artery or basilar artery), thrombectomy was also performed with (ii—EVT + rtPA) or without (iii—EVT alone) systemic thrombolysis. Patients with an ASPECT score < 6 on admission were considered to have a poor collateral network [13].

2.3. Laboratory Analysis

The blood samples were immediately centrifuged at 3500 r/min for 15 min and aliquots of other samples were immediately stored at -80°C before assay. Biomarker concentrations were measured by investigators blinded to the clinical outcome and neuroimaging findings. The serum periostin level was determined by the workers of the Department of Immunology and Biotechnology, University of Pecs, using ELISA-based kits manufactured by Shanghai YL Biotech Co., Shanghai, China. Samples were all processed by the same laboratory technician using the same equipment and blinded to all clinical data. The detection limit for the assay was 0.251 ng/L.

2.4. Statistical Analysis

Data were evaluated using SPSS (version 11.5; IBM, Armonk, NY, USA). Categorical data were summarized by means of absolute and relative frequencies (counts and percentages). The Kolmogorov–Smirnov test was applied to check for normality. The chi-square test for categorical data and Student's *t*-test as well as Mann–Whitney test for continuous data were used for the analysis of demographic and clinical factors. Non-normally distributed data are presented as median and interquartile range. Correlation analysis was performed calculating Spearman's correlation coefficient (r). To find an independent predictor of ASPECT < 6 , a binary logistic regression was used. Receiver operating characteristic (ROC) curve analysis was performed to evaluate the predictive values of serum periostin concentrations for 90-day unfavorable outcome. Subsequently, area under the curve (AUC) and the corresponding 95% CI were calculated. In a combined logistic-regression model, we estimated the additive benefit of periostin concentrations to NIHSS scores. A *p*-value < 0.05 was considered statistically significant.

3. Results

3.1. Clinical Characteristics

This cross-sectional study enrolled 122 patients with first-ever acute ischemic stroke. A flow chart of the study is shown in Figure 1, and Table 1 shows clinical profiles of patient groups based on their best mRS scores at 3-month as primary outcome measure. The median age of the patients was 71 years (interquartile range: 63–79, min-max. values: 30–91) and 39.3% were female. Fifteen healthy volunteers served as age-matched normal controls. The median age of controls was 66 (interquartile range (IQR): 55–73, range 46–82), and 46.7% were female. The age and sex differences between patients and controls were non-significant. Regarding comorbidities, 100 patients (82%) had hypertension, 35 patients (29%) had diabetes mellitus, and 34 patients (27.9%) presented with atrial fibrillation (AF). The median admission NIHSS score was 8 (IQR: 5–16, min-max: 1–32), and the median systolic and diastolic blood pressure on admission were 150 mmHg (IQR: 130–170, range: 90–240) and 84 mmHg (IQR: 80–93.5, range: 48–118). The median ASPECT score was

9 (IQR: 7–10, min-max: 1–10). In total, 29 patients (24%) underwent endovascular mechanical thrombectomy (EVT), 51 (42%) received intravenous systemic recombinant tissue plasminogen activator (rtPA) treatment, and 17 (14%) underwent a combined EVT + rtPA treatment. A total of 25 patients (20.5%) were not eligible neither for EVT nor for rtPA; therefore, they received conservative treatment. The median serum level of periostin was 498.4 ng/L (IQR, 305–783) in patients with IS, and 280.4 ng/L (IQR, 259–332) in healthy controls ($p < 0.001$, Figure 2A).

Table 1. Baseline characteristics of the study population. Continuous variables are expressed as medians (interquartile ranges). Categorical values are given as frequencies (percentages). Abbreviations: GCS, Glasgow coma scale; NIHSS, National Institutes of Health Stroke Scale; SBP, systolic blood pressure; DBP, diastolic blood pressure; ASPECTs, Alberta stroke programme early CT score; WBC, white blood cell; NLR, neutrophil–lymphocyte ratio; CRP, C-reactive protein; tPA, tissue plasminogen activator; * at 90-day follow-up.

Characteristics	Total (n = 122)	Favorable * Outcome (n = 59)	Unfavorable * Outcome (n = 63)	p-Value
Age, y, median (IQR)	71 (63–79)	71 (62–77)	73 (64–79)	0.127
Male, n (%)	74 (60.7%)	35 (59.3%)	39 (61.9%)	0.770
Hypertension, n (%)	100 (82%)	48 (81.4%)	52 (82.5%)	0.865
Diabetes, n (%)	35 (28.7%)	17 (28.8%)	18 (28.6%)	0.976
Smoking, n (%)	52 (38%)	19 (32.2%)	33 (52.4%)	0.024 *
Atrial fibrillation, n (%)	34 (27.9%)	7 (11.9%)	27 (42.9%)	<0.001 *
Large artery atherosclerosis, n (%)	59 (48.4%)	35 (59.3%)	24 (38.1%)	0.029
Lacunar, n (%)	23 (18.9%)	13 (22%)	10 (15.8%)	0.385
Other, n (%)	4 (3.3%)	3 (5.1%)	1 (1.6%)	0.278
Undetermined, n (%)	2 (1.5%)	1 (1.7%)	1 (1.7%)	0.899
GCS, median (IQR)	15 (12–15)	15 (15)	14 (11–15)	<0.001 *
NIHSS, median (IQR)	8 (5–16)	6 (4–8)	13 (8–19)	<0.001 *
SBP, median (IQR)	150 (130–170)	148 (130–170)	160 (138–180)	0.237
DBP, median (IQR)	84 (80–94)	82 (80–90)	86 (80–100)	0.463
ASPECTs, median (IQR)	9 (7–10)	10 (9–10)	8 (6–9)	<0.001 *
WBC, median (IQR)	8.4 (6.9–10.7)	7.7 (9–10)	8.8 (7–11)	0.264
NLR, median (IQR)	2.9 (2–5.6)	2.5 (1.7)	3.6 (2.5–7.3)	0.002 *
platelet, median (IQR)	242 (188–306)	245 (196–300)	238 (185–305)	0.625
creatinine, median (IQR)	86 (73–102)	83 (70–97)	87 (74–104)	0.411
glucose, median (IQR)	7.2 (6.2–8.9)	6.8 (5.9–8.1)	7.8 (6.8–9)	0.004 *
CRP, median (IQR)	3.7 (1.4–9.5)	2.6 (1.4–5.4)	5.1 (1.7–16)	0.042 *
Thrombectomy, n (%)	29 (23.8)	14 (23.7)	15 (23.8)	0.856
Intravenous tPA, n (%)	51 (41.8)	28 (47.5)	23 (36.5)	0.190
Thrombectomy plus intravenous tPA, n (%)	17 (13.9)	6 (10.2)	11 (17.5)	0.260
Conservative, n (%)	25 (20.5)	11 (18.6)	14 (22.2)	0.658
serum level of periostin, median (IQR), ng/L	462 (297–735)	390 (260–563)	615 (443–1070)	<0.001 *

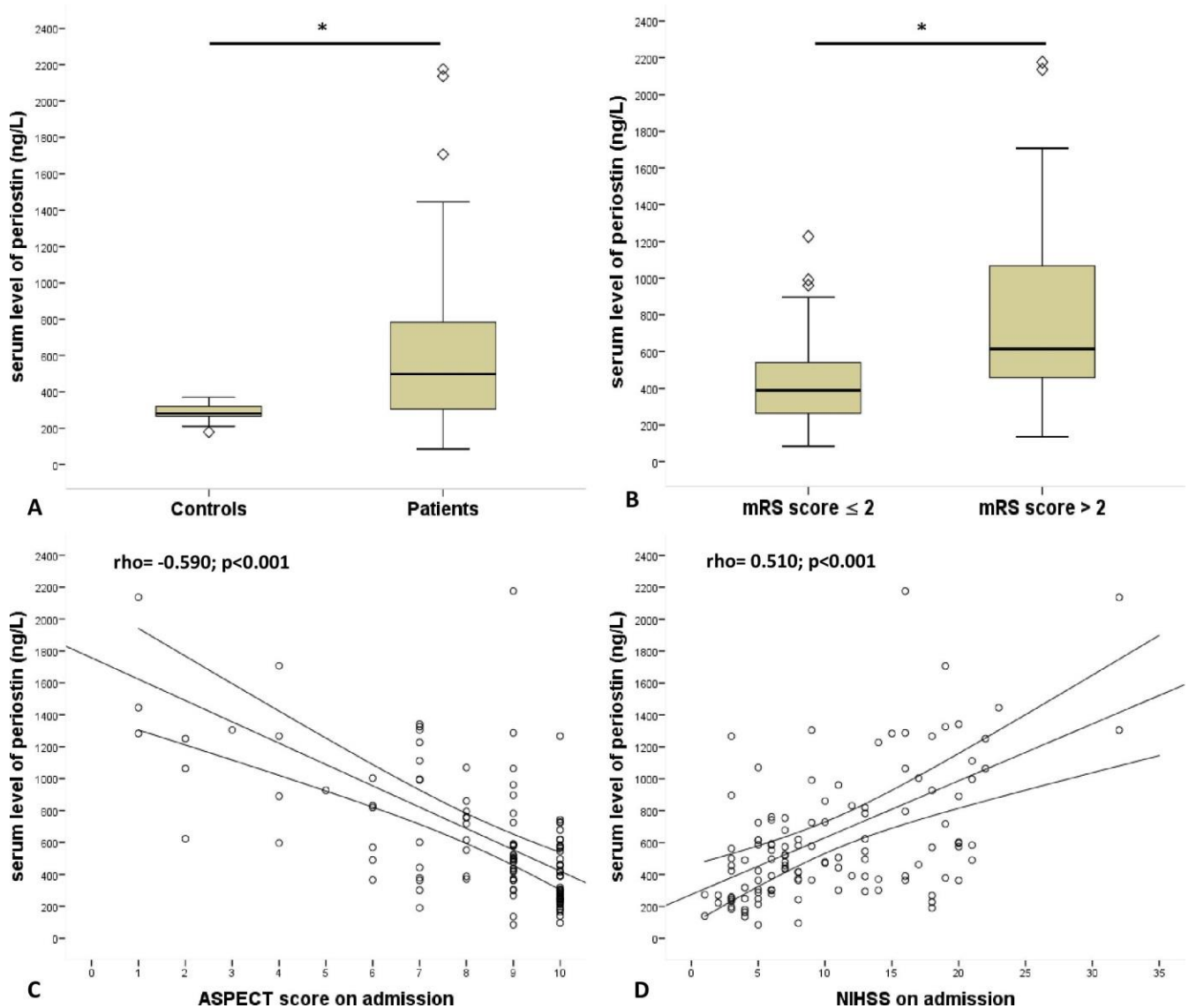


Figure 2. Comparison of serum periostin level (A) among patients with stroke and controls, (B) between patients with favorable outcome (mRS ≤ 2) vs. unfavorable outcome (mRS > 2) on Day 90 follow-up. Correlation of admission serum periostin level with (C) ASPECT score measured on admission and (D) NIHSS score recorded on admission. Serum periostin level was measured at 24 h after stroke onset. * p -value < 0.001 . ASPECT, Alberta stroke program early CT score; mRS, modified Rankin score; NIHSS, National Institutes of Health Stroke Scale. Statistical analysis were performed with Mann–Whitney U-test (A,B) and using Spearman rank correlation (C,D).

3.2. Admission Periostin Level, Comorbidities and Outcome

The admission serum periostin concentration was significantly higher in those patients who later had an unfavorable 90-day outcome compared to patients with favorable outcome (Figure 2B and Table 1). Moreover, the admission concentration of serum periostin showed an inverse correlation with ASPECT score (Figure 2C), while it was positively correlated with admission NIHSS score (Figure 2D). In multivariate analysis, we found positive associations between admission level of periostin and atrial fibrillation, admission white blood cell (WBC) count, neutrophile–lymphocyte ratio (NLR), creatinine, C-reactive protein (CRP), and glucose level (Table 2). In contrast, serum periostin level was negatively associated with GCS and ASPECT score, both measured at admission.

Table 2. Spearman correlation between admission clinical parameters and serum periostin level measured at 24 h after admission. Coefficient (r) values > 0 indicate a positive association; values < 0 indicate a negative association. Statistically significant values are given in bold. ASPECT, Alberta stroke program early CT score.

Variable	Spearman Correlation Coefficient (r)	p-Value
Atrial fibrillation	0.335	<0.001
Systolic blood pressure	0.068	0.459
Diastolic blood pressure	0.119	0.193
Glasgow Coma Scale	−0.308	<0.001
ASPECT score	−0.590	<0.001
White blood cell count, G/L	0.239	0.01
Neutrophil-lymphocyte ratio	0.328	<0.001
Creatinine, μmol/L	0.277	0.003
C-reactive protein, mg/L	0.285	0.002
Glucose, mmol/L	0.257	0.007
Platelet, G/L	−0.059	0.534
Carbamide, mmol/L	0.245	0.01

3.3. Variables Associated with Poor Collaterals

ASPECT score < 6 indicating patients with poor collaterals on admission was positively associated with admission GCS in univariate analysis. In contrast, diabetes, atrial fibrillation, admission NIHSS, periostin level, NLR, CRP as well as creatinine levels were inversely associated with ASPECT score < 6 calculated in univariate analysis. Age and sex were not shown correlation with ASPECT < 6. Although GCS, NIHSS, atrial fibrillation, CRP, diabetes, creatinine and NLR were adjusted in a binary logistic regression model, serum periostin level remained a significant predictor for ASPECT < 6 status on admission (OR, 5.911; CI, 0.990–0.999; $p = 0.015$, Table 3). Next, another binary logistic regression analysis was performed to explore independent predictors of the outcome: NIHSS on admission and atrial fibrillation were independently associated with a favorable 90-day outcome (mRS0–2). Based on ROC analysis, both NIHSS score (AUC, 0.817; 95% CI, 0.743–0.892, cutoff: 8.5, sensitivity: 75%, specificity: 78%, $p < 0.001$) and admission serum concentration of periostin (AUC, 0.757; 95%CI, 0.672–0.841, cutoff: 466.7 ng/L, sensitivity: 75 %, specificity: 65%, $p < 0.001$) showed similar sensitivity and specificity in the prediction of unfavorable 3-month outcome. In contrast, the combination of these two variables had significantly greater predictive power (AUC, 0.842; 95% CI, 0.773–0.911, $p < 0.001$) (Figure 3). The serum concentration of periostin with a cut-off value of ≥ 594.5 independently predicted admission ASPECT < 6 reflecting the poor collateral status with a sensitivity of 84.2% and specificity of 72%.

Table 3. Binary logistic regression analysis of predictors for admission ASPECT score < 6 in patients with acute ischemic stroke. CI, confidence interval. Model 1 included Glasgow Coma Scale and National Institute of Health Stroke Scale. Model 2 included variables in model 1 plus atrial fibrillation and admission level of C-reactive protein. Model 3 included variables in model 2 plus diabetes, admission serum level of creatinine and admission neutrophil-lymphocyte ratio.

	Odds Ratio	95% CI	p-Value
periostin	15.532	0.995–0.998	<0.001
Model 1	6.339	0.995–0.999	0.012
Model 2	5.917	0.993–0.999	0.015
Model 3	5.911	0.990–0.999	0.015

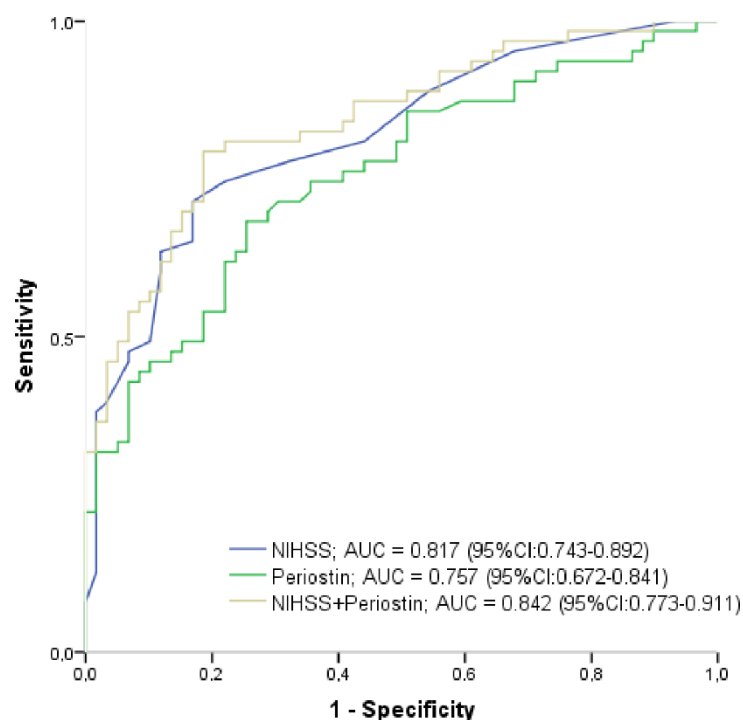


Figure 3. Receiver operating characteristic curve analysis of prognostic predictive ability of serum NIHSS score on admission, serum level of periostin on admission and the combination of NIHSS score and periostin for 3-month unfavorable outcome in patients with acute ischemic stroke. AUC, area under the curve; CI, confidence interval; NIHSS, National Institute of Health Stroke Scale.

4. Discussion

As a novelty, we investigated the matricellular protein periostin in humans in the hyperacute phase of acute ischemic stroke. The major findings were the following: (i) periostin level measured within 6 h after onset of the index event was significantly elevated in patients with unfavorable outcome at 90-day follow-up; (ii) ASPECT score reflecting the collateral circulation was negatively, while NIHSS indicated the severity of IS was positively correlated with systemic concentration of periostin; (iii) finally, periostin level measured on admission was independently associated with ASPECT score < 6 calculated on admission CT scan. Thus, serum periostin level at the time of admission indirectly indicates the quality of the collateral network in the acute phase of ischemic stroke.

Up to now, a growing evidence has suggested that periostin was expressed in high levels in primates and can enhance neurite outgrowth activity of the surrounding neurons [18]. Moreover, periostin significantly enhances neural stem cell proliferation and differentiation after hypoxic-ischemic injury [19]. The upregulation of periostin was also reported in a cerebrovascular clinical setting and in neuronal injury by head trauma. Dong et al. found that serum periostin concentration on admission was an independent predictor for 30-day mortality and overall survival after head trauma [20]. Another study by Ji et al. provided evidence that periostin concentrations of the sera from intracranial hemorrhage (ICH) patients were highly correlated with hematoma volume and baseline NIHSS scores; and serum periostin emerged as an independent predictor for 6-month unfavorable outcome after acute ICH [21]. Moreover, serum periostin concentrations resembled hematoma volume and NIHSS score in terms of predictive value assessed by AUCs for 6-month unfavorable outcome [21]. Lu et al. obtained similar results in a study of subarachnoid hemorrhage, with serum periostin levels showing an independent association with poor outcome and DCI [10]. Serum periostin levels were increased at 6 days and beyond at 4 weeks post-ischemia and were positively correlated with severity in terms of infarct volume and neurological deficit, but not with functional outcome in patients with large-artery

atherosclerotic stroke [11]. Interestingly, in this study the periostin level measured on the first day showed no difference compared to the values measured in the control group. In contrast, in our study, serum periostin levels measured in the hyperacute phase of IS were increased compared to healthy controls. Importantly, our study population shows several differences: (i) in etiology, as almost one-third of the total study population and 43% of the unfavorable outcome subgroup presented with atrial fibrillation on admission; (ii) inflammatory status, as CRP and NLR were higher in patients with poor 90-day outcome; and (iv) metabolic status, as plasma glucose level was significantly elevated among patients with poor outcome. In accordance with He et al., serum concentration of periostin showed strong correlation with NIHSS in our cohort. Additionally, we also find the relationship between systemic concentration of periostin measured in the acute phase of stroke and ASPECT score a valid assessment of the collateral circulation of the ischemic brain. Taken together, these may suggest that matricellular proteins (e.g., apelin, oncostatin M, and periostin) regulating myogenesis/angiogenesis and vessel formation during regeneration processes [22] may have an impact on the collateral circulation determining the salvageable penumbral brain tissue [23].

Based on the aforementioned clinical studies, periostin emerged as a novel prognostic marker in assessing the long-term outcome of diseases with severe neurological damage. However, there is a great need to find markers estimating the cerebral collaterals upon developing an acute ischemic insult. Periostin as a prehospital point-of-care marker might have the potential to provide information about the prior collateral status and the expected outcome, contributing to early diagnostics and the clinical decisionmaking of the stroke care team. In our study, we found that serum periostin concentration is an independent predictor of ASPECT < 6 calculated on admission, and this finding indicates that periostin could reflect the extent of early brain injury in hyperacute stage of ischemic stroke. According to the European Stroke Organisation—European Society for Minimally Invasive Neurological Therapy (ESMINT) Guidelines on Mechanical Thrombectomy in Acute Ischemic Stroke [24], patients with AIS with large vessel occlusion should be treated with mechanical thrombectomy plus best medical management up to approximately 7 h 18 min after stroke onset, without the need for perfusion imaging-based selection if patients have ASPECTS ≥ 6 and moderate-to-good collateral circulation. Since many studies [12–16] prove that ASPECT score is a sensitive marker of the ischemic core, and thus indirectly of the collateral network, its close correlation with periostin can act as an important diagnostic tool. Considering this, periostin as a surrogate marker measured within 6 h after acute stroke might contribute to establish the indication of mechanical thrombectomy in the lack of advanced neuroimaging.

However, the source of elevated periostin is not yet clear. Periostin is generally present at low levels in most adult tissues, but is highly expressed at sites of injury or inflammation and in tumors of adult organisms. Current evidence demonstrates that periostin actively contributes to tissue injury, inflammation, fibrosis and tumor progression [4]. Therefore, these extracerebral sources should be excluded prior to any therapeutic decisions. Given the acute increase in periostin level in our study in patients with poor outcome and ASPECT < 6, it is possible that the acute breakdown of the blood–brain barrier and leakage into circulation may be a significant source. Liu et al. demonstrated that periostin was upregulated in cerebral cortex after experimental SAH in mice and was responsible for early brain injury, which was possibly mediated by p38/ERK/MMP-9 signaling pathways [25]. Furthermore, in our cohort, CRP, NLR, and WBC showed a close correlation with admission periostin levels, indicating a possible link between the early immune response and post-ischemic brain injury. C-reactive protein and NLR have recently been reported as potential novel biomarkers of the baseline inflammatory process and could serve as outstanding predictors in patients with ischemic stroke [26]. Elevated levels of CRP after stroke have been related to poor functional outcome and mortality [27]. In asthma, periostin is recognized as a biomarker of type 2 inflammation and periostin (POSTN) gene expression is up-regulated in bronchial epithelial cells by IL-13 and IL-4 [6]. Our study also found a

strong positive association between atrial fibrillation and the admission level of periostin. As a matricellular protein, periostin has been proved to play an important role in fibrogenesis [28,29]. Wu et al. found that the upregulated expression of transforming growth factor β (TGF- β) and periostin in renin–angiotensin–aldosterone system (RAAS) is correlated with the degree of atrial fibrosis in patients with AF [30]. Furthermore, evidence of a recent review supports the potential role of periostin in the pathophysiology of cardiovascular diseases [31]. These findings suggest that the source of periostin, in addition to brain tissue damage that enters the systemic circulation through damage to the blood–brain barrier, may also be of myocardial origin.

Summarizing, initial periostin level may serve as a surrogate prognostic marker for hyperacute ischemic stroke reflecting stroke severity, long-term outcome, and patient's eligibility for intervention.

However, our study has several limitations. First, data about the changes of circulating periostin concentrations during the progression of ischemic stroke were not reported. Periostin kinetics could provide important information regarding the evolution of stroke. Second, only native and CT angiography were performed on admission, while MR would have been more suitable to determine the size of early infarction. As CT angiography-based collateral score calculation was not performed in all cases, we were not able to include it into our study. Third, various isoforms of periostin have been described in humans [9]; the ELISA kit used in our study detects all periostin isoforms present in the circulation and was not capable to differentiate between them. Fourth, we did not measure other conventional markers of both brain and heart tissue damage such as S100B or troponin, so it is unclear whether the measured periostin level is entirely of cerebral origin [32]. In addition, the relatively small number of cases in our study limits the generalizability of the study results. Therefore, further studies are warranted to explore the real specificity of periostin in early brain damage due to ischemia. As the pathophysiology, prognosis and clinical features of acute small vessel ischemic strokes are different from other types of cerebral infarcts, anethiology-based intergroup comparison of systemic concentration of periostin would be worthwhile in the future [33].

In conclusion, there is an urgent need to find reliable markers reflecting the collateral circulation in patients with acute IS either predicting the extension of early brain damage or supporting decision-making in cases where opportunities for advanced neuroimaging are limited. Reasonably, the concept of endothelial dysfunction as well as other vascular features related to cerebrovascular insults might have to be redefined as we learn more about multiple proteins (e.g., matricellular proteins) secreted by endothelial cells besides nitrogenoxide [34,35]. Overall, periostin may be a useful laboratory marker to identify patients with a poor collateral network and consequently with a more extensive core, especially when advanced neuroradiological procedures, e.g., CT perfusion, are not available. If randomized controlled studies with a higher number of cases confirm our results, measuring periostin serum levels could be developed into a point-of-care diagnostic test. Thus, the prehospital selection of patients suitable for neurointervention could be significantly improved.

Author Contributions: Conceptualization, P.C. and T.M.; methodology, K.B. and T.B.; software, K.B.; validation, T.M. and G.L.; formal analysis, D.S.; investigation, K.B.; resources, A.S.; data curation, P.C.; writing—original draft preparation, P.C., T.M. and D.S.; writing—review and editing, L.Z. and P.C.; visualization, P.C.; supervision, G.L.; project administration, T.M.; funding acquisition, A.S. All authors have read and agreed to the published version of the manuscript.

Funding: This research received no external funding.

Institutional Review Board Statement: The study protocol was approved by the Local Ethics Committee at University of Pecs, Faculty of Medicine and informed consent was obtained from each patient according to the “good clinical practice” (GCP) guidelines (35403-2/2017/EKU).

Informed Consent Statement: Informed consent was obtained from all subjects involved in the study.

Data Availability Statement: The data presented in this study are available on request from the corresponding author.

Acknowledgments: We would like to thank the staff of the Institute of Biotechnology for correct and accurate laboratory measurements.

Conflicts of Interest: The authors declare no conflict of interest.

References

1. Donnan, G.A.; Fisher, M.; Macleod, M.; Davis, S.M. Stroke. *Lancet* **2008**, *371*, 1612–1623. [[CrossRef](#)]
2. Jin, R.; Yang, G.; Li, G. Inflammatory mechanisms in ischemic stroke: Role of inflammatory cells. *J. Leukoc. Biol.* **2010**, *87*, 779–789. [[CrossRef](#)] [[PubMed](#)]
3. Järveläinen, H.; Sainio, A.; Koulu, M.; Wight, T.N.; Penttinen, R. Extracellular Matrix Molecules: Potential Targets in Pharmacotherapy. *Pharmacol. Rev.* **2009**, *61*, 198–223. [[CrossRef](#)] [[PubMed](#)]
4. Liu, A.Y.; Zheng, H.; Ouyang, G. Periostin, a multifunctional matricellular protein in inflammatory and tumor microenvironments. *Matrix Biol.* **2014**, *37*, 150–156. [[CrossRef](#)]
5. Kühn, B.; Del Monte, F.; Hajjar, R.J.; Chang, Y.S.; Lebeche, D.; Arab, S.; Keating, M.T. Periostin induces proliferation of differentiated cardiomyocytes and promotes cardiac repair. *Nat. Med.* **2007**, *13*, 962–969. [[CrossRef](#)]
6. Izuhara, K.; Conway, S.J.; Moore, B.B.; Matsumoto, H.; Holweg, C.T.J.; Matthews, J.G.; Arron, J.R. Roles of Periostin in Respiratory Disorders. *Am. J. Respir. Crit. Care Med.* **2016**, *193*, 949–956. [[CrossRef](#)]
7. Conway, S.J.; Izuhara, K.; Kudo, Y.; Litvin, J.; Markwald, R.; Ouyang, G.; Arron, J.; Holweg, C.T.J.; Kudo, A. The role of periostin in tissue remodeling across health and disease. *Cell. Mol. Life Sci.* **2014**, *71*, 1279–1288. [[CrossRef](#)]
8. Dorn, G.W., 2nd. Periostin and myocardial repair, regeneration, and recovery. *N. Engl. J. Med.* **2007**, *357*, 1552–1554. [[CrossRef](#)]
9. Shimamura, M.; Taniyama, Y.; Katsuragi, N.; Koibuchi, N.; Kyutoku, M.; Sato, N.; Allahtavakoli, M.; Wakayama, K.; Nakagami, H.; Morishita, R. Role of central nervous system periostin in cerebral ischemia. *Stroke* **2012**, *43*, 1108–1114. [[CrossRef](#)]
10. Luo, W.; Wang, H.; Hu, J. Increased concentration of serum periostin is associated with poor outcome of patients with aneurysmal subarachnoid hemorrhage. *J. Clin. Lab. Anal.* **2018**, *32*, e22389. [[CrossRef](#)]
11. He, X.; Bao, Y.; Shen, Y.; Wang, E.; Hong, W.; Ke, S.; Jin, X. Longitudinal evaluation of serum periostin levels in patients after large-artery atherosclerotic stroke: A prospective observational study. *Sci. Rep.* **2018**, *8*, 11729. [[CrossRef](#)] [[PubMed](#)]
12. Seker, F.; Potreck, A.; Möhlenbruch, M.; Bendszus, M.; Pham, M. Comparison of four different collateral scores in acute ischemic stroke by CT angiography. *J. Neurointerv. Surg.* **2016**, *8*, 1116–1118. [[CrossRef](#)] [[PubMed](#)]
13. Dehkharghani, S.; Bammer, R.; Straka, M.; Bowen, M.; Allen, J.W.; Rangaraju, S.; Kang, J.; Gleason, T.; Brasher, C.; Nahab, F. Performance of CT ASPECTS and Collateral Score in Risk Stratification: Can Target Perfusion Profiles Be Predicted without Perfusion Imaging? *AJNR* **2016**, *37*, 1399–1404. [[CrossRef](#)] [[PubMed](#)]
14. Nannoni, S.; Sirimarco, G.; Cereda, C.W.; Lambrou, D.; Strambo, D.; Eskandari, A.; Mosimann, P.J.; Wintermark, M.; Michel, P. Determining factors of better leptomeningeal collaterals: A study of 857 consecutive acute ischemic stroke patients. *J. Neurol.* **2019**, *266*, 582–588. [[CrossRef](#)]
15. Raza, S.A.; Barreira, C.M.; Rodrigues, G.M.; Frankel, M.R.; Haussen, D.C.; Nogueira, R.G.; Rangaraju, S. Prognostic importance of CT ASPECTS and CT perfusion measures of infarction in anterior emergent large vessel occlusions. *J. Neurointerv. Surg.* **2019**, *11*, 670–674. [[CrossRef](#)]
16. Nogueira, R.G.; Jadhav, A.P.; Haussen, D.C.; Bonafe, A.; Budzik, R.F.; Bhuva, P.; Yavagal, D.R.; Ribo, M.; Cognard, C.; Hanel, R.; et al. Thrombectomy 6 to 24 Hours after Stroke with a Mismatch between Deficit and Infarct. *NEJM* **2018**, *378*, 11–21. [[CrossRef](#)]
17. Albers, G.W.; Marks, M.P.; Kemp, S.; Christensen, S.; Tsai, J.P.; Ortega-Gutierrez, S.; McTaggart, R.A.; Torbey, M.T.; Kim-Tenser, M.; Leslie-Mazwi, T.; et al. Thrombectomy for Stroke at 6 to 16 Hours with Selection by Perfusion Imaging. *NEJM* **2018**, *378*, 708–718. [[CrossRef](#)]
18. Matsunaga, E.; Nambu, S.; Oka, M.; Tanaka, M.; Taoka, M.; Iriki, A. Periostin, a neurite outgrowth-promoting factor, is expressed at high levels in the primate cerebral cortex. *Dev. Growth Differ.* **2015**, *57*, 200–208. [[CrossRef](#)]
19. Ma, S.M.; Chen, L.X.; Lin, Y.F.; Yan, H.; Lv, J.W.; Xiong, M.; Li, J.; Cheng, G.Q.; Yang, Y.; Qiu, Z.L.; et al. Periostin Promotes Neural Stem Cell Proliferation and Differentiation following Hypoxic-Ischemic Injury. *PLoS ONE* **2015**, *10*, e0123585. [[CrossRef](#)]
20. Dong, X.Q.; Yu, W.H.; Du, Q.; Wang, H.; Zhu, Q.; Yang, D.B.; Che, Z.H.; Shen, Y.F.; Jiang, L. Serum periostin concentrations and outcomes after severe traumatic brain injury. *Clin. Chim. Acta* **2017**, *471*, 298–303. [[CrossRef](#)]
21. Ji, W.J.; Chou, X.M.; Wu, G.Q.; Shen, Y.F.; Yang, X.G.; Wang, Z.F.; Lan, L.X.; Shi, X.G. Association between serum periostin concentrations and outcome after acute spontaneous intracerebral hemorrhage. *Clin. Chim. Acta* **2017**, *474*, 23–27. [[CrossRef](#)] [[PubMed](#)]
22. Latroche, C.; Weiss-Gayet, M.; Muller, L.; Gitiaux, C.; Leblanc, P.; Liot, S.; Ben-Larbi, S.; Abou-Khalil, R.; Verger, N.; Bardot, P.; et al. Coupling between Myogenesis and Angiogenesis during Skeletal Muscle Regeneration Is Stimulated by Restorative Macrophages. *Stem Cell Rep.* **2017**, *9*, 2018–2033. [[CrossRef](#)] [[PubMed](#)]
23. Jiang, W.; Hu, W.; Ye, L.; Tian, Y.; Zhao, R.; Du, J.; Shen, B.; Wang, K. Contribution of Apelin-17 to Collateral Circulation Following Cerebral Ischemic Stroke. *Transl. Stroke Res.* **2019**, *10*, 298–307. [[CrossRef](#)] [[PubMed](#)]

24. Turc, G.; Bhogal, P.; Fischer, U.; Khatri, P.; Lobotesis, K.; Mazighi, M.; Schellinger, P.D.; Toni, D.; De Vries, J.; White, P.; et al. European Stroke Organisation (ESO)—European Society for Minimally Invasive Neurological Therapy (ESMINT) Guidelines on Mechanical Thrombectomy in Acute Ischemic Stroke. *J. Neurointerv. Surg.* **2019**, *11*, 535–538. [[CrossRef](#)]
25. Liu, L.; Kawakita, F.; Fujimoto, M.; Nakano, F.; Imanaka-Yoshida, K.; Yoshida, T.; Suzuki, H. Role of Periostin in Early Brain Injury After Subarachnoid Hemorrhage in Mice. *Stroke* **2017**, *48*, 1108–1111. [[CrossRef](#)]
26. Lux, D.; Alakbarzade, V.; Bridge, L.; Clark, C.; Clarke, B.; Zhang, L.; Khan, U.; Pereira, A.C. The association of neutrophil-lymphocyte ratio and lymphocyte-monocyte ratio with 3-month clinical outcome after mechanical thrombectomy following stroke. *J. Neuroinflamm.* **2020**, *17*, 60. [[CrossRef](#)]
27. Molnar, T.; Papp, V.; Banati, M.; Szereday, L.; Pusch, G.; Szapary, L.; Bogar, L.; Illes, Z. Relationship between C-reactive protein and early activation of leukocytes indicated by leukocyte antisedimentation rate (LAR) in patients with acute cerebrovascular events. *Clin. Hemorheol. Microcirc.* **2010**, *44*, 183–192. [[CrossRef](#)]
28. Mael-Ainin, M.; Abed, A.; Conway, S.J.; Dussaule, J.-C.; Chatziantoniou, C. Inhibition of periostin expression protects against the development of renal inflammation and fibrosis. *J. Am. Soc. Nephrol.* **2014**, *25*, 1724–1736. [[CrossRef](#)]
29. Liu, W.; Zi, M.; Tsui, H.; Chowdhury, S.K.; Zeef, L.; Meng, Q.J.; Travis, M.; Prehar, S.; Berry, A.; Hanley, N.A.; et al. A novel immunomodulator, FTY-720 reverses existing cardiac hypertrophy and fibrosis from pressure overload by targeting NFAT (nuclear factor of activated T-cells) signaling and periostin. *Circ. Heart Fail.* **2013**, *6*, 833–844. [[CrossRef](#)]
30. Wu, H.; Xie, J.; Li, G.N.; Chen, Q.H.; Li, R.; Zhang, X.L.; Kang, L.N.; Xu, B. Possible involvement of TGF- β /periostin in fibrosis of right atrial appendages in patients with atrial fibrillation. *Int. J. Clin. Exp. Pathol.* **2015**, *8*, 6859–6869.
31. Azharuddin, M.; Adil, M.; Ghosh, P.; Kapur, P.; Sharma, M. Periostin as a novel biomarker of cardiovascular disease: A systematic evidence landscape of preclinical and clinical studies. *J. Evid. Based Med.* **2019**, *12*, 325–336. [[CrossRef](#)] [[PubMed](#)]
32. Csecsei, P.; Pusch, G.; Ezer, E.; Berki, T.; Szapary, L.; Illes, Z.; Molnar, T. Relationship between Cardiac Troponin and Thrombo-Inflammatory Molecules in Prediction of Outcome after Acute Ischemic Stroke. *J. Stroke Cerebrovasc. Dis.* **2018**, *27*, 951–956. [[CrossRef](#)] [[PubMed](#)]
33. Rudilosso, S.; Rodríguez-Vázquez, A.; Urra, X.; Arboix, A. The Potential Impact of Neuroimaging and Translational Research on the Clinical Management of Lacunar Stroke. *Int. J. Mol. Sci.* **2022**, *23*, 1497. [[CrossRef](#)] [[PubMed](#)]
34. Segers, V.F.M.; Brutsaert, D.L.; De Keulenaer, G.W. Cardiac Remodeling: Endothelial Cells Have More to Say Than Just NO. *Front. Physiol.* **2018**, *9*, 382. [[CrossRef](#)] [[PubMed](#)]
35. Schranz, D.; Molnar, T.; Erdo-Bonyar, S.; Simon, D.; Berki, T.; Nagy, C.; Czeiter, E.; Buki, A.; Lenzser, G.; Csecsei, P. Increased level of LIGHT/TNFSF14 is associated with survival in aneurysmal subarachnoid hemorrhage. *Acta Neurol. Scand.* **2021**, *143*, 530–537. [[CrossRef](#)] [[PubMed](#)]



Article

Biomarker Associations in Delayed Cerebral Ischemia after Aneurysmal Subarachnoid Hemorrhage

Dora Spantler¹, Tihamer Molnar^{2,*}, Diana Simon³, Timea Berki³, Andras Buki⁴, Attila Schwarcz⁵
and Peter Csecsei⁵

¹ Department of Anaesthesiology and Intensive Care and Department of Neurosurgery, Medical School, University of Pecs, 7624 Pecs, Hungary

² Department of Anaesthesiology and Intensive Care, Medical School, University of Pecs, 7624 Pecs, Hungary

³ Department of Immunology and Biotechnology, Medical School, University of Pecs, 7624 Pecs, Hungary

⁴ Department of Neurosurgery, Faculty of Medicine and Health, Örebro University, 702 81 Örebro, Sweden

⁵ Department of Neurosurgery, Medical School, University of Pecs, 7624 Pecs, Hungary

* Correspondence: tihamermolnar2@yahoo.com

Abstract: The prognosis for patients with aneurysmal subarachnoid hemorrhage (aSAH) is heavily influenced by the development of delayed cerebral ischemia (DCI), but the adequate and effective therapy of DCI to this day has not been resolved. Multiplex serum biomarker studies may help to understand the pathophysiological processes underlying DCI. Samples were collected from patients with aSAH at two time points: (1) 24 h (Day 1) and (2) 5–7 days after ictus. Serum concentrations of eotaxin, FGF-2, FLT-3L, CX3CL1, IL-1b, IL-4, IP-10, MCP3, and MIP-1b were determined using a customized MILLIPLEX Human Cytokine/Chemokine/Growth Factor Panel A multiplex assay. The functional outcome was defined by the modified Rankin scale (favorable: 0–2, unfavorable: 3–6) measured on the 30th day after aSAH. One-hundred and twelve patients with aSAH were included in this study. The median level of CX3CL1 and MCP-3 measured on Days 5–7 were significantly higher in patients with DCI compared with those without DCI (CX3CL1: with DCI: 110.5 pg/mL, IQR: 82–201 vs. without DCI: 82.6, 58–119, $p = 0.036$; and MCP-3: with DCI: 22 pg/mL (0–32) vs. without DCI: 0 (0–11), $p < 0.001$). IP-10, MCP-3, and MIP-1b also showed significant associations with the functional outcome after aSAH. MCP-3 and CX3CL1 may play a role in the pathophysiology of DCI.

Keywords: aneurysmal subarachnoid hemorrhage; delayed cerebral ischemia; functional outcome; MCP-3; CX3CL1; IP-10



Citation: Spantler, D.; Molnar, T.; Simon, D.; Berki, T.; Buki, A.; Schwarcz, A.; Csecsei, P. Biomarker Associations in Delayed Cerebral Ischemia after Aneurysmal Subarachnoid Hemorrhage. *Int. J. Mol. Sci.* **2022**, *23*, 8789. <https://doi.org/10.3390/ijms23158789>

Academic Editor: Antonio Pisani

Received: 9 July 2022

Accepted: 4 August 2022

Published: 7 August 2022

Publisher's Note: MDPI stays neutral with regard to jurisdictional claims in published maps and institutional affiliations.



Copyright: © 2022 by the authors. Licensee MDPI, Basel, Switzerland. This article is an open access article distributed under the terms and conditions of the Creative Commons Attribution (CC BY) license (<https://creativecommons.org/licenses/by/4.0/>).

1. Introduction

Despite only accounting for 5% of all strokes, aneurysmal subarachnoid hemorrhage (aSAH) imposes a significant health burden on society due to its estimated 40% mortality rate [1]. Medical complications following aSAH such as rebleeding, hydrocephalus, cerebral vasospasm, and delayed cerebral ischemia (DCI) contribute significantly to disease long-term functional outcome. The prognosis for patients with aSAH is heavily influenced by the development of delayed cerebral ischemia, but adequate and effective therapy of DCI to this day has not been resolved [2]. For decades, the condition was attributed to cerebral vasospasm (CV); however, about 20% of SAH patients develop DCI without evidence of CV and only 30% of patients with CV actually suffer from DCI [3]. Recent evidence suggests that several factors influence the development of DCI, such as vascular dysfunction, elevation of intracranial pressure (ICP), microthrombosis, autoregulatory failure, neuroinflammation, disruption of the blood–brain barrier (BBB), cell death, oxidative stress, and cortical spreading depolarization [4]. Vasospasm is only one of them. These factors, combined with direct injury caused by initial bleeding, form the phenomenon of early brain injury (EBI) [5]. EBI is thought to play an important role in the development

of DCI [6]. A consensus definition of DCI has been developed and is widely used [7]. However, the clinical diagnosis of DCI in conscious or sedated patients is particularly difficult as it is almost impossible to assess consciousness in a sedated patient [8]. In addition, the diagnosis of DCI is easier in patients who are fully conscious, but the prognostic factors affecting the effectiveness of the therapy still remain unknown. The only evidence-based strategy for the prevention and treatment of DCI is nimodipine, which can prevent and reverse spasm of small vessels but has no effect on vasospasm of larger vessels [9]. Endovascular strategies have been used for radiographic vasospasm, including balloon angioplasty and placement of intracranial stents [9]. Considering all this, a laboratory biomarker would be an ideal solution, which would enable timely, specific, and sensitive diagnosis of DCI in SAH patients. Unlike other diseases where serum biomarkers are routinely used, however, there are still no effective serum biomarkers in clinical practice for predicting DCI or monitoring therapeutic efficacy. The study of a single biomarker is not suitable for the complex characterization of the mechanisms underlying DCI, but the analysis of a comprehensive biomarker profile may be more appropriate [10]. To have a broader view of possible pathophysiological processes, we performed a multiplex serum biomarker analysis. The biomarkers measured in this study were selected according to the following criteria: (i) previously their role was investigated in animal models of ischemic stroke or SAH, such as eotaxin [11], fibroblast growth factor-2 (FGF-2) [12,13], chemokine (C-X3-C motif) ligand-1 (CX3CL1) [14], or interleukin-1b (Il-1b) [15]; (ii) its role in the case of SAH has already been investigated, but the studies mainly focused on its level in the CSF, such as monocyte chemoattractant protein-3 (MCP-3) [10]; or (iii) its pathophysiological role was primarily investigated in human ischemic stroke such as Fms related receptor tyrosine kinase-3 ligand (FLT-3L) [16] and in SAH (interferon gamma-induced protein 10, IP-10) [17,18], macrophage inflammatory protein 1-beta (MIP-1b) [17], and, further, a more detailed investigation may be promising in the case of SAH. The great variability of temporal patterns of inflammation-related proteins is an indicator of the complexity of the inflammatory response following aSAH. Their exact role is not easy to establish, especially considering the fact that many of these substances are described to play both a detrimental and a beneficial role in the disease course depending on the time after bleeding [10]. We planned to investigate the relationship of the above markers to DCI and the functional outcome and their relationship to each other in the present study.

2. Results

2.1. Patients' Characteristics

One-hundred and twelve patients with aSAH (Table 1) were included in this study. Patients were enrolled between November 2018 and December 2021. All (100%) of the aneurysms were secured by coiling. Patients had a mean age of 57 (SD13) and 62% were female. Of them, 38 patients with aSAH (34%) presented to the emergency department with a WFNS Grade I. Almost half of the patients had a history of arterial hypertension (43.8%) and 11% had a history of smoking. Nearly one-third of the patients had DCI (29.1%) during their in-hospital stay. A description of the of these aSAH patients is shown in Table 1.

Table 1. Patients characteristics. SAH, subarachnoid hemorrhage.

Number of Patients with Aneurysmal SAH, <i>n</i> = 112		
Age	(years, mean ± SD)	57 ± 13
Female	(N, %)	69 (61.6%)
Hypertension	(N, %)	49 (43.8%)
Diabetes	(N, %)	11 (9.8%)
Smoking	(N, %)	12 (10.7%)
Aneurysm location		

Table 1. Cont.

Number of Patients with Aneurysmal SAH, <i>n</i> = 112		
– Internal carotid artery	(N, %)	16 (14.3%)
– Middle cerebral artery	(N, %)	22 (19.6%)
– Anterior communicating artery	(N, %)	31 (27.7%)
– Posterior communicating artery	(N, %)	13 (11.6%)
– Anterior cerebral artery	(N, %)	14 (12.5%)
– Vertebrobasilar	(N, %)	16 (14.3%)
WFNS		
– 1	(N, %)	38 (33.9%)
– 2	(N, %)	24 (21.4%)
– 3	(N, %)	8 (7.1%)
– 4	(N, %)	14 (12.5%)
– 5	(N, %)	28 (25%)
modified Fischer grade		
– 1	(N, %)	1 (0.9%)
– 2	(N, %)	18 (16.1%)
– 3	(N, %)	57 (50.9%)
– 4	(N, %)	36 (32.1%)
Glasgow coma scale, on admission	median, IQR	13 (6–15)
Neutrophile-lymphocyte ratio, on admission	median, IQR	5.9 (4–10)
C-reactive protein, on admission	median, IQR	13 (4–61)
Creatinine, on admission	median, IQR	61 (50–72)
Extraventricular drainage	(N, %)	53 (47.3%)
Infection, CSF	(N, %)	7 (6.3%)
Infection, systemic	(N, %)	18 (16.1%)
Infection, CSF + systemic	(N, %)	5 (4.5%)
Mechanical ventilation	(N, %)	50 (44.6%)
Decompressive craniotomy	(N, %)	14 (12.5%)
Lumbar drainage	(N, %)	14 (12.5%)
Delayed cerebral ischemia	(N, %)	32 (29.1%)
Angiographic vasospasm	(N, %)	28 (28.3%)
Transcranial Doppler positivity	(N, %)	41 (41.8%)
Ischemic lesion on MRI	(N, %)	16 (15.8%)
Favorable outcome on Day 30 (mRS = 0–2)	(N, %)	58 (51.8%)
In-hospital death	(N, %)	15 (13.4%)

SAH, subarachnoid hemorrhage; WFNS, World Federation of Neurological Societies Score; MRI, magnetic resonance imaging; the categorical variables are displayed presented as frequency (%) and the continuous variables are displayed presented as mean \pm standard deviation (SD) or median with interquartile range (IQR).

2.2. Cytokines Associated with DCI and Functional Outcome

None of the cytokines tested on Day 1 were associated with DCI, whereas only cytokines measured on Day (IP-10, MCP-3, MIP-1b) were associated with functional outcome (Table 2). CX3CL1 and MCP-3 measured on Days 5–7 were significantly higher in patients with DCI compared to those without DCI (CX3CL1: Day 5–7, without DCI: 82.6 pg/mL, IQR: 58–119 vs. Day 5–7, with DCI: 110.5 (82–201), $p = 0.036$ and MCP-3: Day 5–7, without DCI: 0 (0–11) vs. Day 5–7, with DCI: 22 (0–32), $p < 0.001$, Figure 1). Serum IP-10 levels in patients with poor outcomes were significantly higher than in patients with favorable outcomes at both time points (Day 1, favorable outcome: 74.7 pg/mL, IQR: 43–97 vs. Day 1, unfavorable outcome: 100, 68–146, $p = 0.005$ and Day 1, favorable outcome: 74.7 pg/mL, IQR: 43–97 vs. Day 5–7, unfavorable outcome: 98.8, 65–157, $p = 0.004$). For MCP-3 and MIP-1b, the serum concentrations measured on Day 1 showed significantly higher levels in patients with unfavorable outcome compared with the group with favorable Day 30 outcome (MCP-3: Day 1, favorable: 0 pg/mL, IQR: 0–15 vs. Day 1, unfavorable: 11.8, 0–25, $p = 0.045$ and MIP-1b: Day 1, favorable: 31.8 pg/mL, 23–42 vs. Day 1, unfavorable: 40, 28–56, $p = 0.025$, Figure 1).

Table 2. Cytokines associated with DCI during hospitalization and functional outcome on Day 30.

Cytokines	DCI during Hospitalization		mRSScore at Day 30	
	DCI – (n = 78 (71%)) vs. DCI + (n = 32 [29%])		Unfavorable Outcome (mRS ≥ 3, n = 54 (48.2%)) vs. Favorable Outcome (mRS ≤ 2, n = 58 (51.8%))	
	Day 1	Day 5–7	Day 1	Day 5–7
Eotaxin	-	-	-	-
FGF-2	-	-	-	-
FLT-3L	-	-	-	-
CX3CL1	-	H *	-	-
IL-1b	-	-	-	-
IL-4	-	-	-	-
IP-10	-	-	H *	-
MCP-3	-	H **	H *	-
MIP-1b	-	-	H *	-
Total	0	2	3	0

DCI, delayed cerebral ischemia; mRS, modified-Rankin scale; FGF-2, fibroblast growth factor-2; FLT-3L, Fms-related tyrosine kinase 3 ligand; CX3CL1, chemokine ligand 1, also known as fractalkine; IL-1b, interleukin-1b; IL-4, interleukin-4; IP-10, interferon gamma-induced protein 10, also known as C-X-C motif chemokine ligand 10 (CXCL10); MCP-3, Monocyte chemoattractant protein-3; MIP-1b, macrophage inflammatory protein 1-beta; H, high level; * $p < 0.05$; ** $p < 0.001$.

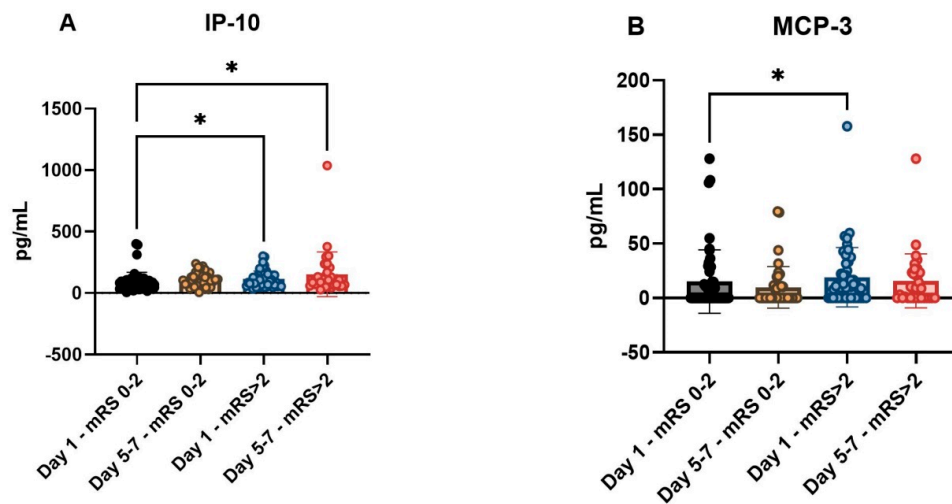


Figure 1. Cont.

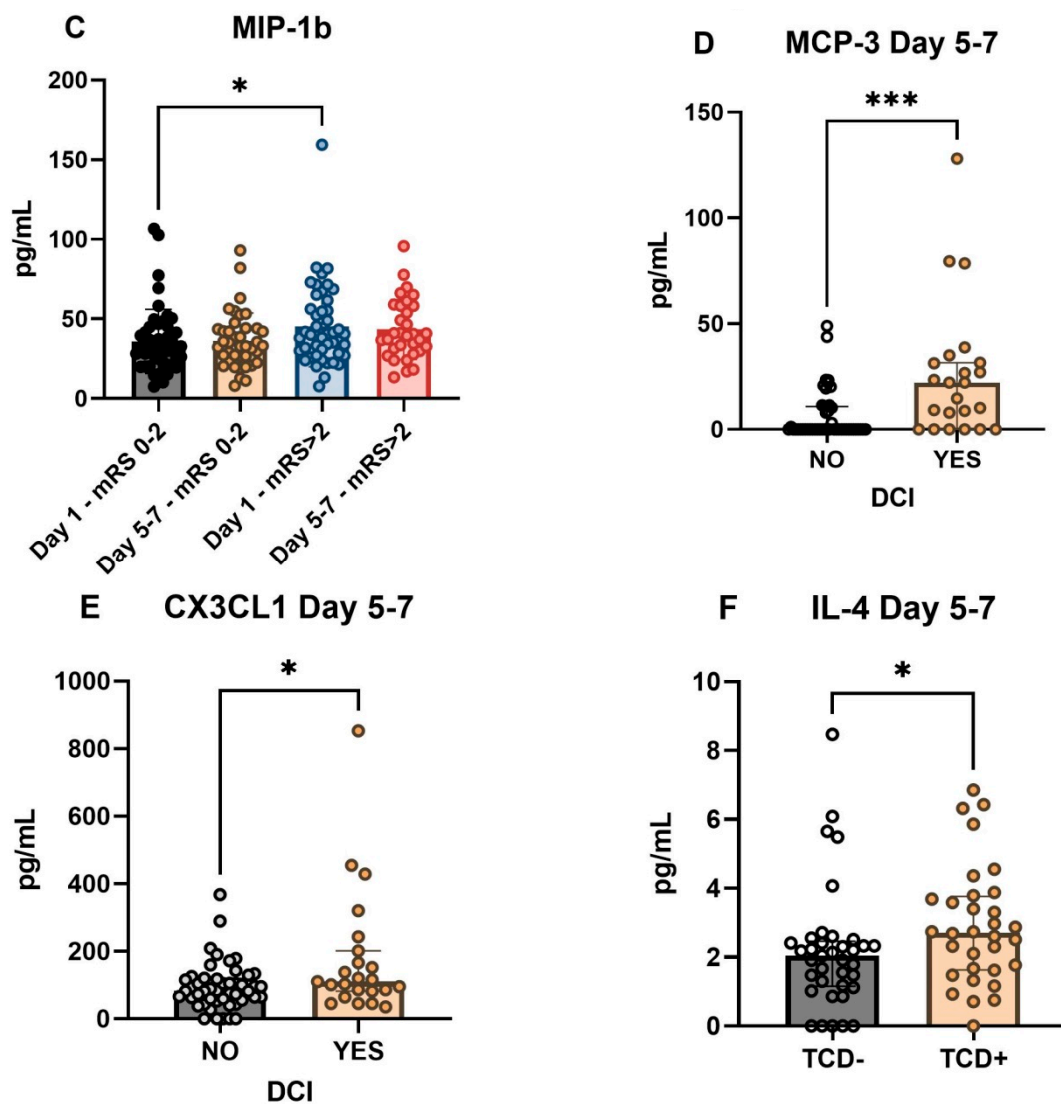


Figure 1. Characteristics of serum biomarker levels in different clinical subgroups in patients with aSAH. Correlation of the functional outcome with the investigated biomarkers, in the case of IP-10 (A), MCP-3 (B) and MIP-1b (C). Correlation of MCP-3 (D) and CX3CL1 (E) measured at T2 with DCI. Association of IL-4 (F) with TCD positivity. The functional outcome was examined 30 days after admission and characterized on the modified Rankin scale (mRS). Biomarker sampling times: Day 1, 24 h after aSAH, Day 5–7, 5–7 days after aSAH. DCI, delayed cerebral ischemia; aSAH, aneurysmal subarachnoid hemorrhage; TCD, transcranial Doppler ultrasound; CX3CL1, chemokine ligand 1, also known as fractalkine; IL-4, interleukin-4; IP-10, interferon gamma-induced protein 10, also known as C-X-C motif chemokine ligand 10 (CXCL10); MCP-3, Monocyte chemoattractant protein-3; MIP-1b, macrophage inflammatory protein 1-beta. * denotes $p < 0.05$, *** denotes $p < 0.001$.

In order to clarify how the increase of MCP-3 and CX3CL1 seen in DCI is related to the time of DCI, we performed an additional analysis. Average time of onset of DCI in our cohort was 6 ± 3.2 days (mean \pm SD). We grouped the DCI cases based on the sampling dates: the cases before T2 were in group A, while the cases after T2 were in group B, Table 3.

Table 3. Association of MCP-3 and CX3CL1 levels measured at T2 with the time of DCI detection.

	No DCI (<i>n</i> = 78)	Group A: DCI before T2 (<i>n</i> = 7)	Group B: DCI after T2 (<i>n</i> = 25)	<i>p</i> -Value (between A and B)
MCP-3 T2, pg/mL, median (IQR)	0 (0–11)	22 (8–27)	18 (0–32)	0.857
CX3CL1 T2, pg/mL, median (IQR)	83 (58–119)	116 (103–138)	106 (65–243)	0.691

T1, serum sample at Day 1 after aSAH; T2, serum sample at Day 5–7 after aSAH. DCI, delayed cerebral ischemia; MCP-3, Monocyte chemotactic protein-3; CX3CL1, chemokine ligand 1, also known as fractalkine.

2.3. Clinical Variables Associated with DCI and Day 30 Functional Outcome

We found no significant association between admission WFNS and Fischer scores and the development of DCI in aSAH patients. Similarly, there was no association between demographic (female, age) and clinical risk factors (hypertension, diabetes, smoking) and the emergence of DCI during hospital stay (Table 4). The admission GCS score was significantly lower in the DCI group than in the non-DCI group (DCI: 9, IQR: 5–14 vs. no DCI: 14, 10–15, $p = 0.02$). Decompressive craniotomy was required more frequently in the DCI group, but there was no difference between the two groups in terms of EVD use. Other factors related to DCI and Day 30 functional outcome are shown in Table 4. We found that regardless of whether the patient had an infection or not during hospitalization, the serum level of MCP-3 was significantly higher in the DCI group than in the non-DCI group. In contrast, de CX3CL1 concentration measured at T2 did not show a significant difference in the two groups of DCI, regardless of the presence of an infection (Table 5).

Table 4. Comparison of clinical and biochemical characteristics between patients with and without DCI and between patients with unfavorable vs. favorable outcome (Day 30) in patients with aneurysmal subarachnoid hemorrhage.

Variable	DCI		<i>p</i> -Value	Functional Outcome at Day 30		<i>p</i> -Value
	DCI (<i>n</i> = 32)	No-DCI (<i>n</i> = 78)		Unfavorable (<i>n</i> = 54)	Favorable (<i>n</i> = 58)	
Age (years, mean \pm SD)	54.8 \pm 11	57.9 \pm 14	0.223	61.8 \pm 12	52.6 \pm 12	<0.001
Female, N (%)	17 (53%)	50 (64%)	0.284	29 (53.7%)	40 (69%)	0.097
Hypertension, <i>n</i> (%)	11 (34.4%)	37 (47.4%)	0.210	28 (51.9%)	21 (36.2%)	0.095
Diabetes, <i>n</i> (%)	3 (9.4%)	8 (10.3%)	0.889	10 (18.5%)	1 (1.7%)	0.003
Smoking, <i>n</i> (%)	2 (6.3%)	10 (12.8%)	0.315	4 (7.4%)	8 (13.8%)	0.275
WFNS, median (IQR)	3 (1–5)	2 (1–4)	0.412	4 (3–5)	1 (1–2)	<0.001
modified Fischer grade, median (IQR)	3 (2–4)	3 (2–4)	1.000	4 (3–4)	2 (1–3)	<0.001
Glasgow coma scale, median (IQR)	9 (5–14)	14 (10–15)	0.02	6 (3–12)	14 (13–15)	<0.001
Neutrophile-lymphocyte ratio, median (IQR)	7 (5–10)	5 (3–11)	0.092	7 (4–12)	5.3 (3–8)	0.054
C-reactive protein, median (IQR)	24 (5–75)	9.5 (3–43)	0.104	41 (9–89)	6.8 (3–17)	<0.001
Creatinine, median (IQR)	61 (50–72)	60 (50–72)	0.744	63 (50–76)	59 (50–67)	0.122
Extraventricular drainage, <i>n</i> (%)	18 (56.3%)	33 (42.3%)	0.183	41 (75.9%)	12 (20.7%)	<0.001
Mechanical ventilation, <i>n</i> (%)	19 (59.4%)	29 (37.2%)	0.033	43 (79.6%)	7 (12.1%)	<0.001
Decompressive craniotomy, <i>n</i> (%)	8 (25%)	5 (6.4%)	0.006	11 (20.4%)	3 (5.2%)	0.015
Angiographic vasospasm, <i>n</i> (%)	27 (84.4%)	1 (1.5%)	<0.001	22 (52.4%)	6 (10.5%)	<0.001
Transcranial Doppler positivity, N (%)	30 (96.8%)	11 (16.4%)	<0.001	23 (54.8%)	18 (32.1%)	0.025

Table 4. Cont.

Variable	DCI		p-Value	Functional Outcome at Day 30		p-Value
	DCI (n = 32)	No-DCI (n = 78)		Unfavorable (n = 54)	Favorable (n = 58)	
Ischemic lesion on MRI, N (%)	16 (50%)	0 (0%)	<0.001	16 (35.6%)	0 (0%)	<0.001

Favorable outcome = modified Rankin score 0–2, unfavorable = 3–6. The categorical variables are presented as frequency and percentage, and the continuous variables are presented as mean ± standard deviation or median (percentile 25–75). The significances of inter-group differences were assessed using chi-square test or Fisher exact test for categorical data as well as Student t test or Mann–Whitney U test for continuous variables. IQR, interquartile range; DCI, delayed cerebral ischemia; WFNS, World Federation of Neurological Surgeons; MRI, magnetic resonance imaging.

Table 5. Correlation between the occurrence of infection the appearance of DCI and biomarker values in aSAH patients.

	No Infection			Infection during Hospitalization		
	No DCI	DCI	p-Value	No DCI	DCI	p-Value
CX3CL1 T2, pg/mL, median (IQR)	82 (53–118)	102 (46–201)	0.221	94 (60–179)	116 (95–166)	0.152

IQR, interquartile range; DCI, delayed cerebral ischemia; MCP-3, Monocyte chemotactic protein-3; CX3CL1, chemokine ligand 1, also known as fractalkine; T2, serum sample at Day 5–7 after aSAH.

2.4. Correlations between Biomarkers in aSAH Patients

Correlations for all measured serum biomarkers at both measurement time points were examined. The Spearman r coefficient of correlation between all these parameters is presented as a heat-map in Figure 2. The heat-map confirmed a positive and strong correlation between IL-1b and FGF-2, CX3CL1 and MCP-3, as well as between MCP-3 and FGF-2 at T1 time point. For biomarkers measured at T2, only the correlation between MCP-3 and CX3CL1 remained strong. For more correlations see Figure 2.

	Eotaxin T1	FGF-2 T1	FLT-3L T1	CX3CL1 T1	IL-1b T1	IL-4 T1	IP-10 T1	MCP-3 T1	MIP-1b T1	Eotaxin T2	FGF-2 T2	FLT-3L T2	CX3CL1 T2	IL-1b T2	IL-4 T2	IP-10 T2	MCP-3 T2	MIP-1b T2
Eotaxin T1	1.000	0.233	0.237	0.060	0.233	0.153	0.095	0.116	0.185	0.654	0.278	0.118	0.144	0.233	0.220	-0.122	0.208	0.039
FGF-2 T1	0.233	1.000	0.295	0.461	0.694	0.346	-0.086	0.524	0.151	0.259	0.724	0.367	0.257	0.580	0.219	-0.337	0.247	-0.116
FLT-3L T1	0.237	0.295	1.000	0.241	0.268	0.330	0.193	0.226	0.218	0.323	0.197	0.607	0.075	0.342	0.036	0.021	0.088	0.052
CX3CL1 T1	0.060	0.461	0.241	1.000	0.356	0.516	0.239	0.778	0.242	0.069	0.174	0.013	0.857	0.226	0.352	0.226	0.424	0.145
IL-1b T1	0.233	0.694	0.268	0.356	1.000	0.276	0.039	0.438	0.239	0.224	0.530	0.214	0.206	0.833	0.200	-0.181	0.210	0.102
IL-4 T1	0.153	0.346	0.330	0.516	0.276	1.000	0.261	0.435	0.235	0.163	0.134	0.084	0.395	0.180	0.694	0.064	0.223	0.121
IP-10 T1	0.095	-0.086	0.193	0.239	0.039	0.261	1.000	0.216	0.411	-0.184	-0.243	-0.071	0.085	-0.126	0.046	0.519	-0.076	0.371
MCP-3 T1	0.116	0.524	0.226	0.778	0.438	0.435	0.216	1.000	0.210	0.054	0.298	0.044	0.615	0.260	0.348	0.002	0.687	0.128
MIP-1b T1	0.185	0.151	0.218	0.242	0.239	0.235	0.411	0.210	1.000	0.038	0.017	0.055	0.073	0.140	0.013	0.177	-0.039	0.643
Eotaxin T2	0.654	0.259	0.323	0.069	0.224	0.163	-0.184	0.054	0.038	1.000	0.194	0.242	0.095	0.037	0.196	-0.112	0.053	-0.058
FGF-2 T2	0.278	0.724	0.197	0.174	0.530	0.134	-0.243	0.298	0.017	0.194	1.000	0.182	0.415	0.486	0.247	-0.413	0.445	-0.121
FLT-3L T2	0.118	0.367	0.607	0.013	0.214	0.084	-0.071	0.044	0.055	0.242	0.182	1.000	-0.019	0.203	0.071	0.044	0.018	0.149
CX3CL1 T2	0.144	0.257	0.075	0.857	0.206	0.395	0.085	0.615	0.073	0.095	0.415	-0.019	1.000	0.237	0.443	0.133	0.637	-0.022
IL-1b T2	0.233	0.580	0.342	0.226	0.833	0.180	-0.126	0.260	0.140	0.037	0.486	0.203	0.237	1.000	0.248	-0.213	0.325	0.035
IL-4 T2	0.220	0.219	0.036	0.352	0.200	0.694	0.046	0.348	0.013	0.196	0.247	0.071	0.443	0.248	1.000	0.008	0.430	0.107
IP-10 T2	-0.122	-0.337	0.021	0.226	-0.181	0.064	0.519	0.002	0.177	-0.112	-0.413	0.044	0.133	-0.213	0.008	1.000	-0.134	0.328
MCP-3 T2	0.208	0.247	0.088	0.424	0.210	0.223	-0.076	0.687	-0.039	0.053	0.445	0.018	0.637	0.325	0.430	-0.134	1.000	-0.096
MIP-1b T2	0.039	-0.116	0.052	0.145	0.102	0.121	0.371	0.128	0.643	-0.058	-0.121	0.149	-0.022	0.035	0.107	0.328	-0.096	1.000

Figure 2. Correlation between different serum biomarkers in patients with aSAH. (Note: red indicates that the two parameters were positively correlated, and blue indicates that the two parameters were negatively correlated; the darker the color, the stronger the correlation). T1, serum sample at Day 1 after aSAH; T2, serum sample at Day 5–7 after aSAH. FGF-2, fibroblast growth factor-2; FLT-3L, Fms-related tyrosine kinase 3 ligand; CX3CL1, chemokine ligand 1, also known as fractalkine; IL-1b, interleukin-1b; IL-4, interleukin-4; IP-10, interferon gamma-induced protein 10, also known as C-X-C motif chemokine ligand 10 (CXCL10); MCP-3, Monocyte chemotactic protein-3; MIP-1b, macrophage inflammatory protein 1-beta; aSAH, aneurysmal subarachnoid hemorrhage; Statistical method: Spearman.

The binary logistic regression analysis identified serum Day 5–7 MCP-3 levels as an independent predictor for DCI status, Table 6. Serum level of FGF-2 showed a strong negative correlation with serum level of IP-10 in patients with favorable outcome, while this correlation disappeared in the case of the group with an unfavorable outcome (Figure 3).

Table 6. Binary logistic regression model of independent predictors of DCI status after aSAH.

	B	Wald	Sig.	Exp(B)
MCP-3 T2	0.045	5.221	0.022	1.046
GCS on admission	−0.031	−0.062	0.803	0.97
Mechanical Ventilation	−0.954	0.638	0.424	0.385
Gender	−0.974	2.496	0.114	0.378
Age	−0.026	1.062	0.303	0.974
Constant	1.593	0.922	0.337	4.917

T2, sample time: Day 5–7 after aSAH; GCS, Glasgow coma scale; aSAH, aneurysmal subarachnoid hemorrhage; MCP-3, Monocyte chemotactic protein-3; DCI, delayed cerebral ischemia.

A	FGF-2 T1	CX3CL1 T1	IL-1b T1	IP-10 T1	MCP-3 T1	FGF-2 T2	CX3CL1 T2	IL-1b T2	IP-10 T2	MCP-3 T2
FGF-2 T1	1.000	0.523	0.684	−0.253	0.613	0.867	0.306	0.467	−0.420	0.320
CX3CL1 T1	0.523	1.000	0.369	0.137	0.730	0.121	0.872	0.195	0.049	0.564
IL-1b T1	0.684	0.369	1.000	−0.126	0.481	0.569	0.216	0.849	−0.345	0.211
IP-10 T1	−0.253	0.137	−0.126	1.000	0.090	−0.570	−0.034	−0.260	0.485	−0.158
MCP-3 T1	0.613	0.730	0.481	0.090	1.000	0.124	0.461	0.179	−0.165	0.729
FGF-2 T2	0.867	0.121	0.569	−0.570	0.124	1.000	0.480	0.495	−0.517	0.475
CX3CL1 T2	0.306	0.872	0.216	−0.034	0.461	0.480	1.000	0.235	0.011	0.697
IL-1b T2	0.467	0.195	0.849	−0.260	0.179	0.495	0.235	1.000	−0.366	0.295
IP-10 T2	−0.420	0.049	−0.345	0.485	−0.165	−0.517	0.011	−0.366	1.000	−0.164
MCP-3 T2	0.320	0.564	0.211	−0.158	0.729	0.475	0.697	0.295	−0.164	1.000
B	FGF-2 T1	CX3CL1 T1	IL-1b T1	IP-10 T1	MCP-3 T1	FGF-2 T2	CX3CL1 T2	IL-1b T2	IP-10 T2	MCP-3 T2
FGF-2 T1	1.000	0.409	0.722	0.068	0.465	0.708	0.260	0.712	−0.210	0.242
CX3CL1 T1	0.409	1.000	0.346	0.345	0.841	0.247	0.866	0.337	0.293	0.350
IL-1b T1	0.722	0.346	1.000	0.194	0.388	0.559	0.215	0.817	0.042	0.250
IP-10 T1	0.068	0.345	0.194	1.000	0.236	−0.006	0.194	−0.017	0.579	−0.115
MCP-3 T1	0.465	0.841	0.388	0.236	1.000	0.464	0.781	0.431	0.150	0.648
FGF-2 T2	0.708	0.247	0.559	−0.006	0.464	1.000	0.326	0.532	−0.300	0.374
CX3CL1 T2	0.260	0.866	0.215	0.194	0.781	0.326	1.000	0.291	0.246	0.559
IL-1b T2	0.712	0.337	0.817	−0.017	0.431	0.532	0.291	1.000	−0.050	0.396
IP-10 T2	−0.210	0.293	0.042	0.579	0.150	−0.300	0.246	−0.050	1.000	−0.108
MCP-3 T2	0.242	0.350	0.250	−0.115	0.648	0.374	0.559	0.396	−0.108	1.000

Figure 3. Correlation between serum biomarkers in different clinical subgroups ((A): favorable, *n* = 58; (B): unfavorable, *n* = 58). Unfavorable, mRS = 3–6 on Day 30; favorable, mRS = 0–2 on Day 30; DCI, delayed cerebral ischemia. (note: red indicates that the two parameters were positively correlated, and blue indicates that the two parameters were negatively correlated. The darker the color, the stronger the correlation). T1, serum sample at Day 1 after aSAH; T2, serum sample at Day 5–7 after aSAH. FGF-2, fibroblast growth factor-2; FLT-3L, Fms-related tyrosine kinase 3 ligand; CX3CL1, chemokine ligand 1, also known as fractalkine; IL-1b, interleukin-1b; IL-4, interleukin-4; IP-10, interferon gamma-induced protein 10, also known as C-X-C motif chemokine ligand 10 (CXCL10); MCP-3, Monocyte chemotactic protein-3; MIP-1b, macrophage inflammatory protein 1-beta; Statistical method: Spearman.

3. Discussion

In this prospective study, we were able to show that: (i) MCP-3 and CX3CL1 levels measured at 5–7 days (T2) after aSAH are associated with the occurrence of DCI, (ii) early (Day 1) high levels of IP-10, MCP-3, and MIP-1b were correlated with Day 30 adverse outcome, and (iii) the serum level of IL-4 measured on Day 5–7 was significantly higher in TCD-positive patients than in TCD-negative ones.

CX3CL1 was successfully analyzed in human CSF after aSAH with an increasing trend in concentration with a late peak at day 10 [10]. CX3CL1 expression is upregulated in intact neurons within the penumbra while both CX3CL1 and CX3CR1 expression are upregulated in infarcted brain in experimental stroke model in rats [14]. This protein may be involved in the inflammatory response to traumatic brain injury (TBI), particularly in the accumulation of leukocytes in the injured parenchyma [19]. CX3CL1 may have dual functions of being neuroprotective and anti-inflammatory in a variety of hypoxic and excitotoxic *in vitro* and *in vivo* models, while proinflammatory and contributing to neuronal damage in others [20]. It has a direct effect on microglia and has the ability to induce the release of soluble factors that orchestrate a neuroprotective response [20]. CX3CL1 and its receptor are involved in a complex network of both paracrine and autocrine interactions between neurons and glia and have a role in microglia polarization [21]. In the acute phase following SAH, the microglia mainly appear to be activated into their pro-inflammatory (M1) phenotype, while the anti-inflammatory (M2) phenotype is more prevalent in the subacute and delayed phases [21]. In the early phase of ischemic stroke, the microglia initially demonstrate the M2-dominated activation which gradually changes into the M1 phenotype in peri-infarct regions. It seems that ischemic neurons lead microglial polarization more towards the M1 phenotype [22]. There is also evidence that while inhibiting inflammatory cytokines contributes to the protective activity of CX3CL1, it also reduces microglial activation, keeping these cells in a “switched off” state [23]. In rodent models, the intracerebroventricular administration of exogenous CX3CL1 provides a long-lasting neuroprotective effect against cerebral ischemia [24]. In our study, CX3CL1 levels on Day 5–7 were significantly higher in DCI patients, which also coincides with the time of microglia polarization of the M2 phenotype. The CX3CL1/CX3CR1 axis may play a protective role after SAH by attenuating microglia activation [25]; thus, the elevated levels of CX3CL1 in the late phase of aSAH may also contribute to the pathogenesis of DCI through its effect on microglia. A study by Zanier E.R. et al. suggested that CX3CL1:CX3CR1 signaling exacerbates the toxic cascades at early time-points whereas it is needed for long-term recovery in TBI [26]. Exogenous CX3CL1 reduced ischemia-induced cerebral infarct size and neurological deficits in rats and these CX3CL1-induced neuroprotective effects mediated by microglia were long lasting, being observed up to 50 days after pMCAO in rats [23].

Two possible mechanisms arise in aSAH: (i) high levels of CX3CL1 may indicate protective mechanisms; (ii) this increase is inadequate to avoid DCI. Based on our findings, a delayed elevation of CX3CL1 in patients with DCI rather suggests an overexpression of CX3CL1 as an adaptive mechanism, and not the insufficient CX3CL1 expression contributing *per se* to DCI development. In contrast, in patients without DCI, the level of secondary ischemic damage does not reach the necessary threshold required for the induction of CX3CL1 expression.

The serum MCP-1 concentrations correlated with vasospasm in patients with SAH, whereas the serum MCP-1 levels did not correlate with DCI; at the same time, concentrations of MCP-1 in the CSF, however, proved to be significantly higher in patients with angiographically demonstrated vasospasm [27]. In rat models, MCP-1 was found to have a significantly increased expression in the major cerebral arteries during cerebral vasospasm [28]. It was demonstrated that MCP-1 concentration measured in the CSF of SAH patients increased between day 1 and 5, peaking at day 3, followed by a gradual decrease thereafter [18]. In rat brain at twelve hours following ischemia, a marked increase of MCP-1 mRNA was observed, which was sustained in the ischemic cortex up to 5 days

post-ischemic injury [29]. In humans, all MCPs have an overlapping chemoattractant activity on basophils and eosinophils, and they express strong chemoattractant features towards monocytes [30]. In our study, MCP-3 concentrations were significantly higher on Day 5–7 in patients with DCI compared with those without DCI, regardless the presence of hospital acquired infection. An increasing trend with a late peak at day 10 of MCP-3 was observed in CSF after SAH in humans [10]. This late peak reflects a more delayed activation post SAH that may indicate an involvement of MCP-3 in the healing processes or the development of late complications such as late vasospasm and DCI.

In our cohort, both Day 5–7 serum MCP-3 and CX3CL1 levels were significantly higher in DCI patients, suggesting that high MCP-3 levels indicate marked inflammatory activity, which is part of the pathogenesis of DCI. At the same time, we did not find a statistically significant difference between the serum MCP-3 and CX3CL1 levels (both measured at the T2 time point) measured in patients who developed DCI before and after T2 sampling. Based on this, it cannot be clearly determined whether the increase in the detected markers is a consequence or a cause.

In terms of functional outcome, we found that early (Day 1) high levels of IP-10, MCP-3, and MIP-1b were correlated with Day 30 adverse outcome. Lower concentration of IP-10 at 24 h after aSAH was independently associated with DCI [17] and its concentrations increased significantly during the first 5 days after SAH and may play a role in the development of delayed ischemic neurological deficits through simultaneous activation of monocytes and lymphocytes [18]. IP-10 have a transient burst of accumulation in the CNS during experimental autoimmune encephalitis (EAE), highlighting that astrocyte-derived IP-10 is a potential chemoattractant for inflammatory cells during EAE [31]. IP-10 and MCP-1 lead to accumulation of activated T cells and monocytes in the CSF compartment in the early stage of viral meningitis [32]. CSF level of iron and heme are associated with an inflammatory response (plasma levels of MIP-1b and IP-10) within the human brain after a hemorrhagic event, suggesting a causal relationship [33]. It has long been known that MCP-1, MCP-2, and MCP-3 are major attractants for human CD4+ and CD8+ T lymphocytes and monocytes [34,35]. Considering the fact that both IP-10 and MCP-3 peak only late in the course of subarachnoid hemorrhage [10], and both have a potent chemoattractant for inflammatory cells, the association of their early high levels with poor outcome, as we found in our study, suggests a prominent role of inflammation in the pathophysiology of early aSAH.

During our investigations, we found that the serum level of IL-4 measured on Day 5–7 was significantly higher in TCD-positive patients than in TCD-negative ones. TCD measurements of cerebral blood flow velocity are commonly used after aSAH to screen for vasospasm; however, their association with cerebral infarction is not well characterized and is still partially controversial [36–38]. In a very recent study, an early, mild, TCD-based vasospasm severity threshold had a high negative predictive value for DCI [39]. Al-Tamimi et al. observed significantly higher levels of IL-4 in CSF in patients with delayed ischemic neurological deficit, with peak-levels on Day 5 [40]. Early intracerebral injection of IL-4 potentially promotes neuro-functional recovery, probably through enhancing the activation of microglia M2 (protective) phenotype and inhibiting the activation of M1 (injurious/toxic) phenotype in patients with intracerebral hemorrhage [41]. Our study supports the assumption that patients with DCI and a putatively larger inflammatory response mount an even greater compensatory anti-inflammatory response reflected by IL-4 elevation. However, since the serum IL-4 level showed a correlation with TCD positivity and not with DCI, the increase in velocity detected with TCD in the arteries is a part of the development of DCI, but not the sole mechanism. Based on the above evidence, we can state that the significantly higher IL-4 level detected in TCD-positive patients shows the pathophysiological role of IL-4 in the development of vasospasm, which may be the basis of DCI.

On correlation analysis, although FGF-2 did not show a direct correlation with the outcome or the occurrence of DCI, a strong negative correlation was observed with IP-10 which was found to be associated with functional outcome. This negative correlation was particularly pronounced in patients with favorable outcome, but negligible in the unfavorable group. FGF-2 suppresses autophagy levels; hence, it may reduce post-SAH neuronal apoptosis, providing a neuroprotective role, at least partially, by activating the PI3K/Akt pathway [12,42]. Recently, triggering by receptor expressed on myeloid cell 2 (TREM2) was identified as regulator of both IP-10 and FGF-2 beside others. TREM2 is involved in the activation of IP-10, MIP-1a, and IL-8, while it inhibits FGF-2, and thus it plays a role in enhancing the microglial function, suggesting that therapeutic strategies that seek to activate TREM2 may not only enhance phagocytosis, but also inhibit apoptosis [43]. Taken together, this novel association between IP-10 as a marker influencing the post-aSAH outcome and FGF-2 suggests independent pathological pathways in the neuroinflammatory response after aSAH. Moreover, it also raises questions which require further studies to clarify the role of the FGF-2/FGFRs neurotrophic system in aSAH. Our study has several limitations. Biomarker samples were only taken at two time points after aSAH, which limits the precise analysis of the long term kinetics of the markers. The relatively lower number of cases also reduces the generalizability of our study. One of the reasons for this is that unfortunately, due to the medical emergency caused by COVID-19, long-term monitoring of patients in our institution was not possible in all cases due to limited access to medical personnel. This significantly limited the number of patients who could be screened. Sampling at two time points is insufficient to provide further information on whether the observed increase in markers is a consequence or a cause.

4. Materials and Methods

4.1. Study Design

This was a prospective observational study from a tertiary stroke treatment center in Pecs, Hungary. All patients ≥ 18 years of age with a newly diagnosed aSAH admitted to our hospital from November 2018 and December 2021 were offered enrollment into this study. Exclusion criteria were: traumatic SAH, pregnancy, hospital admission later than 24 h after ictus, no aneurysm treatment, absence of a signed consent form, underlying SARS-CoV-2 infection, and systemic diseases (chronic neurological disease, tumors, liver and/or renal insufficiency, and chronic lung disease). Written informed consent was obtained from each patient or their legal representative. All included patients underwent computed tomography (CT) or magnetic resonance (MR) angiography before admission and conventional cerebral angiography after admission and received treatment according to clinical treatment guidelines. Following the diagnosis of aSAH, according to our hospital standards, the aneurysm was treated endovascularly within 24 h. In all cases, the patient spent at least 12–14 days in the neurointensive care unit, so that expected complications (e.g., DCI) could be detected in time. DCI was screened by using transcranial doppler from admission in every day of hospital care. If DCI was suspected, MRI and catheter angiography were performed to confirm macrovascular vasospasm and DCI. If vasospasm was confirmed, intra-arterial nimodipine was administered.

4.2. Clinical Definitions

For each patient, data on demographics (age, sex) were collected. Basic comorbidities (hypertension, diabetes, and smoking) were identified. Aneurysm location and admission laboratory parameters (creatinine, C-reactive protein, neutrophile-lymphocyte ratio) were collected according to hospital records. Further, the severity of aSAH was assessed using World Federation of Neurologic Surgeons (WFNS) grade and modified Fisher scale, taking into consideration the amount of blood in the initial CT scan. The presence of mechanical ventilation, need for decompressive craniectomy, and extra ventricular or lumbar drainage were recorded. Transcranial Doppler (TCD) spasm indicated TCD positivity (TCD+) was diagnosed by daily transcranial Doppler measurements and defined as peak-value increase by

>50 cm/s/24 h compared with the previous result or a mean value >120 cm/s in one of the main supply branches [44]. Angiographic vasospasm was defined as moderate-to-severe arterial narrowing on digital subtraction angiography not attributable to atherosclerosis, catheter-induced spasm, or vessel hypoplasia, as determined by a neuroradiologist [45]. We used the widespread, consensus definition of DCI [45]. The definition of infection were symptoms of infection with fever, elevated C-reactive protein and/or procalcitonin, and a positive diagnostic test such as chest X-ray or urine test. The clinical endpoints were DCI and unfavorable outcome (modified Rankin score ≥ 3) after 30 days after aSAH.

4.3. Sampling and Laboratory Analysis

Samples were collected from the patients at two time points: (1) 24 h after ictus (Day 1) and (2) 5–7 days after ictus and were stored at $-80\text{ }^{\circ}\text{C}$ until measurement. Serum concentrations of eotaxin (CCL-11), fibroblast growth factor-2 (FGF-2), Fms related receptor tyrosine kinase-3 ligand (FLT-3L), chemokine (C-X3-C motif) ligand-1 (CX3CL1) also known as fractalkine, interleukin-1b (IL-1b), interleukin-4 (IL-4), interferon gamma-induced protein 10 (IP-10), also known as C-X-C motif chemokine ligand 10 (CXCL10), monocyte-chemotactic protein 3 (MCP3), also known as Chemokine (C-C motif) ligand 7 (CCL7), and macrophage inflammatory protein-1b (MIP-1b) were determined using a customized MILLIPLEX Human Cytokine/Chemokine/Growth Factor Panel A multiplex assay (HCYTA-60K, Merck KGaA, Darmstadt, Germany) according to the manufacturer's protocol. Briefly, 25 μL of each serum sample, standard and control, was added to the appropriate wells of 96-well plates provided with the kit together with 25 μL of assay buffer and 25 μL of the mixture of fluorescent-coded magnetic beads, each of which was coated with a specific capture antibody. After an overnight incubation at $2-8\text{ }^{\circ}\text{C}$ for each analyte to be captured by the beads, and three rounds of washing, 25 μL of biotinylated detection antibody was introduced for an hour at room temperature. The reaction mixture was then incubated for 30 min with 25 μL Streptavidin–phycoerythrin conjugate, the reporter molecule, to complete the reaction on the surface of each bead. Following washing the plate three times it was run on the Luminex MAGPIX instrument (Luminex Corporation, Austin, TX, USA); each individual bead was identified and the result of its bioassay was quantified based on fluorescent reporter signals. Data were analyzed using the Belysa Immunoassay Curve Fitting Software (Merck KGaA, Darmstadt, Germany) in accordance with the manufacturer's instructions. Samples were all processed by the same laboratory technician using the same equipment and blinded to all clinical data.

4.4. Statistical Analysis

SPSS 19.0 (SPSS Inc., Chicago, IL, USA) and Graph Pad Prism 9 software (GraphPad Software, San Diego, CA, USA) was used for statistical analysis of data. The categorical variables are presented as frequency and percentage. The continuous variables are presented as mean \pm standard deviation or median (percentile 25–75). For comparison of data between two groups, the significances of inter-group differences were assessed using chi-square test or Fisher exact test for categorical data as well as Student t test or Mann–Whitney U test for continuous variables. Bivariate correlations were analyzed by Spearman's correlation coefficient. Because a high number of correlations are possible among the 9 cytokines, a hard threshold of 0.50 was used to exclude correlations below this value and to focus only on strong correlations. A binary logistic regression model was used to identify independent predictors with respect to DCI status. All *p* values lower than 0.05 were considered statistically significant.

4.5. Ethical Considerations

The study was approved by the Hungarian Medical Research Council. All procedures were performed in accordance with the ethical guidelines of the 1975 Declaration of Helsinki. Written informed consents were received from all patients according to the guidance of Declaration of Helsinki when they participated in this study.

5. Conclusions

Our results demonstrated that MCP-3 and CX3CL1 may play a role in the pathophysiology of DCI and may be potential therapeutic targets in the pharmacological treatment of DCI. Considering that both markers can be promising in the prediction and treatment of DCI, further studies with a large number of cases are necessary to clearly define their role in the pathophysiology of DCI and thus open up new therapeutic horizons.

Author Contributions: Conceptualization, P.C. and T.M.; methodology, P.C.; software, D.S.(Dora Spantler); validation, T.B., D.S. (Diana Simon); formal analysis, A.B.; investigation, D.S. (Dora Spantler); resources, A.S.; data curation, P.C.; writing—original draft preparation, P.C. and D.S. (Dora Spantler); writing—review and editing, T.M.; visualization, D.S. (Dora Spantler); supervision, A.B.; project administration, T.M.; funding acquisition, A.S. All authors have read and agreed to the published version of the manuscript.

Funding: This project and the open access funding was supported by a grant (ÁOK-KK Kollaboráció Alap (ÁOK-TANDEM)) from University of Pecs, Hungary.

Institutional Review Board Statement: Study was approved by the Hungarian Medical Research Council (IV/8468-1/2021/EKU). All procedures were performed in accordance with the ethical guidelines of the 1975 Declaration of Helsinki.

Informed Consent Statement: Informed consent was obtained from all subjects involved in the study.

Data Availability Statement: All relevant data are within the manuscript.

Acknowledgments: We would like to thank the work of Attilane Pal who performed the laboratory sampling and processing very precisely and she did not spare the time to deal with the study.

Conflicts of Interest: The authors declare no conflict of interest. The funders had no role in the design of the study; in the collection, analyses, or interpretation of data; in the writing of the manuscript, or in the decision to publish the results.

References

1. De Rooij, N.K.; Linn, F.H.H.; Van Der Plas, J.A.; Algra, A.; Rinkel, G.J.E. Incidence of subarachnoid haemorrhage: A systematic review with emphasis on region, age, gender and time trends. *J. Neurol. Neurosurg. Psychiatry* **2007**, *78*, 1365–1372. [[CrossRef](#)] [[PubMed](#)]
2. Velat, G.J.; Kimball, M.M.; Mocco, J.; Hoh, B.L. Vasospasm after Aneurysmal Subarachnoid Hemorrhage: Review of Randomized Controlled Trials and Meta-Analyses in the Literature. *World Neurosurg.* **2011**, *76*, 446–454. [[CrossRef](#)] [[PubMed](#)]
3. Alaraj, A.; Charbel, F.T.; Amin-Hanjani, S. Peri-operative measures for treatment and prevention of cerebral vasospasm following subarachnoid hemorrhage. *Neurol. Res.* **2009**, *31*, 651–659. [[CrossRef](#)] [[PubMed](#)]
4. Dodd, W.S.; Laurent, D.; Dumont, A.S.; Hasan, D.M.; Jabbour, P.M.; Starke, R.M.; Hosaka, K.; Polifka, A.J.; Hoh, B.L.; Chalouhi, N. Pathophysiology of Delayed Cerebral Ischemia after Subarachnoid Hemorrhage: A Review. *J. Am. Heart Assoc.* **2021**, *10*, e021845. [[CrossRef](#)]
5. Sehba, F.A.; Pluta, R.M.; Zhang, J.H. Metamorphosis of Subarachnoid Hemorrhage Research: From Delayed Vasospasm to Early Brain Injury. *Mol. Neurobiol.* **2011**, *43*, 27–40. [[CrossRef](#)]
6. Macdonald, R.L. Delayed neurological deterioration after subarachnoid haemorrhage. *Nat. Rev. Neurol.* **2014**, *10*, 44–58. [[CrossRef](#)]
7. Vergouwen, M.D.; Vermeulen, M.; van Gijn, J.; Rinkel, G.J.; Wijdeveld, E.F.; Muizelaar, J.P.; Mendelow, A.D.; Juvela, S.; Yonas, H.; Terbrugge, K.G.; et al. Definition of delayed cerebral ischemia after aneurysmal subarachnoid hemorrhage as an outcome event in clinical trials and observational studies: Proposal of a multidisciplinary research group. *Stroke* **2010**, *41*, 2391–2395. [[CrossRef](#)]
8. Abdel-Tawab, M.; Hasan, A.A.; Ahmed, M.A.; Seif, H.M.A.; Yousif, H.A. Prognostic factors of delayed cerebral ischemia after subarachnoid hemorrhage including CT perfusion: A prospective cohort study. *Egypt. J. Radiol. Nucl. Med.* **2020**, *51*, 61. [[CrossRef](#)]
9. Koenig, H.M.; Chen, J.; Sieg, E.P. Delayed Cerebral Ischemia: Is Prevention Better than Treatment? *J. Neurosurg. Anesthesiol.* **2021**, *33*, 191–192. [[CrossRef](#)]
10. Vlachogiannis, P.; Hillered, L.; Enblad, P.; Ronne-Engström, E. Temporal patterns of inflammation-related proteins measured in the cerebrospinal fluid of patients with aneurysmal subarachnoid hemorrhage using multiplex Proximity Extension Assay technology. *PLoS ONE* **2022**, *17*, e0263460. [[CrossRef](#)]
11. Lieschke, S.; Zechmeister, B.; Haupt, M.; Zheng, X.; Jin, F.; Hein, K.; Weber, M.S.; Hermann, D.M.; Bähr, M.; Kilic, E.; et al. CCL11 Differentially Affects Post-Stroke Brain Injury and Neuroregeneration in Mice Depending on Age. *Cells* **2019**, *9*, 66. [[CrossRef](#)] [[PubMed](#)]
12. Wang, Y.; Pan, X.-F.; Liu, G.-D.; Liu, Z.-H.; Zhang, C.; Chen, T.; Wang, Y.-H. FGF-2 suppresses neuronal autophagy by regulating the PI3K/Akt pathway in subarachnoid hemorrhage. *Brain Res. Bull.* **2021**, *173*, 132–140. [[CrossRef](#)] [[PubMed](#)]

13. Huang, B.; Krafft, P.R.; Ma, Q.; Rolland, W.B.; Caner, B.; Lekic, T.; Manaenko, A.; Le, M.; Tang, J.; Zhang, J.H. Fibroblast growth factors preserve blood-brain barrier integrity through RhoA inhibition after intracerebral hemorrhage in mice. *Neurobiol. Dis.* **2012**, *46*, 204–214. [[CrossRef](#)] [[PubMed](#)]
14. Tarozzo, G.; Campanella, M.; Ghiani, M.; Bulfone, A.; Beltramo, M. Expression of fractalkine and its receptor, CX₃CR1, in response to ischaemia-reperfusion brain injury in the rat. *Eur. J. Neurosci.* **2002**, *15*, 1663–1668. [[CrossRef](#)] [[PubMed](#)]
15. Wang, B.; Li, X.; Dong, T.; Gao, F.; Li, Z.; Ma, Z. Expression of interferon regulatory factor 4 and inflammation in secondary injury of intracerebral haemorrhage. *Folia Neuropathol.* **2021**, *59*, 291–297. [[CrossRef](#)]
16. Li, X.; Lin, S.; Chen, X.; Huang, W.; Li, Q.; Zhang, H.; Chen, X.; Yang, S.; Jin, K.; Shao, B. The Prognostic Value of Serum Cytokines in Patients with Acute Ischemic Stroke. *Aging Dis.* **2019**, *10*, 544–556. [[CrossRef](#)]
17. Ahn, S.-H.; Savarraj, J.; Parsha, K.; Hergenroeder, G.W.; Chang, T.R.; Kim, D.H.; Kitagawa, R.S.; Blackburn, S.L.; Choi, H.A. Inflammation in delayed ischemia and functional outcomes after subarachnoid hemorrhage. *J. Neuroinflamm.* **2019**, *16*, 1–10. [[CrossRef](#)]
18. Niwa, A.; Osuka, K.; Nakura, T.; Matsuo, N.; Watabe, T.; Takayasu, M. Interleukin-6, MCP-1, IP-10, and MIG are sequentially expressed in cerebrospinal fluid after subarachnoid hemorrhage. *J. Neuroinflamm.* **2016**, *13*, 217. [[CrossRef](#)]
19. Rancan, M.; Bye, N.; Otto, V.I.; Trentz, O.; Kossman, T.; Frenz, S.; Morganti-Kossmann, M.C. The Chemokine Fractalkine in Patients with Severe Traumatic Brain Injury and a Mouse Model of Closed Head Injury. *J. Cereb. Blood Flow Metab.* **2004**, *24*, 1110–1118. [[CrossRef](#)]
20. Lauro, C.; Catalano, M.; Trettel, F.; Limatola, C. Fractalkine in the nervous system: Neuroprotective or neurotoxic molecule? *Ann. N. Y. Acad. Sci.* **2015**, *1351*, 141–148. [[CrossRef](#)]
21. Zheng, Z.V.; Wong, K.C.G. Microglial activation and polarization after subarachnoid hemorrhage. *Neuroimmunol. Neuroinflamm.* **2019**, *6*. [[CrossRef](#)]
22. Wang, G.; Zhang, J.; Hu, X.; Zhang, L.; Mao, L.; Jiang, X.; Liou, A.K.-F.; Leak, R.; Gao, Y.; Chen, J. Microglia/Macrophage Polarization Dynamics in White Matter after Traumatic Brain Injury. *J. Cereb. Blood Flow Metab.* **2013**, *33*, 1864–1874. [[CrossRef](#)] [[PubMed](#)]
23. Cipriani, R.; Villa, P.; Chece, G.; Lauro, C.; Paladini, A.; Micotti, E.; Perego, C.; de Simoni, M.G.; Fredholm, B.B.; Eusebi, F.; et al. CX3CL1 Is Neuroprotective in Permanent Focal Cerebral Ischemia in Rodents. *J. Neurosci.* **2011**, *31*, 16327–16335. [[CrossRef](#)] [[PubMed](#)]
24. Pawelec, P.; Ziemka-Nalecz, M.; Sypecka, J.; Zalewska, T. The Impact of the CX3CL1/CX3CR1 Axis in Neurological Disorders. *Cells* **2020**, *9*, 2277. [[CrossRef](#)] [[PubMed](#)]
25. Chen, X.; Jiang, M.; Li, H.; Wang, Y.; Shen, H.; Li, X.; Zhang, Y.; Wu, J.; Yu, Z.; Chen, G. CX3CL1/CX3CR1 axis attenuates early brain injury via promoting the delivery of exosomal microRNA-124 from neuron to microglia after subarachnoid hemorrhage. *J. Neuroinflamm.* **2020**, *17*, 209. [[CrossRef](#)]
26. Zanier, E.R.; Marchesi, F.; Ortolano, F.; Perego, C.; Arabian, M.; Zoerle, T.; Sammali, E.; Pischiutta, F.; De Simoni, M.-G. Fractalkine Receptor Deficiency Is Associated with Early Protection but Late Worsening of Outcome following Brain Trauma in Mice. *J. Neurotrauma* **2016**, *33*, 1060–1072. [[CrossRef](#)]
27. Kim, G.H.; Kellner, C.P.; Hahn, D.K.; Desantis, B.M.; Musabbir, M.; Starke, R.M.; Rynkowski, M.; Komotar, R.J.; Otten, M.L.; Sciacca, R.; et al. Monocyte chemoattractant protein-1 predicts outcome and vasospasm following aneurysmal subarachnoid hemorrhage. *J. Neurosurg.* **2008**, *109*, 38–43. [[CrossRef](#)]
28. Lu, H.; Shi, J.-X.; Chen, H.-L.; Hang, C.-H.; Wang, H.-D.; Yin, H.-X. Expression of monocyte chemoattractant protein-1 in the cerebral artery after experimental subarachnoid hemorrhage. *Brain Res.* **2009**, *1262*, 73–80. [[CrossRef](#)]
29. Wang, X.; Li, X.; Yaish-Ohad, S.; Sarau, H.M.; Barone, F.C.; Feuerstein, G.Z. Molecular cloning and expression of the rat monocyte chemotactic protein-3 gene: A possible role in stroke. *Mol. Brain Res.* **1999**, *71*, 304–312. [[CrossRef](#)]
30. Dahinden, C.A.; Geiser, T.; Brunner, T.; Von Tscharner, V.; Caput, D.; Ferrara, P.; Minty, A.; Baggiolini, M. Monocyte chemotactic protein 3 is a most effective basophil- and eosinophil-activating chemokine. *J. Exp. Med.* **1994**, *179*, 751–756. [[CrossRef](#)]
31. Ransohoff, R.M.; Hamilton, T.A.; Tani, M.; Stoler, M.H.; Shick, H.E.; Major, J.A.; Estes, M.L.; Thomas, D.M.; Tuohy, V.K. Astrocyte expression of mRNA encoding cytokines IP-10 and JE/MCP-1 in experimental autoimmune encephalomyelitis. *FASEB J.* **1993**, *7*, 592–600. [[CrossRef](#)] [[PubMed](#)]
32. Lahrtz, F.; Piali, L.; Nadal, D.; Pfister, H.-W.; Spanaus, K.-S.; Baggiolini, M.; Fontana, A. Chemotactic activity on mononuclear cells in the cerebrospinal fluid of patients with viral meningitis is mediated by interferon- γ inducible protein-10 and monocyte chemotactic protein-1. *Eur. J. Immunol.* **1997**, *27*, 2484–2489. [[CrossRef](#)] [[PubMed](#)]
33. Righy, C.; Turon, R.; De Freitas, G.; Japiassú, A.M.; Neto, H.C.D.C.F.; Bozza, M.; Oliveira, M.F.; Bozza, F.A. Hemoglobin metabolism by-products are associated with an inflammatory response in patients with hemorrhagic stroke. Subprodutos do metabolismo da hemoglobina se associam com respostainflamatóriaempacientes com acidente vascular cerebral hemorrágico. *Rev. Bras. Ter. Intensiv.* **2018**, *30*, 21–27. [[CrossRef](#)] [[PubMed](#)]
34. Loetscher, P.; Seitz, M.; Clark-Lewis, I.; Baggiolini, M.; Moser, B. Monocyte chemotactic proteins MCP-1, MCP-2, and MCP-3 are major attractants for human CD4⁺ and CD8⁺ T lymphocytes. *FASEB J.* **1994**, *8*, 1055–1060. [[CrossRef](#)] [[PubMed](#)]
35. Taub, D.D.; Proost, P.; Murphy, W.J.; Anver, M.; Longo, D.L.; Van Damme, J.; Oppenheim, J.J. Monocyte chemotactic protein-1 (MCP-1), -2, and -3 are chemotactic for human T lymphocytes. *J. Clin. Investig.* **1995**, *95*, 1370–1376. [[CrossRef](#)]
36. Carrera, E.; Schmidt, J.M.; Oddo, M.; Fernandez, L.; Claassen, J.; Seder, D.; Lee, K.; Badjatia, N.; Connolly, E.S., Jr.; Mayer, S.A. Transcranial Doppler for predicting delayed cerebral ischemia after subarachnoid hemorrhage. *Neurosurgery* **2009**, *65*, 316–324. [[CrossRef](#)]

37. Chang, J.J.; Triano, M.; Corbin, M.J.; Desale, S.; Liu, A.-H.; Felbaum, D.R.; Mai, J.C.; Armonda, R.A.; Aulisi, E.F. Transcranial Doppler velocity and associations with delayed cerebral ischemia in aneurysmal subarachnoid Hemorrhage. *J. Neurol. Sci.* **2020**, *415*, 116934. [[CrossRef](#)]
38. Papaioannou, V.E.; Budohoski, K.P.; Placek, M.M.; Czosnyka, Z.; Smielewski, P.; Czosnyka, M. Association of transcranial Doppler blood flow velocity slow waves with delayed cerebral ischemia in patients suffering from subarachnoid hemorrhage: A retrospective study. *Intensiv. Care Med. Exp.* **2021**, *9*, 11. [[CrossRef](#)]
39. Snider, S.B.; Migdady, I.; LaRose, S.L.; Mckeown, M.E.; Regenhardt, R.W.; Lai, P.M.R.; Vaitkevicius, H.; Du, R. Transcranial-Doppler-Measured Vasospasm Severity is Associated with Delayed Cerebral Infarction after Subarachnoid Hemorrhage. *Neurocrit. Care* **2022**, *36*, 815–821. [[CrossRef](#)]
40. Al-Tamimi, Y.Z.; Bhargava, D.; Orsi, N.M.; Teraifi, A.; Cummings, M.; Ekbote, U.V.; Quinn, A.C.; Homer-Vanniasinkam, S.; Ross, S. Compartmentalisation of the inflammatory response following aneurysmal subarachnoid haemorrhage. *Cytokine* **2019**, *123*, 154778. [[CrossRef](#)]
41. Eyang, J.; Eding, S.; Ehuang, W.; Eqichuan, Z.; Huang, S.; Ezhang, Y.; Zhuge, Q. Interleukin-4 Ameliorates the Functional Recovery of Intracerebral Hemorrhage through the Alternative Activation of Microglia/Macrophage. *Front. Neurosci.* **2016**, *10*, 61. [[CrossRef](#)] [[PubMed](#)]
42. Okada, T.; Enkhjargal, B.; Travis, Z.D.; Ocak, U.; Tang, J.; Suzuki, H.; Zhang, J.H. FGF-2 Attenuates Neuronal Apoptosis via FGFR3/PI3k/Akt Signaling Pathway after Subarachnoid Hemorrhage. *Mol. Neurobiol.* **2019**, *56*, 8203–8219. [[CrossRef](#)] [[PubMed](#)]
43. Akhter, R.; Shao, Y.; Formica, S.; Khrestian, M.; Bekris, L.M. TREM2 alters the phagocytic, apoptotic and inflammatory response to A β 42 in HMC3 cells. *Mol. Immunol.* **2021**, *131*, 171–179. [[CrossRef](#)]
44. Grosset, D.G.; Straiton, J.; du Trevou, M.; Bullock, R. Prediction of symptomatic vasospasm after subarachnoid hemorrhage by rapidly increasing transcranial Doppler velocity and cerebral blood flow changes. *Stroke* **1992**, *23*, 674–679. [[CrossRef](#)] [[PubMed](#)]
45. Frontera, J.A.; Fernandez, A.; Schmidt, J.M.; Claassen, J.; Wartenberg, K.E.; Badjatia, N.; Connolly, E.S.; Mayer, S. A Defining vasospasm after subarachnoid hemorrhage: What is the most clinically relevant definition? *Stroke* **2009**, *40*, 1963–1968. [[CrossRef](#)] [[PubMed](#)]